Graduate School in Molecular Sciences and Plant, Food and Environmental Biotechnology

UNIVERSITA' DEGLI STUDI DI MILANO

FACOLTA' DI AGRARIA

Study of Chemical and Molecular Information Related to NIR and IR Spectroscopic Data for Dairy Sector

LAURA MARINONI

2010-2011

UNIVERSITÀ DEGLI STUDI DI MILANO
FACOLTÀ DI AGRARIA

Scuola di dottorato in Scienze Molecolari e Biotecnologie Agrarie,
Alimentari ed Ambientali

Dottorato in Biotecnologia degli alimenti

Study of Chemical and Molecular Information Related to NIR and IR Spectroscopic Data for Dairy Sector

AGR/15 - BIO/10 - CHIM/10

Laura MARINONI

Matr. n.: R08221

Tutor: Prof.ssa Stefania IAMETTI

Coordinatore: Prof.ssa Maria Grazia FORTINA

Anno Accademico 2010/2011

1. INTRODUCTION

1.1 Infrared spectroscopy

1.1.1 Theoretical principles of infrared spectroscopy (Workman & Weyer, 2008; Burns & Ciurczak, 2001; Siesler, 2002)

Infrared spectroscopy can be defined as the analysis of materials regarding their tendency to absorb light in a certain area of the electromagnetic radiation. In particular, it is used to indicate the separation, detection and recording of changes in energy (resonance peaks) involving nuclei, atoms or entire molecules. These energetic variations are due to the interaction between radiation and matter, specifically the emission, absorption or diffusion of electromagnetic radiation or particles. Infrared spectroscopy is applied for quantitative and qualitative analysis. Its most important and characteristic application field is the identification of organic compounds that give rise, especially in the mid-infrared region, to generally complex spectra with several maxima and minima absorption peaks. In many cases, in fact, the infrared spectrum of an organic compound provides a unique fingerprint that is easily distinguishable from other compounds.
The high selectivity of the method often allows the quantitative determination of an analyte in a complex mixture without prior separation. The theoretical basis of the interaction between matter and radiation is the quantum nature of energy transfer from the radiation to matter and vice versa. In fact both the matter and the electromagnetic field have a "dual nature", i.e. the ability to behave both as waves and as particles. Electromagnetic radiations, the best known of which is light, are nothing but a form of transport of energy electromagnetic thought space. According to studies of James Clerck Maxwell, the movement of electrical charges can generate waves of radiant energy in space. They are the result of the superposition of an electric field and a magnetic field orthogonal mutually coupled: each of them is the source of the other and propagates with a sinusoidal movement in both space and time (Figure 1.1).

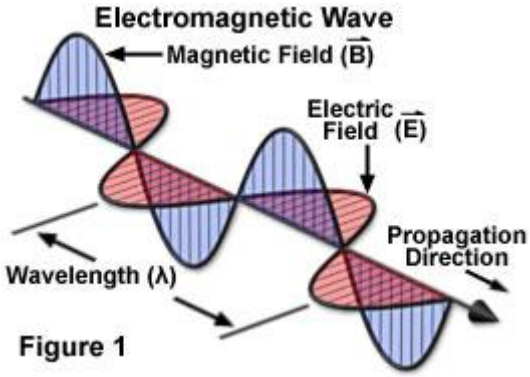

Figura 1.1: Representative model of the electromagnetic radiation.

The directions of oscillation in space of electric and magnetic fields are perpendicular to the direction of propagation which has a wave nature. The wave character of the electromagnetic radiation is commonly described by its wavelength (λ), measured in nanometers (nm = 10^{-9} m), the wave number (ν), which represents the number of waves present in a unit length, measured in reciprocal centimeters (cm^{-1}), the speed (V) with the wave advance, and the number of wavelengths that pass in a given point per unit of time, frequency (ν), measured in hertz (Hz = s^{-1}). The relationship between these quantities is given by the expression formula

$$v = \frac{l}{\lambda} = \frac{\nu}{V}$$

where V is the velocity of the electromagnetic wave in vacuum, i.e. the rate of radiation diffusion. Maxwell discovered that the propagation speed was constant for all the electromagnetic waves in vacuum, and it was equal to 2.998x1010 cm s^{-1}, i.e. the speed of light. Thus, being the speed propagation constant, the frequency can be deduced from the wavelength and vice versa. The entire electromagnetic spectrum is composed of several areas defined by specific wavelengths as shown in Figure 1.2. This division gives rise to five major groups: the visible region, the ultraviolet and ionizing radiation, characterized by high frequencies and short wavelengths, and the infrared and radio waves, characterized by low frequency and high wavelengths. The infrared region of the spectrum comprises radiation with wave numbers ranging from about 12500 to 10 cm^{-1}. It's usually divided into three regions: the higher energy near-IR (NIR), (4000-10000 cm^{-1}) exciting overtone or harmonic vibrations; the mid-infrared (IR), (4000–400 cm^{-1}) used to study fundamental vibrations and associated rotational-vibrational structure; the far-infrared (FIR) (400–10 cm^{-1}) used for rotational spectroscopy.

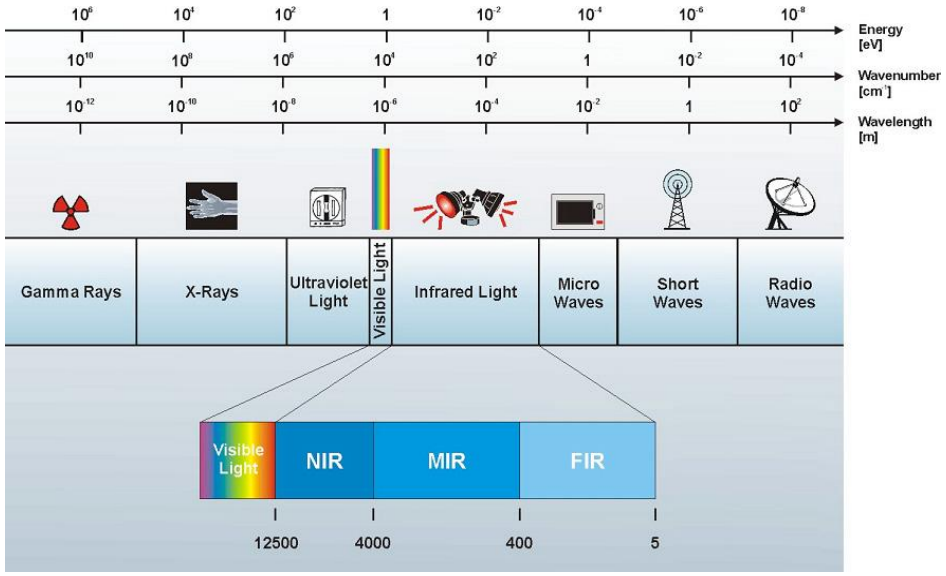

Figure 1.2: Electromagnetic spectrum.

The radiation shows its particle nature when interacts with matter. It does not transmit a continuous quantity of energy, as in classical physics, but "packets" of quantized energy. It can therefore be considered as a stream of particles called photons. The interaction between radiation and matter happens when the quantum energy transfer occurs between the electromagnetic wave and the energy states of matter and vice versa. By considering that the radiation consists of photons and the energy transmitted by a photon is proportional to the frequency of the electromagnetic wave, the amount of energy that a photon of a certain wave transmits to the matters can be calculated through the Einstein -Planck relation:

$$E = h\nu = \frac{hc}{\lambda} = hc\nu$$

where *E* is the energy in Joules, *h* is Planck's constant (6.62x10-34 J / s) and *v* is the frequency of the radiation in Hertz.

This function shows that the energy of a photon or of a monochromatic radiation (single frequency) depends on its wavelength (λ) or by its frequency (ν). A radiation beam can have an intensity more or less strong depending on the amount of photons per unit time and unit area, but the quantum energy (*E*) is always the same for a given frequency of radiation. The electromagnetic spectrum is the radiation set consisting in a series of photons or electromagnetic waves at increasing energy and it can therefore be divided into regions, corresponding to well-defined fields of energy. Thus, the electromagnetic radiation it is not distributed in a continuous way but in a quantized way and consequently also the energetic events occurring at the atomic or molecular level. From these considerations, Bohr (Burns & Ciurczak, 2001) in 1914 laid the foundation for a correct interpretation of the spectra of atoms and molecules with the following postulates:

1. The atomic systems exist in stable states, without emitting electromagnetic energy.
2. The absorption or the emission of electromagnetic energy occurs when an atomic system changes from one energy state to another.
3. The process of absorption or emission corresponds to a photon of radiant energy $h\nu = E' - E''$, where $E' - E''$ is the difference in energy between two states of an atomic system.

So, according to quantum physics, a molecule can not rotate or vibrate freely with any value of energy, but it is subject to what are called quantum restrictions. So when the energy of a radiation goes through the energy of a molecule that is vibrating, there is a transfer of energy that can be measured and graphically represented as a variation of energy (in the ordinate) and wavelength (in the abscissa) as a spectrum. According to the third postulate of Bohr (Burns & Ciurczak, 2001), the passage of energy from a photon to a molecule can take place only if the photon has a frequency, and therefore energy, equal to that is necessary to move the molecule from the ground to the excited state.

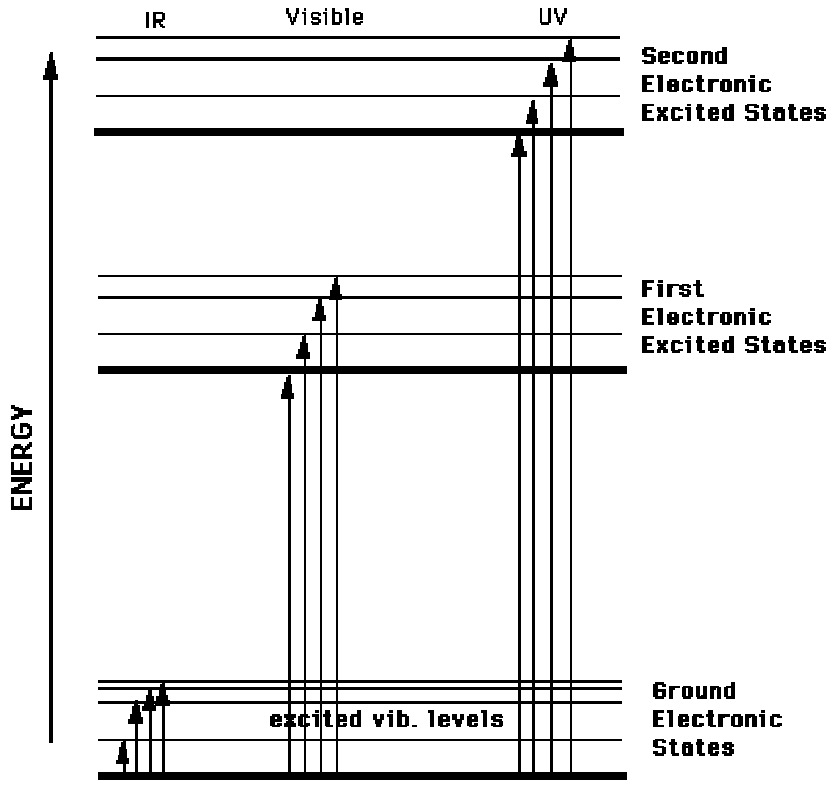

Figure 1.3: Atomic quantum jumps

The three groups of lines, represented in figure 1.3, correspond to three different arrangements of electrons. The lowest energy corresponds to the most stable configuration, called basic configuration. The next level corresponds to the first excited level. If a photon, with an energy equal to the difference between the two considered configurations, strikes the molecule, an electron in the basic state has a certain probability to move to the next level. Thus, the photon is absorbed by the molecule. After some time, typically 10^{-8} seconds, the electron returns to its basic state with the emission of a photon of energy equal to the jump in energy between the two levels. Higher energy photons can lead the electron to a second level or to subsequent levels of excitement. High energy photons in the ultraviolet region can also split the electron from the atom which remains positively charged (ionized). In the infrared region, with low energy, photons are not able to excite the molecule, but they may induce vibrational motions of electrons. Even in this case energies associated with various modes of vibration are quantized. Energy of the ground state and excited states are flanked by vibrational states. The system of the possible levels jumping greatly increases and gives rise to very complicated emission and absorption spectra. Electromagnetic radiations in the microwave, even less energy, are not able to induce vibrations but only the rotation of the molecule. So the effects of radiation on matter vary depending on the frequency of the radiation and are represented in Figure 1.4.

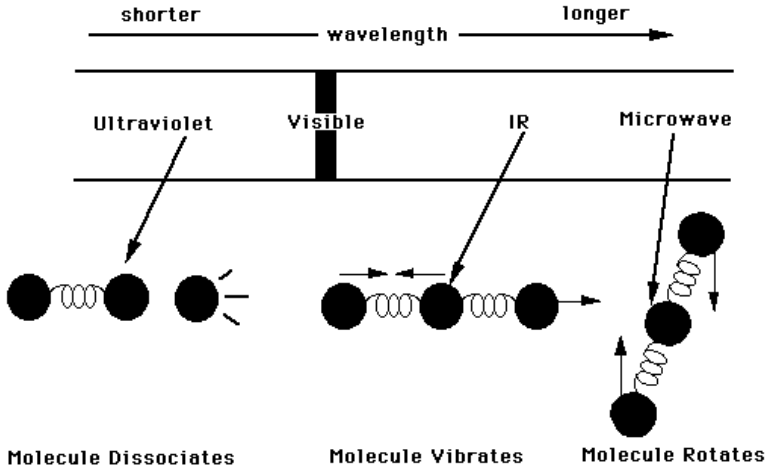

Figura 1.4: Molecular effects of UV, VIS, IR and microwave radiations.

For these reasons the absorption or the emission of energy by matter is one of the most important identification marks provided by nature. When a beam of radiation is passed through an absorbent material, the intensity of the incident radiation (I) will be greater than that emitted (I_0). So it is possible to go back to the frequency of the radiation that was absorbed and thus to the jump of energy of the molecule. Jumps with a given energy level may be restricted to certain molecules; thus it's possible to understand what molecules make up the matter. The total energy of a molecule can be considered as the sum of the contributions of the electronic , rotational and vibrational energies: $E_{tot} = E_{el} + E_{rot} + E_{vib}$

In the atomic spectra, electronic interactions regarding the electrons in the valence shell are the only possible; regarding molecules, for each electronic state, usually several vibrational and rotational states are possible. In the case of NIR, even combinations of these and the presence of overtones occurs.

A photon, that has an amount of energy that is two or three times the energy required to bring a molecule to a higher energy level, will produce changes in the second or third level, thus forming the second or third overtone.

Consequently, the number of possible energy levels for a molecule is much larger than that for an atomic particle. That is why the atomic spectra appear as lines, while those molecular consist of hundreds or thousands of absorption lines so close together that they appear as bands of absorption.

In the area of the electromagnetic spectrum defined as near-infrared, the energies involved seem to result in a change in the vibrational motion of molecules and in particular of the links they contain. In fact, absorptions of the ground states usually fall in the region between 2500 and 15000 nm (4000-660 cm^{-1}) defined as mid-infrared (MIR), while absorptions of states with multiple frequencies to those of the ground state, called overtones, are characteristic of the area of NIR.

A molecule absorbs infrared radiation when it vibrates in such a way that its electric dipole moment changes during vibration. The electric dipole moment μ is a vector quantity $\mu = qd$, where q is the electric charge and d is the vectorial distance of charge q from a defined origin point of coordinates for the molecule. When the molecule vibrates, its charge distribution, with respect to this origin, may change or remain unchanged, depending on the structure of the molecule. Not all the vibrations of a particular molecular structure necessarily absorb infrared

radiation, but only those vibrations that are changing the electric dipole moment of the molecule. Models to explain the vibrations are based on the concept of "harmonic oscillator", which consists of two masses connected by a spring (Figure 1.5):

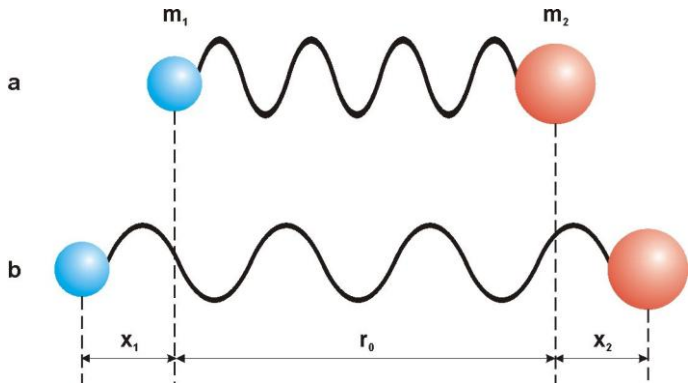

Figure 1.5: Harmonic oscillator

When set in motion, the system will oscillate or vibrate back and forward along the axis determined by the spring, at a certain frequency, depending on the masses of the spheres and the stiffness of the spring. A sphere with small mass is lighter and easier to move than one with a large mass. So the smaller masses oscillate at higher frequencies than large masses. A very stiff spring is difficult to deform and quickly returns to its original shape when the force of deformation is removed. On the other hand, a weak spring is easily deformed; in addition, a stiffer spring will oscillate at frequencies higher than a weak spring. A generic chemical bond between two atoms can be considered as a simple harmonic oscillator. The link is the spring, and the two atoms or groups of atoms, held together by the binding, are the masses. Each atom has a different mass, and a single, double and triple bond have different degrees of stiffness, so that each combination of atoms and bonds has its particular harmonic frequency. Mathematically, the system behavior is described by Hooke (Burns & Ciurczak, 2001):

$$\nu = \frac{1}{2\pi c}\sqrt{\frac{k(m_1+m_2)}{m_1 m_2}}$$

where c is the speed of light, k is the spring constant (dyne * 5 * 105 cm-1) and m_1 and m_2 are the masses of the atoms involved.

At any temperature above absolute zero, all the small and simple harmonic oscillators that make up any molecule vibrate intensely. The frequency of vibration of the molecules matches the frequencies that characterize the infrared radiation. If a vibrating molecule is hit with IR light, the molecule could absorb energy delivered by radiation, if this exactly combines with the frequencies of the different harmonic oscillators that make up the molecule. When light is absorbed in the small molecule oscillators continue to vibrate at the same frequency, but since they have absorbed the energy of light, have greater amplitude, resulting in a lengthening of the "spring". The absorption intensity is also influenced by the polarity of the bond on which the radiation affects: the more polarity of a bond, the greater is its absorption. This model represents, with a good approximation, only the symmetric diatomic molecules. Although the harmonic model is often used to explain the vibrational spectroscopy, it has some limitations

because it fails to describe the possible energetic transitions that can occur in a molecule that has a large number of atoms and especially not symmetrically arranged, as in most of organic molecules in food.
The infrared radiation is absorbed by a molecule when the radiation has enough energy to induce vibrational transitions on the molecule itself. The basic types of vibration caused by the incidence of IR radiation are divided into two categories: stretching and bending, as shown in Figure 1.6 Stretching is the vibration of the bond along the plane, due to the inter-atomic distance which varies rhythmically and can be symmetrical or asymmetrical; the bending vibrations are characterized by a variation of the angle between two atoms in the plane (scissoring and rocking) and out of the plane (wagging and twisting).

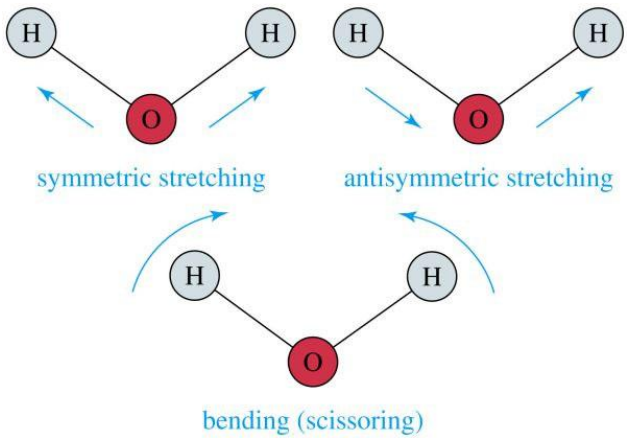

Figure 1.6: Molecular vibrations in a water molecule

The vibrational frequencies can be approximately related to molecular properties by means of Hooke's law, already described in the previous paragraph. This approximation is valid for diatomic molecules, but can also be applied, without significant differences of the average values, for stretching and bending vibrations of two atoms in a polyatomic molecule.
Since the values of the reduced mass of the groups -OH, -NH and -CH are quite similar, the spectral information is determined primarily by the *k* value, which depends not only on the length and strength of the bond, but also from the surrounding environment, thus creating differences in energy of absorption for each bond, making them specific, and are used in the spectrum interpretation. Actually, however, we analyze diatomic asymmetrical molecules, which change their responses to excitation caused by the incident radiation. The phenomena of mechanical anharmonicity, or the loss of equidistance between different energy levels, and of electrical anharmonicity, i.e. the change of the equation of electric dipole moment, move away from the ideal conditions. The anharmonicity leads to the appearance of overtone bands, or non-harmonic band, whose frequency is not a numeral multiple of the fundamental frequency in which the dipole bond of the molecule ranges.
These phenomena are even more dominant in a polyatomic molecule in which the mutual influences between atoms increase exponentially. In bonds involving hydrogen atoms, which have a very small mass, the lack of harmonicity is even more evident, and leads to a vibration with a great amplitude and more intense absorption bands. The absorption of electromagnetic radiation in the NIR region is therefore mainly due to overtones and their combination arising from the absorptions of the fundamental vibrations in the mid-infrared. The intensity of these

bands decreases significantly when the probability that the corresponding transitions occur decrease. Since the absorptions are up to 10-100 times weaker than the intensity of the fundamental bands, only the first 2 or 3 overtones for each fundamental band are observable. They are progressively less intense, located at higher and higher frequencies and therefore absorb at lower wavelengths.
The stretching motion of the hydrogen atom, because of its small mass and then the big difference with the other atom involved in the binding (usually oxygen, carbon or nitrogen) shows a particularly high deviation from the harmonic behavior. This implies that the fundamental stretching bands located in the mid-infrared between 3000 and 2400 cm^{-1}, at the limit with the NIR region, induce overtones and combination bands in the NIR region, thus making the absorption related to the secondary vibrational modes of hydrogen, the main feature of a near infrared spectrum. In fact most of the absorptions in this region are derived from the first, second and third overtones, corresponding to the fundamental vibrations of the bonds -CH, -NH, -OH, -SH, and their combination bands. The interactions due to the presence of hydrogen bonds between molecules of the sample are particularly noticeable, since they cause enlargement of the bands and shifts to lower frequencies. Very weak bands are related to the vibrations of C-C, C-F and C-Cl bonds.
The low-intensity of absorption in the NIR region may at first seem to be a limit, since it seems to decrease the sensitivity of the technique. Actually, at a practical level, this is a big advantage because it allows the direct analysis of a sample, without diluting or dispersing it into inert matrices as normally happens in traditional spectroscopic techniques, and also to obtain representative spectra of the whole sample, since the optical paths used are very long. Moreover, even if NIR bands are larger and liable to overlap more than in other spectral regions, chemometric techniques available today are able to extract a lot of information even from complex spectra such as NIR spectra.
IR measurements can be performed both in transmission and in reflectance mode; in the case of transmission mode, the intensity of light transmitted through the sample compared to the intensity of incident light is measured:

$$T = I/I_0$$

Lambert and Beer (Burns & Ciurczak, 2001) observed that the amount of radiation absorbed or transmitted from a solution or a medium was the exponential function of the concentration of the adsorbent and the radiation path length through the sample:

$$A = log\ 1/T = k_a\ cl$$

where k_a is the molar extinction coefficient, c is the concentration and l is the optical path length of incident radiation through the sample. In the case of acquisition of reflectance data, the intensity of the reflected light compared to the intensity of incident light is measured:

$$R = I_{rifl}/I_0$$

According to the Kubelka-Munk law (Burns & Ciurczak, 2001), reflectance depends on the coefficient of absorption k_r and the coefficient of dispersion of a sample s:

$$f(R_\infty) = k_r/s$$

where R_∞ is the absolute reflectance.

Experimentally the relative reflectance, i.e. the intensity of light that is reflected from the sample compared to the intensity of the reflected light in a referee material with a high and constant absolute reflectance, will be measured; examples of used materials are Teflon, MgO, discs of high purity ceramic material. In practice, the relative reflectance is often converted into apparent absorbance *A'*, using an empirical relationship between analyte concentration and reflectance, similar to the Lambert and Beer's law:

$$A' = \log 1/R = a'c$$

where *c* is the concentration and *a'* is a constant of proportionality.
However, if the matrix is highly absorbent or the analyte shows intense absorption bands, the linear relationship between absorbance and concentration fails. Both for the transmittance and the reflectance mode, the proposed equations are obtained from ideal situations, and are applicable only when the absorptions are weak or the product between concentration and molar extension coefficient is small. In the case of NIR spectroscopy, the matrix, which cannot be separated from the analyte, has the major absorption and can absorb at the same wavelengths of the analyte.
Often, the spectroscopic measurement is affected by scattering phenomena, or light diffusion on the surface, especially in the case of the acquisition of solid samples: in fact, the more the incident radiation is scattered, the less the beam penetrates deep into and therefore the lower will be the absorbance (apparent or real). The scattering phenomena depends primarily on the physical properties of the sample (particle size, crystal environment) and can cause shifts in the baseline of the spectrum and lead to phenomena of collinearity at different wavelengths.
The signal dependence of the signal from the physical properties of the sample is a significant disadvantage when NIR is used for qualitative determinations such as product identification or monitoring of process chemical parameters (humidity, homogeneity), and quantitative analysis of one or more components. To avoid this, some mathematical spectra pre-treatments have been developed to be applied before the data processing.

1.1.2 IR instrumentation (Settle, 1997; Da-Wen Sun, 2008)

A generic IR instrument is formed by a number of basic components: the source of radiation, a wavelength selector, a system of sample exposure to radiation and a detector.

Radiation sources

For FTIR instrumentation nichrome coil source is commonly used. Helium neon laser source is used for timing operations in an FTIR.
The NIR radiation sources are mainly incandescent bulbs or emitting diodes (LEDs). Each source has a specified emission range of wavelengths; for example, incandescence sources are effective for visible radiation while LEDs are limited to specific wavelengths depending on the material used. For each of these sources, especially with incandescent lamps, filters must be still used to eliminate the portion of radiation irrelevant for the analysis purposes and which can lead to excessive sample heating . For some very specific applications the use of lasers is emerging.

Wavelength selectors

The selection refers to the method used to separate specific wavelengths, in order to obtain the best resolution. The most common method for selecting wavelengths is the use of filters, made by layers of clear or colored glass and covered with aluminum, in order to pass only specific

wavelengths or groups of them. More filters can be put together to make more accurate selections. In modern systems, the diffraction grating is used: this is a surface that reflects infrared radiation and is engraved with a number of parallel lines, which leads, for the diffraction, the division of the incident radiation into separate wavelengths. The selection of wavelengths to be addressed to the sample or to the detector occurs by rotating the grating and thus changing the incident angle of the radiation source. The critical point of the system is just the rotation mechanism, which must be extremely precise.
Another category of monochromators, which today is widely used for being fast and precise, and characterizes all the instruments based on the Fourier transform, is the interferometers. The traditional model of spectrometer is modified by replacing the monochromator with the interferometer discovered by Michelson in 1891, which is still widely used in most of the NIR instruments (Figure 1.7)

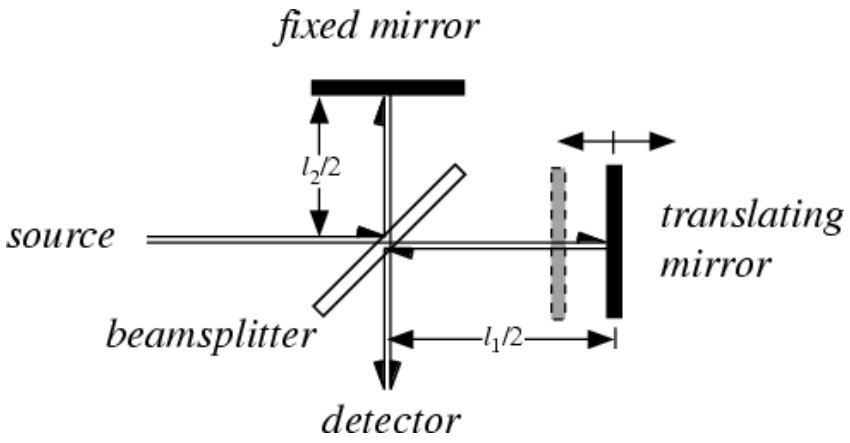

Figura 1.7: Michelson inteferometer.

It is based on the principle that two different waves can add up and then combined constructively each other in a peak with maximum intensity when they are involved, or they can combine annulling each other when are out of phase (Figure 1.8). To do so, the radius from the source is split into two parts so that they have the same propagation conditions. The first part will be reflected on a fixed mirror, while the second on a moving mirror. The two mirrors are positioned at right angles to each other and the two parts of the radius from the source are orthogonally directed and separated with a semi-transparent mirror (beamsplitter) with reflectivity equal to 50%. Once reflected, the two parts are recombined, but with different phases, since the displacement of the moving mirror causes a delay which in turn induces the out of phase of the fixed mirror. After recombination, only a certain wavelength will be enhanced with a peak, while the other will be deleted (Figure 1.8).

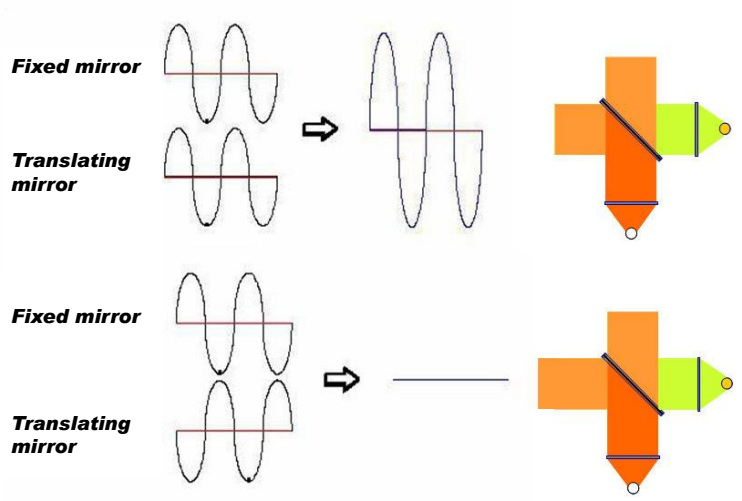

Figura 1.8: Generation of interference through the interferometer.

Therefore, the moving mirror is able to select all the wavelengths in a fixed range. The transmitted, diffused or reflected light reaches the detector, which sends a signal to the analog-digital converter that converts the signal into digital data which are then analyzed by a software that, applying the Fourier transform, translates the data into a spectral interferogram.
FT spectroscopy has the advantage to simultaneously analyze all frequencies; conversely, traditional spectroscopy, using the grating monochromator, sends to the detector a single wavelength at each time.

MIR Sample presentation systems (Settle, 1997)

It is possible to obtain an IR spectrum from samples in many different forms, such as liquid, solid, and gas. However, many materials are opaque to IR radiation and must be dissolved or diluted in a transparent matrix in order to obtain spectra. Alternatively, it is possible to obtain reflectance or emission spectra directly from opaque samples.
Liquid cells are used for dilute solutions of solid and liquid samples that are dissolved in relatively IR-transparent solvents. Sampling in solution results in enhanced reproducibility and is often the preferred choice. Unfortunately, no single solvent is transparent through the entire mid IR region, thus the analyst usually chooses solvents that have transparent windows in the region of interest.

Attenuated total reflectance (ATR) system

The development of FT-MIR instruments has been followed by the development of adequate sampling presentation techniques. Maybe one of the most interesting developments has been the introduction of simple reflectance techniques as the attenuated total reflectance (ATR) system.
Attenuated total reflectance (ATR) accessories are especially useful for obtaining IR spectra of difficult samples that cannot be readily examined by the normal transmission method. They are suitable for studying thick or highly absorbing solid and liquid materials, including films, coatings, powders, threads, adhesives, polymers, and aqueous samples. ATR requires little or no sample preparation for most samples and is one of the most versatile sampling techniques.

However, the ATR crystal absorbs energy at lower energy levels, and most of the used crystals have pH limitations. Moreover, there must be good contact between the sample and the crystal to be sure that the data obtained is accurate.
ATR occurs when a beam of radiation enters from a more-dense (with a higher refractive index) into a less-dense medium (with a lower refractive index). The fraction of the incident beam reflected increases when the angle of incidence increases. All incident radiation is completely reflected at the interface when the angle of incidence is greater than the critical angle (a function of refractive index). The beam penetrates a very short distance beyond the interface and into the less-dense medium before the complete reflection occurs. This penetration is called the evanescent wave and typically is at a depth of a few micrometers (μm). Its intensity is reduced (attenuated) by the sample in regions of the IR spectrum where the sample absorbs. Figure 1.9 illustrates the basic ATR principles.

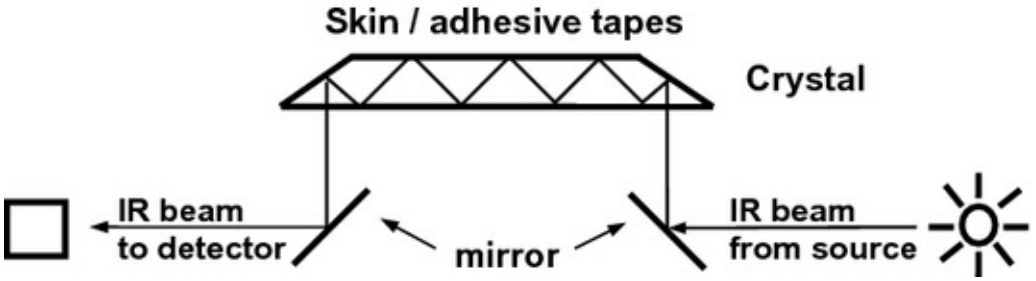

Figure 1.9: Schematic representation of multiple internal reflection effect in Attenuated Total Reflectance (ATR).

The sample is normally placed in close contact with a more-dense, high-refractive-index crystal such as zinc selenide, thallium bromide–thallium iodide, germanium, silicium or diamond. The IR beam is directed onto the beveled edge of the ATR crystal and internally reflected through the crystal with a single or multiple reflections. Both the number of reflections and the penetration depth decrease with increasing angle of incidence. For a given angle, the higher length-to-thickness ratio of the ATR crystal gives higher numbers of reflections. A variety of types of ATR accessories are available, such as 25 to 75° vertical variable-angle ATR, horizontal ATR, and Spectra-Tech Cylindrical Internal Reflectance Cell for Liquid Evaluation (CIRCLE®) cell.
Diffuse reflectance technique is mainly used for acquiring IR spectra of powders and rough surface solids such as coal, paper, and cloth. It can be used as an alternative to pressed-pellet or mull techniques.

Diffuse reflectance infrared Fourier transform spectroscopy (DRIFTS)

IR radiation is focused onto the surface of a solid sample in a cup and results in two types of reflections: specular reflectance, which directly reflects off the surface and has equal angles of incidence and reflectance, and diffuse reflectance, which penetrates into the sample, then scatters in all directions. Special reflection accessories are designed to collect and refocus the resulting diffusely scattered light by large ellipsoidal mirrors, while minimizing or eliminating the specular reflectance, which complicates and distorts the IR spectra. This energy-limited technique was not popular until the advent of FTIR instruments. This technique is often called diffuse reflectance infrared Fourier transform spectroscopy (DRIFTS).

The sample can be analyzed either directly in bulk form or as dispersions in IR-transparent matrices such as KBr and KCl. Dilution of analyte in a nonabsorbing matrix increases the proportion of diffuse reflectance in all the light reflected. Typically the solid sample is diluted homogeneously to 5 to 10% by weight in KBr. The spectra are s plotted in units such as log 1/*R* (*R* is the reflectance) or Kubelka–Munk units. The Kubelka–Munk format relates sample concentration to diffuse reflectance and applies a scattering factor.

MIR detectors (Settle, 1997)

The two most popular detectors for a FTIR spectrometer are deuterated triglycine sulfate (DTGS) and mercury cadmium telluride (MCT). The response times of many detectors (for example, thermocouple and thermistor) used in dispersive IR instruments are too slow for the rapid scan times (1 sec or less) of the interferometer. The DTGS detector is a pyroelectric detector that delivers rapid responses because it measures the changes in temperature rather than the value of temperature. The MCT detector is a photon (or quantum) detector that depends on the quantum nature of radiation and also exhibits very fast responses. Whereas DTGS detectors operate at room temperature, MCT detectors must be maintained at liquid nitrogen temperature (77 °K) to be effective. In general, the MCT detector is faster and more sensitive than the DTGS detector.

MIR advantages

MIR spectroscopy rapidly provides information on a very large number of analytes, and the absorption bands are sensitive to the physical and chemical states of individual constituents. Table 1.1 illustrated some advantages and drawbacks of MIR. The high spectral signal-to-noise ratio obtained from modern instrumental analysis, as when using the Fourier transform infrared (FT-MIR) spectroscopy, allows the detection of constituents present in low concentrations, as well as subtle compositional and structural differences between and among multi-constituent specimens (Da-Wen Sun, 2008). MIR spectroscopic methods, and particularly FT-MIR spectroscopy, can be considered routine applications among standard laboratory techniques and can a molecular fingerprinting method (Baeten et al. ,2000; Baeten & Dardenne, 2002 Mazarevica et al., 2004).

Advantages	Drawback
Reliesen part of the spectrum that contains fundamental vibrations.	The available energy decreases with wavelength.
Useful for qualitative and quantitative identification of functional groups.	Expensive transmitting materials.
Characteristic and well defined bands for organic functional groups.	Cells need to have short effective pathlength, since most of the material absorb in this region.
Unknown species can be identified.	

Table 1.1: Advantages and drawbacks of MIR spectroscopy.

NIR Sample presentation systems (Burns & Ciurczak, 2001)

When a sample is exposed to radiation, interaction with matter can be occur in several ways: the light can be absorbed by the sample, reflected, and in part or completely transmitted through the sample (Figure 1.10).

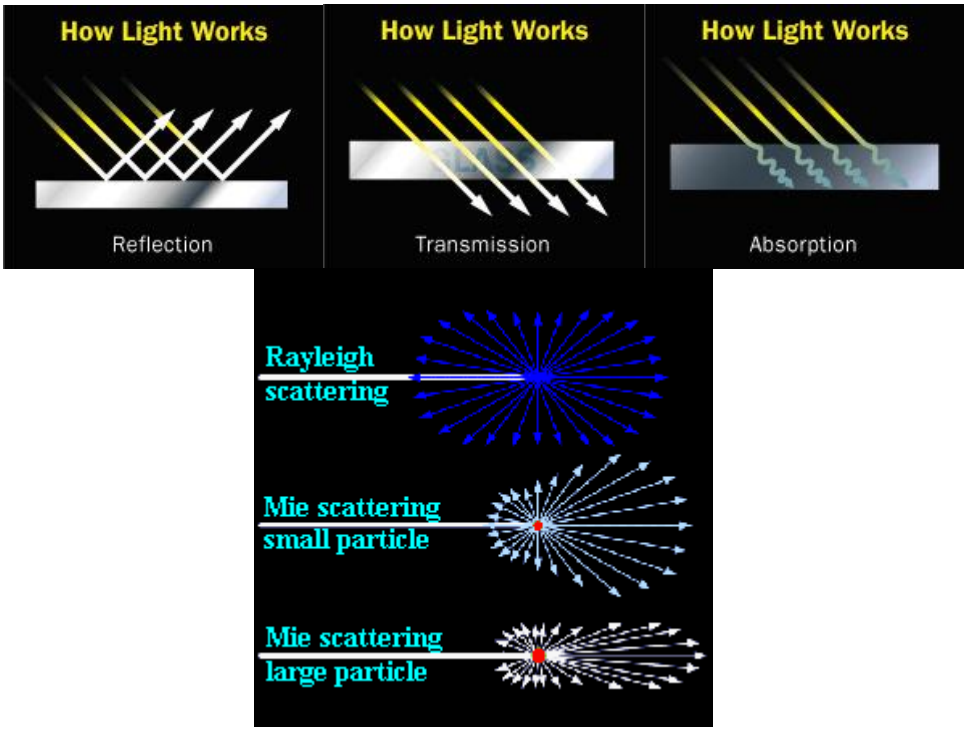

Figure1.10: Light and matter interaction modes

The mode and the degree to which these effects occur depends on the physical state of the sample and the reading system used. The radiation transmission systems are mainly used for liquid samples or for thin layers solids, while the reflection mode is most useful for solid samples. If the sample does not reflect or transmit radiation well enough, the transflectance can be used as a measuring parameter. In this mode, the radiation penetrates the sample, part is absorbed, the rest is then reflected on a non-absorbent surface on the bottom of the cell and re-transmitted through the sample to the detector. Several types of presentation systems are currently available, strictly dependent on the construction technology.

Fiber-optics

NIR instrumentation is a growing field, thanks to the development of optical fibers that allow the direct and simple acquisition of spectra by placing the tip of the fiber on the surface and / or inside the sample. The fibers can have two different optical geometries: diffuse reflectance fibers (for solid matrices) and transmission fibers (for liquid matrices). The operating principle of diffuse reflectance fibers is illustrated in Figure 1.11: the radiation beam from the NIR source strikes the sample, the fraction not absorbed by the sample is reflected and reaches the detector.

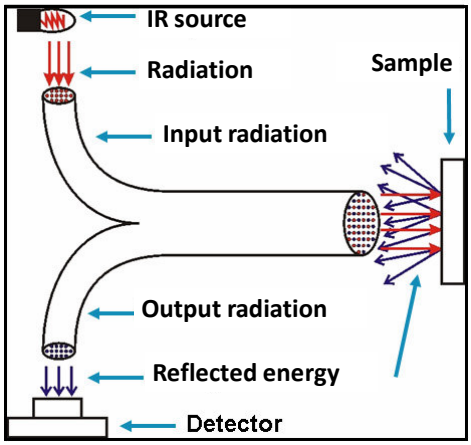

Figura 1.11: Operating principle of diffuse reflectance fiber optic.

In fiber transmission (Figure 1.12), the light beam strikes the sample, passes through it and it is collected by the detector. In this optical geometry light passes through the sample once.

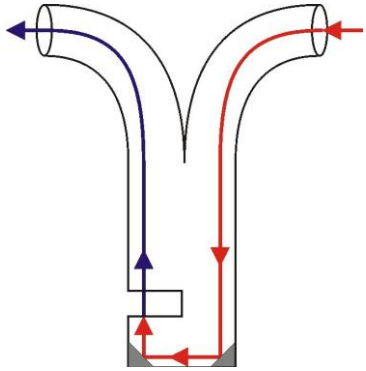

Figure 1.12: Operating principle of transmission optical fiber.

Optical fibers withstand stressful environmental conditions, are easily integrated into machines and allow conveying the signal unchanged for tens of meters, permitting the centralization of the measurement devices into a single structure. Moreover, the use of optical fiber, positioned directly on the sample surface, allows for non-invasive, non destructive and in line measurements.

Integrating sphere

For measurements on heterogeneous solid samples, the most suitable sampling system is integrating sphere, whose operating principle is illustrated in Figure 1.13.

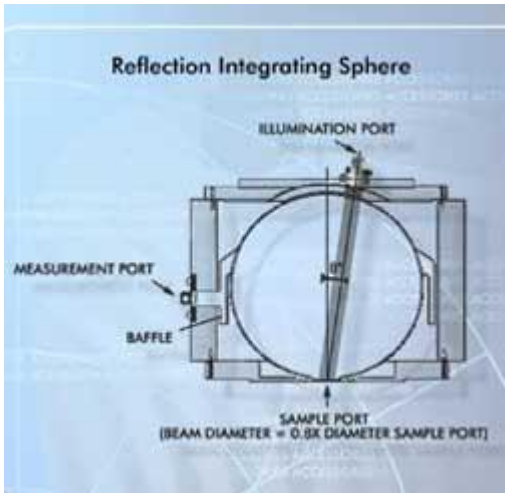

Figure 1.13: Operating principle of the integrating sphere

The radiation strikes a mirror outside the sphere which in turn directs the radiation to the sample. The part of radiation not absorbed by the sample is reflected back to the inner surface of the sphere to be collected by the detector. The sample is usually collected in a container with a bottom transparent to radiation and equipped with a geometry that allows the rotation of the sample, which is necessary when working with non-homogeneous samples.

Scanning transmission system for solids

Although transmission systems are mainly used for liquid samples or for thin layers of solids, it is possible to scan solid samples in transmission mode. In this case, the light beam strikes the sample, passes through it and it is collected by the detector. This sampling technique is used to measure the whole mass of the sample, especially to determine hardness or composition.
Table 1.2 shows the advantages and disadvantages between diffuse reflectance and transmission measurements on solid samples. As the table shows, diffuse reflectance measurements allow to work on the whole spectral range and therefore to have information on combination bands and overtone spectral region, while transmission measurements, characterized by a low energy, allow to acquire spectra in a smaller range of wavelengths.

Diffuse reflectance measurements	Ttransmission measurements
High energy	Low energy due to the high sample absorption
The analysis requires sample homogeneity (the surface should be representative of the whole mass of the sample)	The whole mass of the sample is measured
Analysis lasting from 1 to 30 seconds	Analysis lasting from 10 seconds to 2 minutes
Whole spectral range: from 12500 to 3600 cm^{-1} (800-2780 nm)	Reduced spectral range: from 12500 to 7000 cm^{-1} (800-1400 nm)
Combination bands and overtone working zone	Overtone bands working zone
Usually applied to samples surface (coatings etc.)	Usually applied to the sample core (hardness or composition etc.)

Table 1.2: Comparison between diffuse reflectance and transmission measurements.

NIR detectors (Burns & Ciurczak, 2001)

The most characteristic element for the instrument is the detector. Its task is to receive the radiation from the sample and turn it into an electrical signal. The detector must be sensitive to the wavelength of interest: generally sulphide or lead selenide detector are used for the spectral region between 1100 and 2500 nm and silicon detectors for the NIR region at short length (SWNIR) between 400 and 1100 nm. Most applications of the NIR technique are intended to obtain the spectrum of a sample, i.e. the graphical representation of absorbance or transmittance as a function of wavelength or wavenumber. An additional request is the ability of the tool to acquire a white or a background to subtract from the sample spectrum. This can be done before the scan or, in some cases, i.e. in dual-beam instruments, continuously and simultaneously with the reading.

NIR advantages (Burns & Ciurczak, 2001)

The practical advantages offered by FT-NIR are:
• Improved signal to noise ratio. The high value of this ratio allows the well resolved spectra with fast scans in few seconds
• Less energy loss and hence a greater energy to the detector. The optics of the FT-NIR in fact allows to have a passing energy greater than that of dispersive instruments, where the available energy is limited by the need of the use of splits.
• Improved accuracy and precision in the wavelengths discrimination.
• Increased speed of spectra collection.

1.1.3. References

Burns DA, Ciurczak EW Handbook of near-infrared analysis**.** Burns DA, Ciurczak EW eds, CRC Press, Marcel Dekker Inc, New York, 2001

Da-Wen Sun Infrared Spectroscopy for Food Quality Analysis and Control. Da-Wen Sun ed, Academic Press, Elsevier Inc, USA, 2008.

Siesler HW Near-infrared spectroscopy: principles, instruments, applications. Siesler HW, Ozaki Y, Kawata S, Heise HM eds, John Wiley & Sons, Weinheim, Germany, 2002.

Workman J, Weyer L Practical guide to interpretive near-infrared spectroscopy CRC Press, Taylor & Francis Group, New York, 2008

1.2 The casein

1.2.1 Milk and milk proteins

Milk is the characterizing secretion of mammals, produced to meet the complete nutritional requirements of the neonate of the species, as well assume defensive and other physiological requirements. Milk is an aqueous solution of lactose, inorganic and organic salts, and numerous compounds at trace levels (milk serum), in which are dispersed colloidal particles of three size ranges: whey proteins dissolved at the molecular level, caseins dispersed as large (50–500 nm) colloidal aggregates (micelles) and lipids emulsified as large (1–20 μm) globules (Walstra, 2006).
The properties of milk and most dairy products are affected more by the proteins they contain than by any other constituent. The milk proteins also have many unique properties; because of their technological importance, the milk proteins have been studied extensively and are probably the best characterized food protein system (Walstra, 2006).
Approximately 3.0-3.5% of normal bovine milk is made up of protein; the concentration and composition of which can change during lactation. The function of milk is to supply essential amino acids that are required for the development of muscular and other protein-containing tissues in young mammals and also for biological by active proteins providing immunoglobulins, vitamin-binding and metal-binding proteins and several protein hormones (Fox & McSweeney, 1998). In addition, milk proteins also play a very important role in dairy and food products, e.g. during processing, including undesirable behavior such as fouling on heated surfaces and gelling inside process equipments (Sawyer et al., 2002).
Originally, milk proteins were believed to be a simple homogeneous protein, but since a century or more ago, milk proteins were divided into two broad classes (Fox & McSweeney, 1998). The first fraction, which is about 80% of the protein in bovine milk, is precipitated at pH 4.6 (isoelectric pH) at 30ºC, and is now called casein. The second minor fraction, makes up about 20% of protein, is soluble under those conditions, and is now referred to as whey protein or serum protein or non-casein nitrogen (Dalgleish, 1982; Fox & McSweeney, 1998).
In addition to, milk contains trace fractions of glycoproteins (Walstra et al., 1999) and two other groups of proteinaceous materials, proteose peptones (PPs) and non-protein nitrogen (NPN).

1.2.2 **Caseins** (Thompson et al., 2008)

The caseins are phosphoproteins and constitute about 80% of the protein in milk (Swaisgood, 2003). They are assembled in a colloidal complex with calcium phosphate and small amounts of other minerals. Although obviously important for the provision of amino acids, calcium and phosphorus for infant nutrition, the casein micelle structure is also critical in determining the physical properties of milk.

Molecular properties of casein

- **Solubility at pH 4.6**. The caseins are insoluble at pH 4.6. The isoelectric precipitation of casein is exploited in the production of caseins and caseinates, fermented milk products and acid-coagulated cheeses.
- **Coagulability** following limited proteolysis. The caseins are coagulable (clotted) following specific, limited proteolysis. This property of the caseins is exploited in the production of rennet-coagulated cheese and rennet casein.

- **Heat stability**. The caseins have a high thernostability. Milk at pH 6.7 may be heated at 100ºC for 24 h without coagulation and withstands heating at 140ºC for up to 20–25 min; aqueous solutions of sodium caseinate may be heated at 140ºC for several hours without apparent changes. The high thermostability of caseins, which is probably due to their lack of typical stable secondary and tertiary structures, allows the production of heat-sterilized dairy products with relatively small physical changes. The lack of stable tertiary structures means that the caseins are not denaturable *stricto senso* and, consequently, are extremely heat stable; sodium caseinate, at pH 7, can withstand heating at 140ºC for several hours without visible change.
- **Amino acid composition**. Caseins are hydrophobic; they have a fairly high charge, many proline (17% of all residues in β -casein), and few cysteine residues. They do not form anything more than short lengths of α-helix and have slight tertiary structure. This does not imply that the casein molecules are random coils, though in dilute solution the chains are partly unfolded. The caseins are phosphorylated. Whole isoelectric casein contains approximately 0.8% phosphorus, but the degree of phosphorylation varies among the individual casein fractions. The phosphate is attached to the polypeptides as phosphomonoesters of serine: the presence of phosphate groups has major significance for the casein properties, e.g., (i) molecular charge and related properties and heat stability; and (ii) metal binding which affects their physico-chemical, functional and nutritional properties. Metal binding by casein is regarded as a biological function because it enables a high concentration of calcium phosphate to be carried in milk in a soluble form.

  The caseins lack stable secondary structures; classical physical measurements indicate that the caseins are unstructured, but theoretical considerations indicate that, rather than being unstructured, the caseins are very flexible molecules and have been referred to as rheomorphic (Holt & Sawyer, 1993; Horne, 2002; Farrell et al., 2006). The inability of the caseins to form stable structures is due mainly to their high content of the structure-breaking amino acid proline; β -casein is particularly rich in proline, with 35 of the 209 residues. Casein is very susceptible to proteolysis, which facilitates their natural function as a source of amino acids, due to its open and flexible structure.

  The caseins are generally regarded as very hydrophobic proteins but, with the exception of β -casein, they are not exceptionally hydrophobic. Because of their lack of stable secondary and tertiary structures, most of their hydrophobic residues are exposed and, consequently, they have a high surface hydrophobicity.

  One of the more notable features of the amino acid sequence of the caseins is that the hydrophobic and hydrophilic residues are not distributed uniformly, thereby giving the caseins a distinctly amphipatic structure.

  This feature, coupled with their open flexible structure, gives the caseins good surface activity, and good foaming and emulsifying properties, making casein the functional protein used for many applications.

  Also because of their open structure, the caseins have a high specific volume and, consequently, form highly viscous solutions, which is a disadvantage in the production of caseinates.

  The caseins are low in sulfur (0.8%). The sulfur in casein is mainly due to the methionine presence, with little amount of cystine or cysteine; the principal caseins are devoid of the latter two amino acids.
- **Physical state in milk**. The caseins have a very strong tendency to associate, due mainly to hydrophobic bonding. Even in sodium caseinate, the most soluble form of casein, the molecules form aggregates of 250–500 kDa, i.e. containing 10–20 molecules. This strong tendency to associate makes it difficult to fractionate the caseins, for which a dissociating

agent, e.g. urea or SDS, is required. On the other hand, a tendency to associate is important for some functional applications and in the formation and stabilization of casein micelles. In contrast, the whey proteins are molecularly dispersed in solution. The high charge of casein is partly caused by the phosphate groups. These are for the most part esterified to serine residues; near the pH of milk they are largely ionized. The groups strongly bind divalent ions like Ca^{2+}, especially at a higher pH. This property has many major consequences; the most important from a technological viewpoint is that proteins are insoluble at calcium concentrations > 6 mM at temperatures > 20°C. As bovine milk contains = 30 mM calcium, one would expect that the caseins would precipitate under the conditions prevailing in milk. However, κ -casein, which contains only one organic phosphate group, binds calcium weakly and is soluble at all calcium concentrations found in dairy products. Furthermore, when mixed with the calcium-sensitive caseins, κ -casein can stabilize and protect = 10 times its mass of the former by forming large colloidal particles called casein micelles. The micelles act as carriers of inorganic elements, especially calcium and phosphorus, but also magnesium and zinc, and are, therefore, very important from a nutritional viewpoint. Through the formation of micelles, it is possible to dissolve much higher levels of calcium and phosphate than would otherwise be possible.

Table 1.3 summarizes the principal properties of caseins.

Properties	Caseins			
	α_{s1}	α_{s2}-	β-	κ-
MW	23612	25228	23980	19005
Residues	199	207	209	169
Conc in milk (g/L)	12–15	3–4	9–11	2–4
Phosphate residues	8–9	10–13	4–5	1–2
½ Cystine	0	2	0	2
Sugars	0	0	0	Yes
Prolyl residue per molecule	17	10	35	20
A_{280}, 1% 1 cm	10.1	11.1	4.6	9.6
Secondary structure	Low	Low	Low	Low
$H\phi_{ave}$	4.89	4.64	5.58	5.12
pI	4.96	5.27	5.20	5.54
Partial specific volume (ml/g)	0.728	0.720	0.741	0.734

Table1.3: Casein properties

Heterogeneity and fractionation of casein (Walstra et al., 1999)

Several different caseins occur in milk, but their separation is not easy. It was only after electrophoresis came into use that resolution of the caseins was feasible. Currently, the complete primary structures are known. This has revealed that there are four different peptide chains, αs1, αs2, β, and κ, of which the molar ratio is about 11:3:10:4. Differences in phosphorylation and glycosylation, as well as some proteolysis, cause additional heterogeneity.

α_s1-Casein

α_s1-Casein has a high net negative charge and a high phosphate content. α_s1-Casein associates in two steps at pH 6.6 and 0.05 M ionic strength. Reducing the ionic strength, and increasing the range of the electrostatic repulsion, the association decreases. Hydrophobic interactions are also involved in the association. At higher pH, the association decreases and eventually disappears, even if casein concentration and ionic strength are high. A variant that occurs in small amounts has nine rather than eight phosphate groups.

α_s2-Caseins

Some variants of this protein exist. They differ in the number of ester phosphate groups, i.e., 10 to 14 per molecule. α_s2-Casein fractions contain two cysteine residues (forming an –S–S– bridge) and no carbohydrate groups. They are rather Ca^{2+} sensitive. The association pattern is similar to that of α_s1-Casein.

β-Casein

β-Casein is the most hydrophobic casein, and it has a large number of proline residues. Its charge is irregularly distributed and this make β-Casein like a soap molecule, with a polar 'head' and a long-chain, apolar 'tail.' The association of β-Casein in micelles, which usually comprises some 20 or 30 molecules, doesn't occur below 5°C and the molecule remains unfolded. In milk, part of the β-casein goes into solution at low temperature, thereby increasing the viscosity of the milk.

κ-Casein

κ-Casein greatly differs from the other caseins. It has two cysteine residues that form intermolecular disulfide bonds. Because of this, κ–Casein is present in milk as oligomers containing 5 to 11 monomers, with an average MW (Molecular Weight) about 120 kDa. About two thirds of the (monomeric) molecules contain a carbohydrate group, which is esterified to one of the threonines (131, 133, 135, or 142) and has galactosamine, galactose, and one or two N-acetyl neuraminic acid (NANA or *o*-sialic acid) residues. These groups are hydrophilic. Some other, minor configurations occur as well. This so-called microheterogeneity always occurs, even within individual milking of one cow. The peptide bond between residues 105 and 106 is rapidly hydrolyzed by proteolytic enzymes. κ-Casein also strongly associates to yield micelles that contain over 30 molecules including protruding carbohydrate groups.

1.2.3 Casein micelles

It has been known, since the work of Schuler in 1818, that almost all casein in fresh uncooled milk is present in roughly spherical particles, mostly 40 to 300 nm in diameter, called casein micelles. The micelles are voluminous, holding more water than dry matter and they have a negative charge. Casein micelles also contain inorganic matter, mainly calcium phosphate, about 8 g per 100 g of casein and also small quantities of some other proteins, such as part of the proteose peptone and certain enzymes. The stability of the micelles is critically important for many of the technologically important properties of milk and consequently has been the focus of many researches, especially during the past 50 years.

Electron microscopy shows that casein micelles are not quite spherical particles with a bumpy surface and a diameter in the range 50–500 nm (average = 120 nm) and a mass ranging from 10^6 to 3 x 10^9 Da (average = 10^8 Da). There are 10^{14} –10^{16} micelles/mL of milk, and they are roughly two micelle diameters (= 250 nm) apart. They scatter light, and the white color of milk is due largely to light scattering by the casein micelles.

Properties of casein micelles (Fox & McSweeney, 1998)

There are some observations relevant for micelle structure:
• In a solution of whole casein in (simulated) milk ultra-filtrated, association occurs as well; the small aggregates show mixed composition. If calcium and phosphate ions are slowly added at constant pH to such a solution, it becomes white, and shows particles that look just like native casein micelles.
• In the lactating cell, it is seen that most of the Golgi vesicles contain many small particles, about 15 nm in size, whereas in other vesicles these particles have apparently aggregated into casein micelles.
• The micelles show high variability in size distribution. Authors do not fully agree about the size distribution. In early-lactation milk, a small number of very large micelles are found, with a diameter up to 600 nm. Variations between the micelles of one milking of one cow and variations between different lots of milk, from different cows, are to be noticed. Different cows produce milk with a different particle size distribution. The protein composition is also variable. In particular, the proportion of κ-Casein varies, since it largely determines the casein micelle size.
• After determination of the casein micelle composition with different diameters, it has been calculated that the core of a micelle consists of roughly equal amounts of αs- and β-Casein, with a very little amount of κ-Casein, whereas the outer layer appears to consist of about equal amounts of κ- and α_s-Casein, and very little quantity of β-Casein. The κ-Casein concentration is nicely proportional to the specific surface area of the micelles.
• The micelle shows a 'hairy layer,' consisting of the C-terminal end (about 75 amino acid residues) of κ-Casein. (The cross-links between the molecules are in the N-terminal part). The hairs are quite hydrophilic and are negatively charged; they also contain the carbohydrate moieties of κ-Casein. The hydrodynamic thickness of the layer is about 7 nm. The layer is essential in providing colloidal stability.
• Nearly all of the κ-Casein is present in the form of polymers of 2 to 9 (average about 6) molecules, linked to each other by –S–S– bridges.
• The forces keeping the structural elements of a micelle together are, at least at physiological conditions, hydrophobic bonds between protein groups and cross-links between peptide chains by the nano-clusters. Probably, ionic bonds are also involved.
• NMR studies have shown that the protein molecules in a casein micelle are almost fully static, except for the hairs, which will show continuous Brownian motion. This concerns immobility at very short timescales (on the order of nanoseconds). At longer timescales, molecules can move in and out of a micelle.
• Nano-clusters of calcium-phosphate of about 3nm diameter are present. The clusters contain the inorganic phosphate and much of the calcium in the micelles (the CCP), but also the organic phosphate of the SerP residues, and probably some glutamic acid residues.

Micelle structure

Due to the importance of casein and casein micelles for the functional behavior of dairy products, the nature and structure of casein micelles have been studied extensively, but the exact structure of casein micelles is still under debate. Various models for casein micelle structure have been proposed (Brunner, 1977; Brule et al., 2000). There has been speculation since the beginning of the twentieth century on how the casein particles (micelles) are stabilized (Fox & Brodkorb, 2008). The first attempt to describe the structure of the casein micelle was made by Waugh in 1958 and, since then, numerous models have been made and refined. (Rollema, 1992 ; Holt & Horne, 1996 ; Horne, 1998; Walstra, 1999; Horne, 2002)
The most commonly accepted model in the sub-micelle model category was proposed by Walstra in 1984 (Rollema, 1992). This model suggests that casein micelles are built of roughly spherical subunits or sub-micelles. The composition of sub-micelles is variable and the size is in range 12-15 nm in diameter, and each sub-micelle has 20-25 casein molecules. The sub-micelles are kept together by hydrophobic interactions between proteins, and by calcium phosphate linkages. There are two main types of sub-micelles; one mainly consisting of αs- and β-Caseins, hydrophobic regions buried in the center of the sub-micelle, another type consisting of αs- and κ-Caseins, which is more hydrophilic because of the sugar residues on κ-Caseins. The κ-Caseins are located near the outside of the micelle with the hydrophilic part of the C-terminal end protruding from the micelle surface to form a 'hairy' layer that will avoid further aggregation of sub-micelles by steric and electrostatic repulsion. Consequently, micelles are stable, and they do not usually flocculate (Walstra, 1999; Walstra et al., 1999). Figure 1.14 shows the structure of casein micelles from the sub-micelles model.

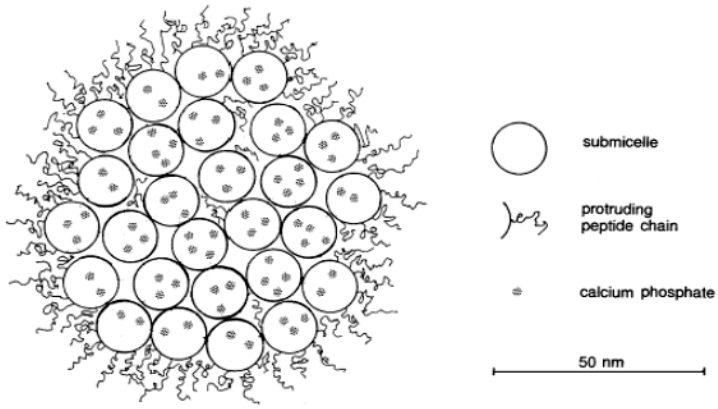

Figure 1.14: Casein sub-micelles model

Although the sub-micelles casein model as extended by Walstra (Walstra, 1999) has been widely accepted, two alternative models, which fall into internal structure category, have been proposed by Holt in 1992 (Holte, 1992) and by Horne (Horne, 1998). Holt delineated the casein micelle as a tangled web of flexible casein networks forming a gel-like structure with micro-granules of colloidal calcium phosphate through the casein phosphate center, and the C terminal region of κ-Casein extends to form a hairy layer (Figure…). The two main features of this model are the cementing role of colloidal calcium phosphate and the surface location of hairy layer of κ-Casein. In addition, casein micelles are stabilized by two main factors, which are a surface (zeta) potential of approximately -20mV at pH 6.7,and steric stabilization owing to the

protruding κ-Casein layer hairs (Holt, 1994; Holt & Horne,1996; Fox & Mc Sweeney, 1998). Furthermore, the dual bonding model of Horne (Horne, 1998), which fits into the category of internal structure models, was proposed.

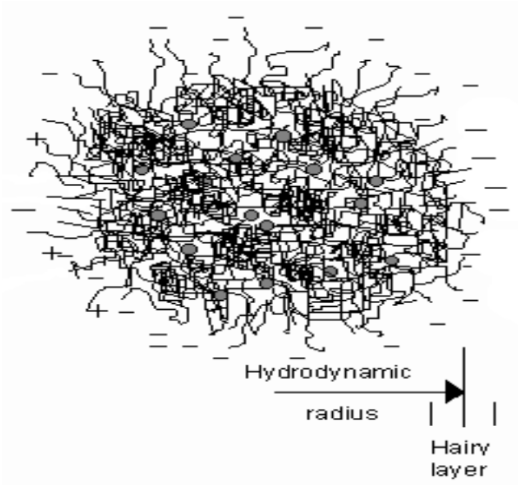

Figure 1.15: Hairy casein micelle model proposed by Holt, where a tangled web and open structure of polypeptide chains cross-linked by calcium phosphate nanocluster (colloidal calcium phosphate) in the core provides rise to an external region of lower segment density known as the hairy layer. The gray circles represent the calcium phosphate nanoclusters. (Source: http://www.foodsci.uoguelph.ca/deicon/casein.html)

This model suggests that the proteins in casein micelles are bound together by two types of bonding and it is a balance between the attractive hydrophobic interactions and electrostatic repulsion. Hydrophobic interaction is the driving force for the formation of casein micelles, while electrostatic repulsions are limiting the growth of polymers or in other words defining the degree of polymerization. The conformation of αs1- and β-Caseins when they are adsorbed at hydrophobic interfaces forms train-loop-train and a tail-train structure, respectively and both caseins polymerize or self-associate, by hydrophobic interactions. Accordingly, the self-association of caseins makes it possible for polymerization to occur. Calcium phosphate nano-clusters, or CCP, are considered to be one of the linkages between casein micelles and neutralizing agents of the negative charge of the Pserine residues by binding to those residues; consequently, electrostatic repulsion is reduced, and the hydrophobic interaction between caseins is still dominant, resulting in more associations of proteins. Unlike other caseins, κ-Caseins can only interact hydrophobically and acts as a propagation terminator, because they do not have a Pserine cluster to bind calcium and also another hydrophobic point to prolong to chain. The dual bonding model for the casein micelle structure is shown in Figure 1,16. The αs-, β-, and κ-Caseins are shown as indicated. Bonding between caseins first takes place in the hydrophobic regions, shown as rectangular bars, and also the linkage between CCP and Pserine residues of casein molecules. κ-Caseins limit further growth (Horne, 1998).

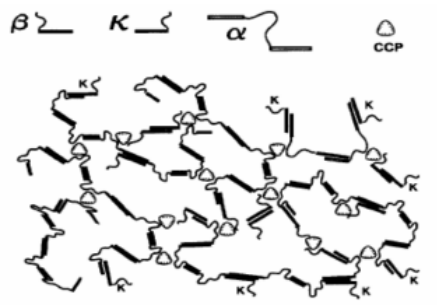

Figure 1.16: The dual bonding model of casein micelle structure, with α-, β-, κ-casein portrayed as indicated. (Source: Horne, 1998)

Micelle stability (Thompson et al., 2008)

During milk storage, the casein micelles slowly alter, because there is no thermodynamic equilibrium between the micelles and their surroundings. The main change probably is proteolysis of β-Casein into γ-Casein and proteose peptone by plasmin. From a physicochemical point of view, micelles are not stable because the colloidal phosphate is not in the stablest form. The phosphate thus will be converted to stabler phosphates (octa calcium phosphate or hydroxyapatite), associated with the casein in another way, or in the form of a precipitate that is separated from the micelles.
Furthermore, the casein micelles will alter during changes in the external conditions, especially temperature and pH. Some of these alterations are reversible, whereas others are not or partly so.

Dynamic equilibria

A casein micelle and its surroundings keep exchanging components. Part of the mineral compounds exchanges the fastest. Some of the components of the colloidal phosphate, including Ca, phosphate, and citrate, also exchange fairly rapidly. Casein can diffuse in and out of each micelle, presumably mainly in the form of submicelles, and the equilibrium situation depends on such factors as temperature and pH. Casein micelles can be broken up to smaller units by mechanical forces, e.g., by very intensive homogenization; the formed fragments then rapidly reaggregate into the original size distribution.

Low temperature

By lowering the temperature, dissolution of a considerable part of the β-Casein occurs. The main reason of the dissolution of β-Casein is that the hydrophobic bonds, which are predominantly responsible for its binding, are much weaker at low temperature. Other caseins will dissolve as well, although to a lesser extent (α_s-Caseins least). Proteolytic enzymes can far better attack casein in a dissolved state. Because of this, for example, β-Casein is fairly rapidly converted by plasmin at low temperature. The size of the micelles increases markedly at low temperature. This increase should be partly ascribed to the formation of another category of hairs. In addition to some β-Casein molecules going into solution, others may be loosened so that β-Casein chains now may protrude from the core surface of the micelles.

Collapse of micelles upon cooling may also be due to dissolution of a part of the CCP. In fact, the association of Ca^{2+} ions with caseins decreases with decreasing temperature. The loss of CCP presumably causes a weaker binding of individual casein molecules in the micelles. Consequently milk viscosity increases significantly. The colloidal stability of the casein micelles is definitely greater; consequently, the milk shows poor rennet ability during cheese making. All of these changes do not occur immediately on cooling, but they take some 24 h at 4°C before being more or less completed.

High Temperature

Micelles are quite stable to the principal thermal processes to which milk is normally subjected. On increasing the temperature, the micelles shrink somewhat and the amount of colloidal phosphate increases with different properties as the natural phosphate. At temperatures above 70°C the casein molecules become more flexible, as if part of the micelle structure melts. At still higher temperatures (above 100°C), dissolution of part of the κ-Casein occurs. The extent closely depends on pH; no dissolution occurs below pH 6.2, but there is almost complete dissolution at pH 7.2. This is due to the increased effect of entropy at high temperature and also to the absence of serine phosphate in the part of the κ-Casein chain that is inside the micelle. However, micelle-like particles remain at high temperatures, even at 140°C. Serum proteins become largely associated with the casein micelles during their heat denaturation, and they largely become bound to the micelle surface. The association should at least partly be ascribed to formation of –S–S– linkages. An example is the association of β-lactoglobulin with κ-Casein. Most of these associations are irreversible on cooling.

Acidity

The colloidal phosphate goes into solution, with a complete dissolution at pH 5.25. Removal of all of the calcium requires a still lower pH, i.e., until below the isoeletric pH of casein. On further decrease of the pH, the negative charge of casein increases, due to dissociation of the calcium ions from the micelles, and eventually decreases again, due to association with H+ ions. At still lower pH, casein becomes positively charged. Furthermore, lowering the pH leads at first to swelling of the particles and eventually to considerable shrinkage. When the pH is lowered to 5.3, a large part of the caseins goes into 'solution'. The average particle size changes little in the considered pH region. At physiological pH, it is primarily the colloidal calcium phosphate that keeps the micelles unbroken. When the pH is lowered, the phosphate dissolves, resulting in increasingly weaker bonds. Consequently, swelling of the micelles occurs, along with dissolution of part of the casein. At low pH, internal salt bridges between positive and negative groups on the protein keep the molecules together. Milk pH increasing causes swelling of the micelles and their eventual disintegration. Presumably, the colloidal phosphate passes into another state.

Disintegration

Weakening of the bonds between the sub-micelles or those between protein molecules in the sub-micelles can lead to micelles disintegration. The former may be due to dissolution of the colloidal phosphate at constant pH, e.g., by adding an excess of a Ca binder like citrate, EDTA, or oxalate. The second type of disintegration occurs by addition of reagents like sodium dodecyl sulfate or large urea amounts, which break hydrogen bonds and/or hydrophobic interactions.

Reagents that break –S–S– linkages do not disintegrate the micelles, but it is not known if less rigorous changes occur.

Salts

The typical concentrations of the principal macro-elements of milk are shown in Table 1.4.
Although the salts are relatively minor constituents of milk, they are critically important for many technological and nutritional properties of milk.
Some of the salts in milk are fully soluble but others, especially calcium phosphate, exceed their solubility under the conditions in milk and occur partly in the colloidal state, associated with the casein micelles; these salts are referred to as CCP, although some magnesium, citrate and traces of other elements are also present into the micelles. CCP plays a critical role in the structure and stability of the casein micelles. The solubility and the ionization status of many of the principal ionic species are interrelated, especially H^+, Ca^{2+}, PO_4^{3-} and citrate^{3-} . These relationships have major effects on the stability of the caseinate system and consequently on the technological properties of milk. The status of various species in milk can be modified by adding certain salts to milk, e.g. the Ca^{2+} concentration is reduced by adding PO_4^{3-} or citrate^{3-}; addition of $CaCl_2$ affects the distribution and ionization status of calcium and phosphate, and the milk pH .

Species	Concentration (mg/l)	%	Soluble form	Colloidal
Sodium	500	92	Completely ionized	8
Potassium	1450	92	Completely ionized	8
Chloride	1200	100	Completely ionized	—
Sulfate	100	100	Completely ionized	—
Phosphate	750	43	10% bound to Ca and Mg 54% $H_2PO_4^-$ 36% HPO_4^{2-}	57
Citrate	1750	94	85% bound to Ca and Mg (undissociated) 15% $Citr^{3-}$	6
Calcium	1200	34	35% Ca^{2+} 55% bound to citrate 10% bound to phosphate	66
Magnesium	130	67	Probably similar to calcium	33

Table 1.4: Concentration of the principal macro-elements of milk.

The simplest stoichiometry is $Ca_3(PO_4)_2$ but spectroscopic data suggest that $CaHPO_4$ is the most likely form. The distribution of species between the soluble and colloidal phases is strongly affected by pH and temperature. As the pH is reduced, CCP dissolves and is completely soluble at pH<= 4.9; the reverse occurs when the pH is increased. The solubility of calcium phosphate decreases as the temperature is increased and soluble calcium phosphate is transferred to the colloidal phase, with the release of H^+ and a decrease in pH.
There are substantial changes in the concentrations of the macro-elements in milk during lactation, especially at the beginning and at the end of lactation and during mastitic infection. Changes in the concentration of some salts in milk, especially calcium phosphate and citrate, have major effects on the physico-chemical properties of the casein system and on the processability of milk, especially rennet coagulability and related properties and heat stability.

Other agents and treatments

The micelles are stable to compaction (e.g. they can be sedimented by ultracentrifugation and re-dispersed by mild agitation), to commercial homogenization and to Ca^{2+} concentrations up to at least 200 mM at temperatures up to 50ºC. The effects of high pressure (up to 800 MPa) on the casein micelles in bovine, ovine, caprine and buffalo milks have been studied; the size of the micelles increases up to 200–300 MPa but decreases at higher pressure (Huppertz et al., 2006).
Some proteinases, especially chymosin, catalyze a very specific hydrolysis of κ-Casein, as a result of which the casein coagulates in the presence of Ca^{2+} or other divalent ions. This is the key step in the manufacture of most cheese varieties. The proteinase preparations used for cheesemaking are called rennets. At room temperature, the casein micelles are destabilized by = 40% ethanol at pH 6.7 or by lower concentrations if the pH is reduced. However, if the system is heated to $\geq$ 70ºC, the precipitate re-dissolves and the system becomes translucent. When the system is re-cooled, the white appearance of milk is restored and a gel is formed if the ethanol-milk mixture is held at 4ºC, especially if concentrated milk is used. If the ethanol is removed by evaporation, very large aggregates (average diameter = 3000 nm) are formed. The dissociating effect of ethanol is promoted by increasing the pH (35% ethanol causes dissociation at 20ºC and pH 7.3) or adding NaCl. Methanol and acetone have an effect similar to ethanol, but propanol causes dissociation at = 25ºC. The mechanism by which ethanol dissociates casein micelles has not been established, but it is not due to the solution of CCP, which is unchanged.

References

Brule G, Lenoir J, Remeuf F The casein micelle and milk coagulation. In Cheesemaking: From Science to Quality Assurance, Eck A & Gillis J, eds., 2nd Edition, Lavoisier Publishing, Paris, 2000, pp. 7-40.

Brunner JR Milk proteins. In Food Proteins, Whitaker JR & Tannenbaum SR, eds., AVI Publishing Company, Inc., Connecticut, 1977, pp. 175-208.

Dalgleish DG Milk proteins - chemistry and physics. In Food Proteins, Fox PF & Condon JJ, eds., Applied Science Publishers, Ltd., Essex, 1982, pp. 155-178.

Farrell HM, Malin EL, Brown EM, Qi PX, 2006, Casein micelle structure: What can be learned from milk synthesis and structural biology? Curr opin colloid In 11:135–147.

Fox PF, Brodkorb A, 2008, The casein micelle: historical aspects, current concepts and significance. Int Dairy J 18: 677-684.

Fox PF, McSweeney PLH Dairy chemistry and biochemistry, Blackie Academic & Professional, 1998.

Holt C, 1992, Structure and Stability of Bovine Casein Micelles. Adv Protein Chem 43: 63-151.

Holt C, Horne DS, 1996, The hairy casein micelle: Evolution of the concept and its implications for dairy technology. Neth Milk Dairy J 50: 85-111.

Holt C, The biological function of casein, in Yearbook 1994, the Hannah Research Institute, Ayr, UK, 1994, pp. 60–68.

Horne DS, 1998, Casein interactions: casting light on the black boxes, the structure in dairy products. Int Dairy J 8: 171-177.

Horne DS, 2002, Casein structure, self-assembly and gelation. Curr opin colloid In 7:456-461.

Huppertz T, Kelly Al, de Kruif CG, 2006, Disruption and reassociation of casein micelles under high pressure. J Dairy Res 73: 294-298.

Rollema HS Casein association and micelle formation. In Advanced Dairy Chemistry, Vol. 1: Proteins, Fox PF, ed., Elsevier Science Publisher, Ltd., Essex, 1992, pp. 111-140.

Sawyer L, Barlow PN, Boland MJ, Creamer LK, Denton H, Edwards PJB, Holt C, Jameson GB, Kontopidis G, Norris GE, Uhrinova S, Wu S, 2002, Milk protein structure – what can it tell the dairy industry?: A Review. Int Dairy J 12: 299-310.

Smit G Dairy processing: improving quality. Woodhead Publishing, 2003.

Swaisgood HE Chemistry of caseins. In Advanced dairy chemistry, Vol 1: Proteins, Fox PF & McSweeney PLH eds, 3rd ed, Kluwer Academic/Plenum Publisher, New York, 2003.

Thompson A, Boland M, Singh H. Milk Proteins: From Expression to Food. Academic Press, 2008.

Walstra P, 1999, Casein sub-micelles: do they exist? Int Dairy J 9: 189-192.

Walstra P, Geurts TJ, Noomen A, Jellema A, van Boekel MAJS Dairy Technology: Principles of Milk Properties and Processes, Marcel Dekker Inc, New York, 1999.

Walstra P, Wouters JTM, Geurts TJ Dairy Science and Technology, Taylor & Francis Group, LLC, 2nd Edition, 2006.

Waugh DF, 1958, The interactions of α_s-, β- and κ-caseins in micelle formation. Discuss Faraday Soc 25: 186-192.

1.3 Milk fat

1.3.1 General overview

Milk of all mammals contains lipids in a concentration which varies widely between species from about 2% to greater than 50%. The principal function of dietary lipids is to serve as a source of energy for the newborn and the fat content in milk largely reflects the energy requirements. Milk lipids are also important as a source of essential fatty acids especially those which cannot be synthesized by animals, like linoleic acid, and fat soluble vitamins (A, D, E, K), and for the flavor and rheological properties of dairy products and foods in which they are used. (Fox & McSweeney, 1998).

Bovine milk contains on average 3.5% fat but its level varies widely, depending on several factors including: breed, animal individuality, stage of lactation, season, nutritional status, type of feed, health and age, the interval between milking and the sampling point during milking. Of the common European breeds, milk from Jersey cows contains the highest level of fat and that from Friesians the lowest. The fat content of milk decreases during the first 4-6 weeks after delivery and then increases steadily throughout the lactation, especially toward the end. In general, fat content is highest in winter and lowest in summer, due partly to the effect of environmental temperature. For any animal, fat content decreases slightly during successive lactations, by about 0.2% over a typical productive lifetime (about five lactations). The concentration of fat (and of all other milk-specific constituents) decreases markedly under mastitic infection, due to impaired synthesizing ability of the mammary tissue; the effect is more evident in the case of clinical mastitis than for subclinical infection. Milk yield is reduced by underfeeding but the concentration of fat usually increases, with little effect on the amount of fat produced. Diets low in roughage have a marked depressing effect on the fat content, with little effect on milk yield. Ruminants synthesize milk fat mainly from carbohydrate-derived precursors. Feeding of some fish oils (e.g. cod liver oil, in an effort to increase the concentrations of vitamins A and D in milk) has a very marked (about 25%) depressing effect on the fat content, apparently due to the high level of polyunsaturated fatty acids, although oils from some fish species do not cause this effect (Fox & McSweeney, 1998).

The milk fat of ruminants is very complex, due to the diversity of lipid species that are produced by microbial activity in the rumen and are transported to the milk secretory cells in the blood stream. Other lipids are produced by synthesis in the secretory cells. Fatty acids found in milk fat include: (1) saturated even and odd n-chain acids from 2 to 28; (2) at least 50 branched chain fatty acids; (3) *cis* monoenoic fatty acids of 12 and 14 to 24 -chain acids; (4) *trans* 16 to 24 *n* chain fatty acids; (5) various positional and geometric isomers of dienes and trienes of 18, 20, 22, and 24 -chain acids; and (6) small amounts of tetra- and pentanoic acids. Quantitatively, the major fatty acids of milk fat are myristic (11%), palmitic (26%), stearic (10%), and oleic (20%). Saturated fatty acids account for about two-thirds of milk fatty acids, with larger quantities of unsaturated fatty acids found during the summer months (Goffand & Hill, 1993).

Triacylglycerols (triglycerides) represent 97-98% of the total lipids in the milks of most species**.** The diglycerides probably derive from both incompletely synthesized lipids and partially hydrolyzed triglycerides, as indicated by the high concentration of free fatty acids, suggesting damage to the milk fat globule membrane (MFGM) during milking and storage.

Although phospholipids represent less than 1% of total lipid, they play a particular and important role, being present mainly in the MFGM (Milk Fat Globule Membrane) and other membraneous material in milk. The principal phospholipids are phosphatidylcholine, phosphatidylethanolamine and sphingomyelin**.** Trace amounts of other polar lipids, including

ceramides, cerobrosides and gangliosides, are also present. Cholesterol is the principal sterol in milk, representing over 95% of total sterols and 0.3%, w/w, of total lipids. Most of the cholesterol is in the free form, with less than 10% as cholesteryl esters. Several other sterols, including steroid hormones, occur at trace levels.
Several hydrocarbons occur in milk in trace amounts. Of these, carotenoids are the most significant. In quantitative terms, carotenes occur at only trace levels in milk (typically ~200μg l^{-1}) but they contribute 10-50% of the vitamin A activity in milk and are responsible for the yellow color of milk fat.
Milk contains significant concentrations of fat-soluble vitamins, but their actual form in milk appears to be uncertain. Their concentration varies widely with breed of animal, feed and stage of lactation, e.g. the vitamin A activity of colostrum is about 30 times higher than that of mature milk.
Several prostaglandins occur in milk but it is not known whether they play a physiological role; they may not survive storage and processing in a biologically active form (Fox & McSweeney, 1998).

1.3.2 Milk fat globules

More than 95% of the total milk lipid is in the form of a globule, as shown in Figure 1.17 (Michalski et al., 2004).

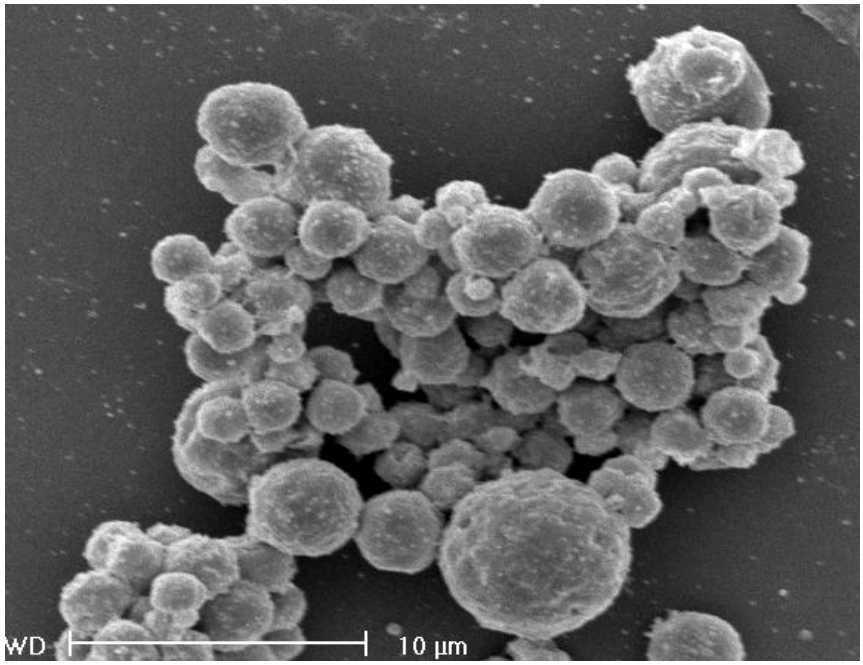

Figure 1.17: Scanning electron micrographs of native milk fat globules (Hintze, et al., 2011)

These fat globules are formed throughout the mammary epithelial cell, grow in size as they move toward the apical cell membrane and are extruded into the alveolar lumen (Figure 1.18). During the extrusion process, the globule is enveloped by portions of the cell membrane that becomes the milk fat globule membrane (MFGM) (El-Loly, 2011). The membrane is about 8–

20 nm in cross-section and owns properties completely different from both milk fat and plasma (Smith & Campbell, 2007).

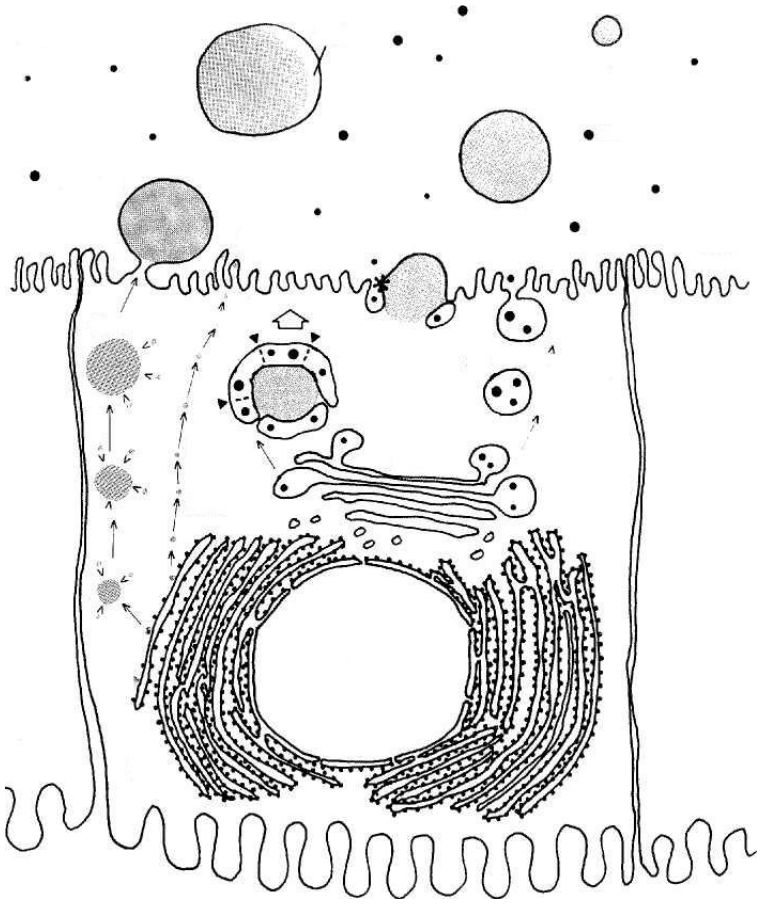

Figure 1.18: Summary of pathways for lipid droplet transit and secretion from mammary epithelial cells (Mather & Keenan, 1998).

Fat globule size ranges from 0.1 to 15 um in diameter (Michalski et al., 2004). Small globules represent 80% of the total milk fat globules but only a few percent of the total fat; the average-sized globules (3-4μm) account for 94% of the total fat whereas the large globules make up only a small portion of the fat and are very few in number. The globules of different sizes have been shown to have different lipid composition, different ratio of triglycerides to phospholipids and physicochemical characteristics (Michalski et al., 2006;Mulder & Walstra, 1974).
The core of the lipid droplet is composed for 98%of triglycerides, di- and monoglycerides, with a substantial amount of short-chain fatty acids (C4:0 to C10:0) and only a small amount of long-chain polyunsaturated fatty acids, cholesterol, carotenoids and fat-soluble vitamins. The average composition of the milk fat globules varies with size, between globules of same size in one milking of one cow, and between cows. The composition of the milk fat globule and its membrane can be modified by processing, animal and environmental factors (Lopez et al., 2008). The processing factors include cooling, stirring, heat treatment, homogenization, drying,

separation, acidification and dilution (Mulder & Walstra, 1974). The animal factors include the breed, the diet and the stage of lactation of the cow and the season. The environmental factors include contamination by bacteria before or after pasteurization, and the presence of mastitis pathogens.
The MFGM surrounds the apolar fat globule with a tri-layer structure through association with the triglycerides in the liquid portion of the fat, as reported in Figure 1.19.

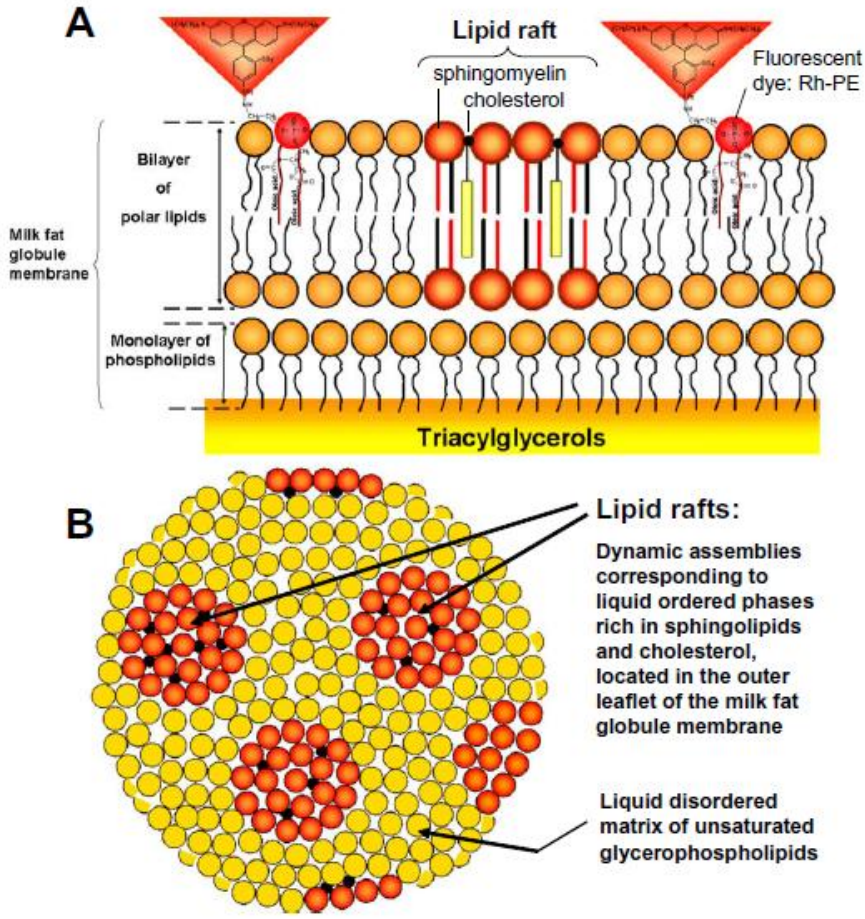

Figure 1.19: Two- and three-dimensional schematic representations of the organisation of polar lipids in the milk fat globule membrane (MFGM). (A) Segregation of sphingomyelin in micro-domains in which the exogenous phospholipid fluorescent dye Rh-PE cannot integrate; (B) three-dimensional representation of the organisation of polar lipids in the MFGM, showing the circular shape of the lipid rafts enriched in sphingomyelin. (Lopez et al., 2010).

The native membrane (FGM) is comprised of apical plasma membrane of the secretory cell which continually envelopes the lipid droplets as they pass into the lumen. The major components of the native FGM, therefore, are proteins and phospholipids. The strength and elasticity of the MFGM, with its ability to reduce interfacial tension, contributes to emulsion

stability and protects globules from enzymatic actions. Moreover, at least 25 different enzyme activities have been found to be associated with the MFGM, which also presents a high water-binding ability (Michalski et al., 2003).

1.3.3 Milk fat technological properties

Milk fat greatly contributes to the texture, flavor and physicochemical properties of many dairy products, especially cheese. Particularly, depending on its solid fat content, it acts more or less as a plasticizer. Several studies pointed out that total fat content and fat globule size distribution significantly influence creaming phenomenon and affect the viscosity of milk (Jaros et al., 2001).

Relative proportions of triglyceride isomers in the fat globules impart unique thermal and structural properties. In general, the structure and texture of dairy gels and cheese are affected by the interactions between the surface of milk fat globules and the casein matrix. In particular, native milk fat globules do not interact with the protein network in dairy gels and act mainly as inert fillers or structure breakers, depending on their size and number (Michalski et al., 2003). Conversely, under milk processing conditions the structure and composition of the MFGM is altered. For example, homogenization and pasteurization of the milk result in a loss of native MFGM material, which is then partially replaced by caseins and whey proteins at the interface (Michalski et al., 2002).

During homogenization, the milk fat globule membrane is break down and the interfacial tension between the lipid core of the globule and the milk serum increases from 2mN/m to 15mN/m (Danthine et al., 2000). The adsorption of caseins and whey proteins stabilizes the interfacial tension back to 3-4mN/m. The use of small globules produced by homogenization, where the native MFGM has been disrupted and replaced by casein micelle fragments, results in structure enforcement by creating links with the casein network (Michalski et al., 2003). Therefore, this type of globule does not possess the genuine characteristics of native globules and could not be compared with products made with small native MFG.

Heat treatment leads to the association of milk proteins, in particular β-lactoglobulin with MFGM, with an increase in cheese yield (Singh, 2006, Molina et al., 2000). During the cream-making process, milk is centrifuged and MFGM phospholipids partition into the serum phase (Anderson & Brooker, 1975).

The smaller the globules, the more the crystallization process takes place with small and unstable crystals (Couvreur & Hurtaud, 2007). Thus a higher pressure and a longer time are required during churning of the cream in the butter-making process for smaller globules. Butter, made from milk containing small fat globules, contains more intact milk fat globules and more wet and, therefore, more spreadable than butter rich in large fat globules. Milk with large fat globules is more suitable for creaming. A cream with small MFGs will have reduced ability to be churned (Walstra et al., 1999). A picture of MFGM isolated from buttermilk produced by ultrafiltration is shown in Figure 1.20.

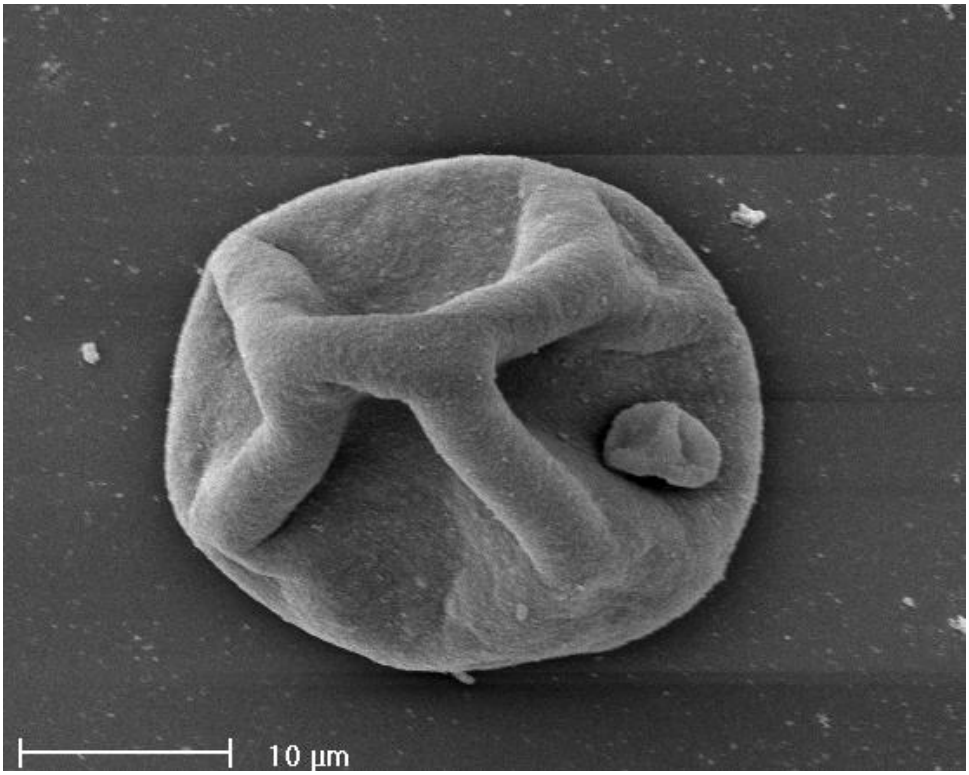

Figure 1.20: Milk fat globular membrane isolated from buttermilk with ultrafiltration (Hintze, et al., 2011)

In cheese, small fat globules easily insert within the protein network, leading to a higher water-retention capacity and higher cheese moisture. The large fat globules tend to be destructive of the protein network as they are often larger than the protein pores. Thus, cheese produced with small fat globules (less than 2µm) is less hard than cheese with globules larger than 2µm (Goudedranche et al., 2000). The size of native milk fat globules, separated by means of microfiltration, affects functional and physicochemical properties of Camembert cheese (Michalski et al., 2003) and Emmental cheese (Michalski et al., 2007) due to an increased surface area of the native MFGM in small globules compared with larger MFGs. Small fat globule Camembert and Emmental cheeses are less firm, and undergo greater proteolysis but reduced lipolysis than large fat globule cheeses: Emmental produced from native small MFG (~3 µm) had 5.0% more moisture on non-fat basis than the cheese made from large MFG (~6 µm) after 52 days of ripening, and 2.2% more moisture in the case of Camembert cheese after 40 days of ripening (Michalski et al., 2003; Michalski et al., 2004). The use of small or large native MFG results in different cheese texture and aroma, as observed in low-fat Cheddar cheese. Proteolysis caused by starter proteases and proteolysis and lipolysis by MFGM enzymes may lead to a richer and more intense flavor in cheese with higher MFGM contents (Michalski et al., 2003). The larger fat globule surface area is likely to enhance aroma perception due to a greater contact surface of fat in the mouth (Michalski et al., 2003). For these reasons, a French research group developed a microfiltration process which allows to obtain native milk fat globules of various sizes from whole milk (Goudédranche et al., 1998).

Due to the high amount of unsaturated FAs, MFGM phospholipids are susceptible to oxidation and may cause a soapy-rancid flavor (Lopez et al., 2007). For the production of non-fat and low fat yoghurt, the reduction on total solids causes adverse effects on textural and sensory properties, such as severe syneresis, a lack of the typical flavor and mouth-feel Trachoo & Mistry, 1998.
A recent study (Wiking et al., 2004b) tending to verify the correlation between the increase in FFA (Free Fatty Acids), the intervals of milking technology and AMS (Automatic Milking System) milk transport to the tank storage, showed that as the fat content increases, the globules average diameter increases as well as their aptitude to be moved with pumps. Moreover, the lipolysis increases when the flow speed increases in the pipeline transportation. Other studies proved a positive relationship between size of fat globules and susceptibility to lipolysis (Svennersten-Sjaunja et al., 2000; Wiking et al., 2004b). The stability of the smaller globules during the transport with pumps is due to their greater total external surface area that requires more energy to be damaged with physical systems. In milk refrigerated at 5° C, the majority of lipids is present in crystalline form and this gives more stability to the globules when subjected to high flow speed of the pumps.
During the cooling of milk, there is a corruption of the fat globules, with release of triglycerides that can be hydrolyzed by the native milk lipase. Short intervals between milkings result in improving the level of FFA.
FFA represent the final product of the lipolytic process and the measurement of their content is a good indicator of such damage. Lipolysis is responsible for the rancid flavor of milk. The fat present in globules is protected from endogenous lipolytic enzymes (mLPL) by the globules membrane. If this membrane is damaged, for example with milk stirring, fatty acids can be removed enzimatically from the glyceridic chain. It has been observed that grazing increases the level of FFA compared to diets richer in concentrates or maize silage-based. Even undernourished animals simply denote a higher level of FFA (Slaghuis et al., 2004). During the final phase of lactation, and in case of high milking frequency (3 or more per day) phenomena linked to spontaneous lipolysis can occur (Cartier et al., 1990).
The adoption of measures limiting the frequency of milking, for less productive animals and in the final phase of lactation, can help to prevent high levels of FFA in milk. The natural creaming of milk fat leads to a diversification in globule dimensions in cream and skim milk. The fat component in milk, that remains after the creaming process, is characterized by decreased size of fat globules, resulting in higher ratio of membrane surface area and volume of fat globules. The greater proportion of membrane can facilitate the lipolysis processes in cheese, because the enzymes responsible for these processes are located inside the membrane. This fact affects the aroma of the final product due to the progress of the hydrolytic process of fat component.

1.3.4 Milk fat globule and MFGM nutritional and nutraceutical aspects

The lipid and protein fractions of the MFGM material have shown to have nutritional properties and several health-promoting effects.
Regarding the fatty acid composition of milk, after fat globules separation by centrifugation, Lopez et al., (2011) observed that in skim milk, globules with 1.5 μm diameter showed lower content of fatty acids from C4:0 to C10:0 as well as C18:0, and with greater amount of C18:1, compared to larger fat globule of the cream, with 3 μm diameter. A more recent study (Wiking et al., 2004) reported positive correlations between the concentration of several fatty acids deriving from the diet and the average diameter: the average diameter of globules is positively correlated with the concentration of fatty acids C16: 1 (palmitoleic acid) and C18 (stearic acid),

but negatively with the concentration of C18: 2 (linoleic acid) + C18: 3 (linolenic acid). of milk fat globules.
Sphingolipids, which constitute the polar lipid fraction of the MFGM together with glycerophospholipids, are functional ingredients, due to their regulatory properties, structural functionality and effectiveness at low concentrations. Sphingomyelin and its metabolites seem to have an influence on triglyceride hydrolysis, cholesterol absorption, lipoprotein formation and mucosal growth in the gut. Studies proved their effect on colon cancer cells, inducing growth arrest, differentiation and/or apoptosis. Sphingolipids were found to inhibit both the early and the late stages of colon carcinogenesis, in tests on mice, and to induce a significant shift in tumor type from the malignant adenocarcinomas to the more benign adenomas. Sphingolipids were found to be chemopreventive as well as chemotherapeutic, and are associated with age-related diseases and the development of Alzheimer's disease. They are also involved in the intestinal uptake of cholesterol: sphingomyelin was found to lower the intestinal absorption of cholesterol and fats in rats (Dewettinck et al., 2008).
Duivenvoorden *et al.* (2006) reported that dietary sphingolipids have great potential to treat multiple aspects of the metabolic syndrome, such as dyslipidemia, insulin resistance and cardiovascular diseases. Dietary sphingolipids could also have protective role against bacterial toxins and infection by bacteria or viruses due to their ability to compete for and act as cellular binding sites. As the adherence of the pathogens to the intestinal mucosa is often the first step in infection, the competition results in an elimination of pathogens from the intestine, which causes a shift in the bacterial population of the colon. Lysophingomyelin appeared highly bactericidal against *Campylobacter jejuni*, *Listeria monocytogenes* and *Clostridium perfringens*, and showed moderately lowered viable counts of *E. coli* and *Salmonella enteritidis.* Many neuronal effects of ageing in animals are attenuated by Phosphatidylserine (PS) and, at elevated doses, clinical trials with patients suffering from Alzheimer's disease showed positive effects. PS supplementation on exercising humans results in alteration of neuroendocrine function and positive influence on perceived muscular soreness and well-being. Phosphatidylcholine (PC) is believed to protect the human gastrointestinal mucosa against toxic attack and to promote synthesis and transmission of neurotransmitters important to memory, and might also be involved in brain development. It is a source of choline, which is an essential nutrient for humans. Furthermore, some phospholipids are digested in the gastrointestinal tract to compounds that might possess antimicrobial activity. Several studies proved the presence of proteins, in bovine and human MFGM, involved in DNA repair processes and showing antibacterial effects. Their antimicrobial activity is related to the production of reactive oxygen species, such as superoxide and hydrogen peroxide in the gut. It may also catalyze the reduction of inorganic nitrite to nitric oxide and, in the presence of oxygen, to peroxynitrite, which both show bactericidal properties. Delipidated bovine MFGM material shows inhibitory power similar to that of the gastric mucins, able to inhibit sialic acid-specific hemagglutination of *H. pylori*, responsible of some forms of stomach diseases, such as chronic gastritis, peptic ulcer disease and stomach cancer (Dewettinck et al., 2008).
The main health benefits associated to MFGM components are reported in Table 1.5.

Component	Health benefit	Reference
BRCA1	Inhibition of breast cancer	Spitsberg and Gorewit, 1997b;
BRCA2	Inhibition of breast cancer	Vissak et al., 2002
Fatty acid binding protein (FABP)	Cell growth inhibitor	Spitsberg et al., 1995; Spitsberg and Gorewit, 2002
Beta-glucuronidase inhibitor	Inhibition of colon cancer	Ito et al., 1993
FABP as selenium carrier	Anticancer factor	Bansal and Medina, 1993; Whanger, 2004
Helicobacter pylori inhibitor	Prevention of gastric diseases	Wang et al., 1998
Cholesterolemia-lowering factor	Anticholesterolemic	Ito et al., 1992
Butyrophilin	Suppression of multiple sclerosis	Mana et al., 2004
Vitamin E and carotenoids	Antioxidants	Lindmark-Mansson and Akesson, 2000; Jensen and Nielsen, 1996
Vitamin B2		Kanno et al., 1991
Xanthine oxidase	Bactericidal agent	Martin et al., 2004; Hancock et al., 2002
Phospholipids	Inhibition of colon cancer	Parodi, 2001
	Anticholesterolemic	Noh and Koo, 2004
	Suppression of gastrointestinal pathogens	Sprong et al., 2002
	Anti-Alzheimer, antidepressant	Horrocks and Farooqui, 2004
	Antistress	McDaniel et al., 2003
Phosphoproteins	Source of organic phosphorus and Ca-phosphate	Spitsberg and Gorewit, 1997c

Table 1.5: Components of bovine milk fat globule membrane (MFGM) associated with health benefits. (Source: Spitsberg, 2005)

1.3.5 References

Anderson M, Brooker BE, 1975, Loss of material during the isolation of milk fat globule membrane. J Dairy Sci, 58: 1442–1448.

Cartier P, Chilliard Y, Paquet D, 1990, Inhibiting and activating effects of skim milks and proteose-peptone fractions on spontaneous lipolysis and purified lipoprotein lipase activity in bovine milk**.** J Dairy Sci 73:1173–1177.

Couvreur S, Hurtaud C, 2007, Globule milk fat: Secretion, composition, function and variation factors. Prod Anim 20: 369-382.

Danthine S, Blecker C, Paquot M, Innocente N, Deroanne C, 2000, Progress in milk fat globule membrane research: a review. Lait 80: 209-222.

Dewettinck K, Rombaut R, Thienpont N, Trung Le T, Messens K, Camp JV, 2008, Nutritional and technological aspects of milk fat globule membrane material. Int Dairy J, 18: 436–457.

Duivenvoorden I, Voshol PJ, Rensen PC, van Duyvenvoorde W, Romijn JA, Emeis JJ, Havekes LM, Nieuwenhuizen WF, 2006, Dietary sphingolipids lower plasma cholesterol and triacylglycerol and prevent liver steatosis in APOE*3Leiden mice. Am J Clin Nutr 84: 312–321.

El-Loly MM, 2011, Composition, Properties and Nutritional Aspects of Milk Fat Globule Membrane – a Review. Pol J Food Nutr Sci 61: 7-32.

Fox PF, McSweeney PLH Dairy Chemistry and Biochemistry, Thomson Science, 1st Edition, 1998.

Goffand HD, Hill AR Chapter 1-Chemistry and Physics. In Dairy Science and Technology Handbook 1 Principles and Properties, Hui YK, ed., Wiley-VCH, Inc, 1993.

Goudedranche H, Fauquant J, Maubois JL, 2000, Fractionation of globular milk fat by membrane microfiltration. Lait 80: 93-98.

Goudédranche H, Maubois JL, Fauquant J, 1998, Produits, en particulier laitiers, comprenant des fractions sélectionnées de globules gras, obtention et applications, Brevet FR 2 776 208-A1.

Hintze JK, Snow D, Burtenshaw I, Ward RE, 2011, Nutraceutical Properties of Milk Fat Biotechnology of Biopolymers, www.intechopen.com.

Jaros D, Petrag J, Rohm H, Ulberth F, 2001, Milk fat composition affects mechanical and rheological properties of processed cheese. Appl Rheol 11: 19-25.

Lopez C, 2007, The composition, supramolecular organisation and thermal properties of milk fat: a new challenge for the quality of food products. Lait 87: 317-336.

Lopez C, Briard-Bion V, Menard O, Beaucher E**,** Rousseau F**,** Fauquant J, Leconte N, Benoit R, 2011, Fat globules selected from whole milk according to their size: Different compositions and structure of the biomembrane, revealing sphingomyelin-rich domains. Food Chem 125: 355-368.

Lopez C, Briard-Bion V, Menard O, Rousseau F, Pradel P, Besle JM, 2008, Phospholipid, sphingolipid, and fatty acid compositions of the milk fat globule membrane are modified by diet. J Agr Food Chem 56: 5226-5236.

Lopez C, Madec MN, Jiménez-Flores R, 2010, Lipid rafts in the bovine milk fat globule membrane revealed by the lateral segregation of phospholipids and heterogeneous distribution of glycoproteins. Food Chem 120: 22-33.

Mather IH, Keenan TW, 1998, Origin and secretion of milk lipids. J Mammary Gland Biol 3:259-273.

Michalski MC, Camier B, Briard V, Leconte N, Gassi JY, Goudédranche H, 2004, The size of native milk fat globules affects physico-chemical and functional properties of Emmental cheese. Le Lait 84: 343–358.

Michalski MC, Camier B, Gassi JY, Briard-Bion V, Leconte N, Famelart MH, Lopez C, 2007, Functionality of smaller vs control native milk fat globules in Emmental cheeses manufactured with adapted technologies. Food Res Int 40: 191-202.

Michalski MC, Gassi JY, Famelart MH, Leconte N, Camier B, Michel F, 2003, The size of native milk fat globules affects physico-chemical and sensory properties of Camembert cheese. Le Lait 83: 131–143.

Michalski MC, Leconte N, Briard-Bion V, Fauquant J, Maubois JL, Goudédranche H, 2006, Microfiltration of raw whole milk to select fractions with different fat globule size distributions: process optimization and analysis. J Dairy Sci 89: 3778-3790.

Michalski MC, Michel F, Geneste C, 2002, Appearance of submicronic particles in the milk fat globule size distribution upon mechanical treatments. Lait 82: 193-208.

Molina E, Alvarez MD, Ramos M, Olano A, Lopez- Fandiño R, 2000, Use of high pressure-treated milk for the production of reduced-fat cheese. Int Dairy J 10: 467-475.

Mulder H, Walstra P, 1974 The milk fat globule emulsion science as applied to milk products and comparable foods. PUDOC, Wageningen, Netherlands, 1974, p.296.

Singh H, 2006, The milk fat globule membrane - A biophysical system for food applications. Curr opin colloid In 11: 154-163.

Singh H, 2006, The milk fat globule membrane-A biophysical system for food applications. Curr opin colloid In 11: 154-163.

Slaghuis BA, Bos K, de Jong O, Tudos AJ, te Giffel MC, de Koning CJAM, Robotic milking and free fatty acids. In: A Better Understanding – Automatic Milking. Meijering A, Hogeveen H, de Konig CJAM eds, Wageningen, The Netherlands: Wageningen Academic, 2004, pp 341–347.

Smith A, Campbell B Microstructure of Milk Components. In: Structure of Dairy Products, Tamime A ed, Blackwell Publishing Ltd, Oxford, UK, 2007.

Spitsberg VL, 2005, Bovine Milk Fat Globule Membrane as a potential nutraceutical, J Dairy Sci 88: 2289–2294.

Svennersten-Sjaunja K, Berglund I, Pettersson G, 2000, The milking process in an automated milking system, evaluation of milk yield, teat condition and udder health. in Proc. Robotic Milking Proc Int Symp, Lelystad, the Netherlands. Wageningen Pers, Wageningen, the Netherlands, pages 277–287.

Trachoo N, Mistry VV, 1998, Application of ultrafiltered sweet buttermilk and sweet buttermilk powder in the manufacture of non fat and low fat yogurt. J Dairy Sci 81: 3163-3171.

Walstra P, Geurts TJ, Noomen A, Jellema A, van Boekel MAJS Dairy technology. Principles of milk properties and processes. Marcel Dekker AG, New York, 1999, p.767.

Wiking L, Bjork L, Nielsen JH, 2004b, Impact of size distribution of milk fat globules on milk quality affected by pumping in automatic milking. A better understanding. Meijering A, Hogeveen H, de Koning CJAM, ed. Wageningen Academic Publishers, Wageningen, The Netherlands. pp 348- 356.

Wiking L, Stagsted J, Bjorck L, Nielsen, 2004, Milk fat globule size is affected by fat production in dairy cows. Int Dairy J 14: 909-913.

2. AIM OF THE RESEARCH ACTIVITY

In the last decades, the spectroscopic techniques, and in particular the near-infrared spectroscopy (NIRS), have acquired reliability, since they are sufficiently accurate and precise for analysis of the macro-composition of food.
The diffusion of instrumentation capable to work in Fourier Transform mode has further increased the analytical precision. The use of fiber optics and the diversification of the available optical geometries have praised the versatility of this non-destructive technique, encouraging studies to demonstrate the potential applications of this technique from "the field" to "the consumer" (Burns & Ciurczak, 2001).
The development of instrumental operating and spectral data processing softwares has provided suitable tools for the correct interpretation of the large amount of information contained into the spectra, for the achievement of specific objectives. The numerous studies, carried out in order to improve the transfer of calibrations from one instrument to another, have allowed the adoption of universal calibrations favoring both the recovery of historical data and the comparison between different instrumental responses (Williams & Norris, 2001).
In this context, this research has set itself the general objective of assessing and deepening of the potential of spectroscopic techniques applied to fields still little studied in dairy sector.
In this work, NIR and IR techniques were applied to study some aspects of cow milk casein and cow milk fat globules.
Caseins from milk of ruminants have been extensively studied as well as the nature of links between the different subunits, but the exact structure of the casein micelle is still debated (Rollema, 1992; Holt & Horne, 1996; Walstra, 1999). Despite the several applications of NIRS in food and agricultural sectors, the relevance of this technique to study the proteins structure of has received minor attention.
The size distribution of fat globules is an aspect influencing the technological and sensorial milk characteristics (Michalski, 2007; Michalski et al., 2003). Despite the importance of this parameter, its measurement requires dedicated instrumentation not available in dairy laboratories and this type of information is not easily available, except for research purposes.
In particular, the research activity was addressed to reach the following specific objectives:

- to verify the ability of spectroscopic techniques in the evaluation of intermolecular interactions between casein sub-fractions and their modifications as function of pH and temperature;
- to assess the NIRS ability in predicting casein fractions content, as a determinant parameter for the cheese yield, and its ability in detecting bonds involved in the micelle complex;
- to evaluate the content of the macronutrients of milk by FT NIR and FT IR spectroscopy, in order to make a comparison between the calibration basis of the two vibrational spectroscopy and to demonstrate the role of light scattering in the NIR fat quantification;
- to study the variability in the distribution of fat globules within cow breedings in Lombardy;
- to develop a rapid and economic method for estimating the distribution of fat globules in milk through a physical-mathematical model based on the study of the scattering component in the NIR spectrum;
- to improve the applicability of the model trough standardization of a portable spectrometer to a bench-top instrument.

References

Holt C and Horne DS, 1996, The hairy casein micelle: Evolution of the concept and its implications for dairy technology. Neth. Milk Dairy J., 50: 85-111.

Rollema HS Casein association and micelle formation. In Advanced Dairy Chemistry, Vol. 1: Proteins (ed. P.F. Fox), Elsevier Science Publisher, Ltd., Essex, 1992, pp. 111-140.

Walstra P, 1999, Casein sub-micelles: do they exist? Int. Dairy J., 9: 189-192.

Williams P, Norris K., Near-infrared technology in the agricultural and food industries. American Association of Cereal Chemists, Inc. St. Paul, Minnesota, USA, 2nd ed., 2001.

Burns DA, Ciurczak EW Handbook of near-infrared analysis**.** Burns DA, Ciurczak EW eds, CRC Press, Marcel Dekker Inc, New York, 2001.

3. RESULTS AND DISCUSSION

3.1 Intermolecular interactions between the different sub-fractions of casein micelles detected by FT-NIR and FT-IR

3.1.1 Introduction

Casein is a complex milk protein consisting of subunits of different nature: α_s, β - and κ-casein- linked by calcium and phosphate ions (Rollema, 1992). The nature of the links between the different subunits has been extensively studied, but the exact structure of the casein micelle is still debated. Several models have been proposed in an attempt to explain the experimental evidence. The first representation of the casein micelle structure shown in Figure 3.1, named "sub- micelles casein", dates back to 20 years ago. According to this theory, not universally accepted, the micelle would consist of spherical units of casein, which are linked together by clusters of calcium phosphate (Walstra, 1999).

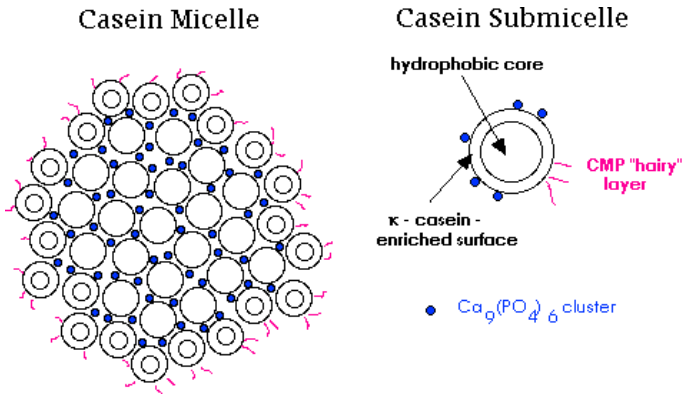

Figure 3.1: Casein micelle structure.

The main shortcoming of this model concerns the distribution of calcium phosphate: it is known that it exists more evenly distributed throughout the micelle, both inside and outside the sub-micelles.
It is therefore considered that well defined casein sub- micelles don't exist, but rather a more open and fluid structure, like a "bowl of spaghetti" shape ("bowl-of-spaghetti" model) (Holt & Horne, 1996).
Inside the micelle, flexible polypeptide chains form a tangle, whose state of association depends on the balance between electrostatic repulsion and attractive forces arising from interactions between hydrophobic and hydrophilic regions of casein containing phosphoserine and calcium phosphate nanoclusters.
On the other hand, the surface layer of the micelle has a lower density, with hydrophilic polypeptide chains derived from the C-terminal region of κ-casein, which protrude outside of the micelle forming a "hairy layer" which provides steric and / or charge stability to particles of native casein. Variations in temperature, pH and ionic strength affect this delicate balance of forces and can change the status of micelles association.
The model in Figure 3.2 shows the interactions between sub-micelles as a function of temperature and pH (Holt & Horne, 1996).

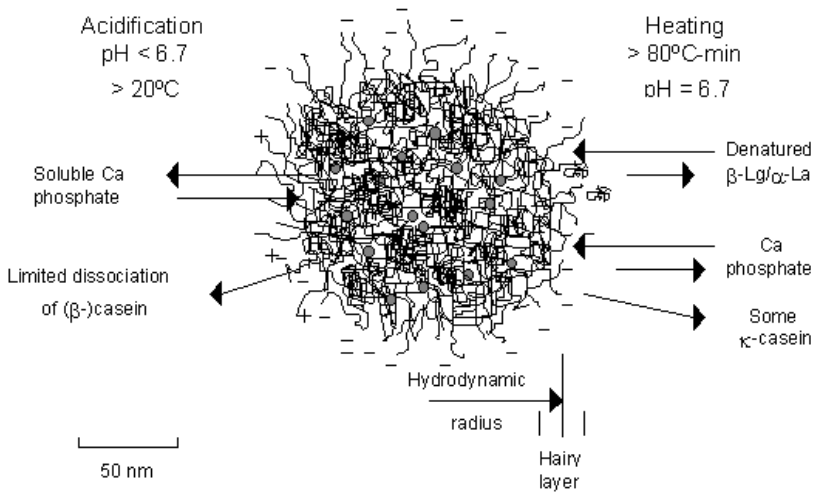

Figure 3.2: Interactions between sub-micelles as a function of temperature and pH.

The objective of this study was to assess the suitability of spectroscopic techniques in the evaluation of intermolecular interactions between the casein sub-fractions and their modifications as a function of temperature and pH.

3.1.2 Materials and methods

Samples and solutions preparation

Preparation of phosphate and phosphate buffer solutions at different pH
The phosphate solutions were prepared by dissolving Na phosphate (Di-Sodium Hydrogen Ortophosphate Anhydrous, Carlo Erba, Italy) in distilled water. The pH was adjusted from 4 to 13 by adding 98% phosphoric acid (phosphoric acid, Sigma-Aldrich Srl, Italy) or NaOH 0.1N (Sodium Hydroxide, Titolchimica, Italy) and measured with a pH meter (Hanna Instruments mod.8417, Singapore). Phosphate buffer solution at pH 6.8 (PBS) was prepared in the same way.

Addition of Ca^{2+} to casein
Preliminary atomic absorption measurements (Perkin Elmer 1100B HGA 700, USA) revealed that calcium concentration in commercial 'technical grade' (TG) casein (Sigma-Aldrich Srl) was much lower than in milk (0.68 mg/g vs. 1.20 mg/g; Mucchetti & Neviani, 2006). Thus, in order to obtain comparable concentrations, powder of $CaCl_2$ (Calcium chloride dehydrate, Merck, Germany) was added slowly with constant mixing to a solution of commercial casein (26 g/L) at room temperature, reaching final concentrations of 0.01, 0.02 and 0.03 M.
The pH of the solution was adjusted to 7.8 by the dropwise addition of 0.1 N NaOH.

Preparation of Ca^{2+}-EDTA solutions
Increasing amounts of powder of $CaCl_2$ (Merck) were added slowly with constant mixing to a solution of 0.03 M EDTA (Sigma-Aldrich Srl), to obtain Ca^{2+} final concentrations of 0.012, 0.018, 0.024 and 0.03 M.

Preparation of citrate solutions
Sodium citrate powder (tri-sodium citrate dehydrate, Merck, Germany) was added to solutions of TG casein in different concentrations, reaching final concentration of 20 mM. The pH of the solution was adjusted at 6.8 by the dropwise addition of 1 N NaOH.
Citrate buffer solution at pH 6.8 (CBS) was prepared in the same way.

Commercial Samples
Commercial preparation of casein fractions (α_s–, β - and κ-casein (Sigma-Aldrich Srl)) and whole TG casein (Sigma-Aldrich Srl) were used to obtain solutions to the concentrations in which these molecules are present in cow milk, ie 26 g / L for casein TG, distributed as follows: 46% for α_s-casein, 34% β–casein and 13% κ-casein. Samples of native casein were obtained by ultracentrifugation (UC) of raw milk previously defatted operating at 24000 rpm x 45 min, T = 4 ° C and pressure = 10 Pa. All the commercial preparations were dissolved in PBS and CBS, both 0.1 M, pH 6.8. Tests to check the influence of pH were carried out in phosphate solutions at pH 6.8 (PBS, native value), 7.0, 8.0, 9.0, 10.0. Tests to verify the effect of temperature were performed using solutions at pH 6.8 at five different temperatures in the range 20° to 60° C (20°, 30°, 40°, 50°, 60° C). All experiments were carried out in duplicate.

Spectroscopic analyses

Mid-infrared spectroscopy
The spectra were recorded using a MIR spectrometer Jasco FT / IR 400 (Jasco Europe, Italy) in the range 4000-500 cm^{-1} using multiple reflection ATR (Attenuated Total Reflectance) system, with a cell of ZnSe crystal for liquids. Spectra were collected using a resolution of 4 cm^{-1}.

Near infrared spectroscopy
The NIR spectra were obtained with spectrometer Buchi NIRFlex N-500 (BUCHI Italy, Italy) and collected between 10000 and 4000 cm^{-1} with a quartz cuvette (optical path = 0.2 mm). All spectra were pretreated by applying the second derivative Savitzy-Golay (SG 15, 2, 0), corrected by the multiplicative scatter correction method and mean centered. Principal Component Analysis was applied with Matlab R2009a (The Mathworks Inc., USA) combined with PLS Toolbox (Egenvector, USA). The loadings of the first three Principal Components (PC1, PC2, PC3) multiplied by the respective scores were used to reconstruct the spectra in order to highlight information relating exclusively to the intermolecular interactions. The sum spectrum of individual casein sub-fractions spectra was also calculated (synthetic casein = SC).

3.1.3 Results and discussion

TG casein samples were dissolved in PBS 0.1M in order to reproduce as well as possible the environment and the interactions that occur in milk.

Interpretation of phosphate solutions MIR spectra at different pH

As a preliminary study, phosphate solutions 0.1M, at different pH from 4 to 13 were scanned in the MIR range in order to recognize spectral signals related to phosphate species deriving from buffer. Spectra are shown in Figures 3.3 and 3.4.

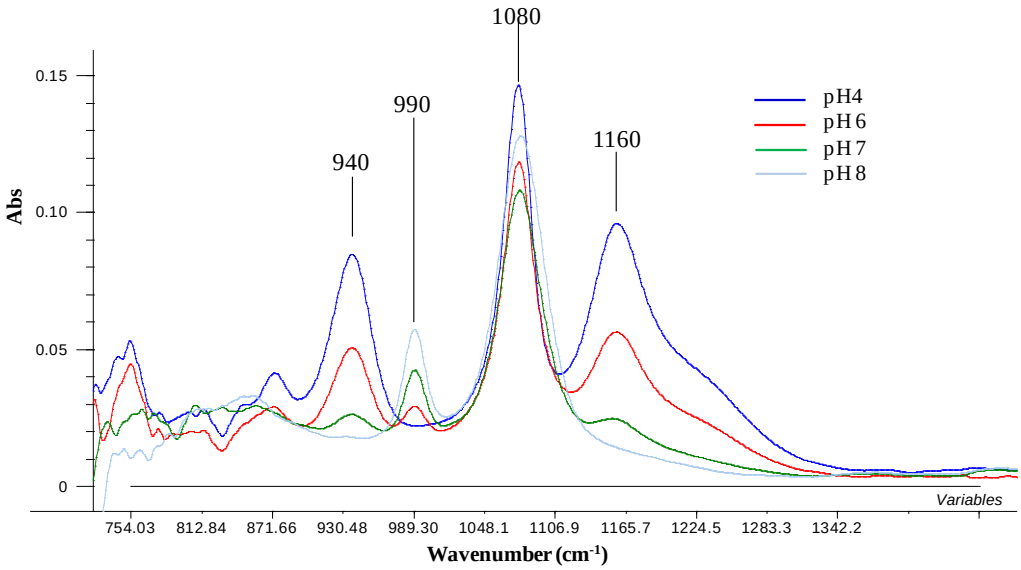

Figure 3.3: MIR spectra of phosphate solutions at pH 4-8.

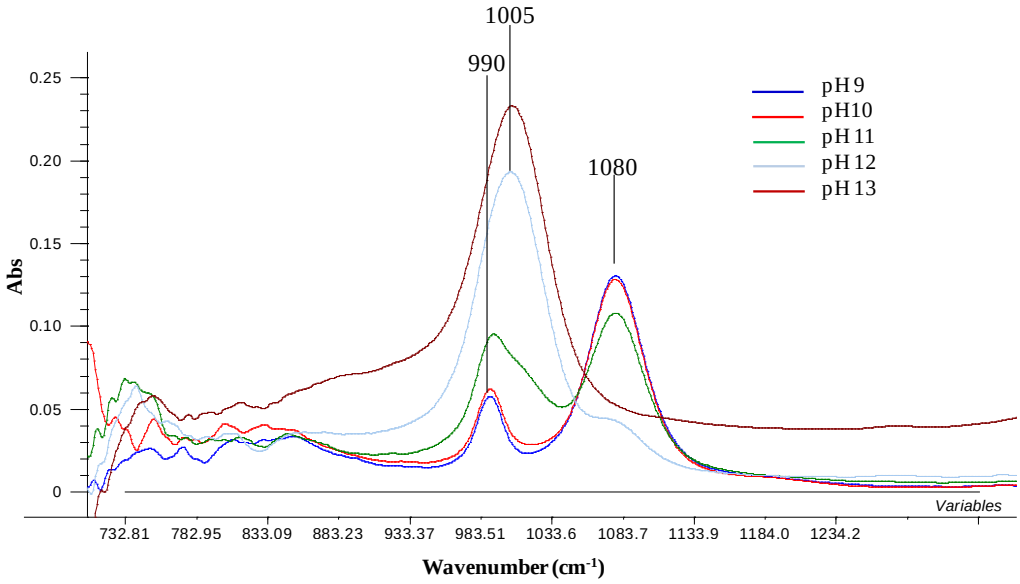

Figure 3.4: MIR spectra of phosphate solutions at pH 9-13.

In order to assign the absorption bands, the distribution diagram (HySS 3.1 Hyperquad Simulation and Speciation, 2003, Protonic Software) of phosphoric acid (pK_{a1}= 2.1; pK_{a2}=7.1; pK_{a3}=12.4) was considered (Figure 3.5). From the diagram, the concentration of the predominant anionic species at each pH were calculated. According to these findings, the wavelengths at 940 and 1160 cm^{-1} were assigned to vibrations related to the monoanion $H_2PO_4^-$: this species, prevalent at low

pH, was evident only in the phosphate solutions from pH 4 to pH 7 and disappeared yet at pH=8. Bands at 990 cm^{-1} were attributed to vibrations of the dianion HPO_4^{2-} with a constant concentration from pH 8 to pH 10. Some bands are present at all pH because they plausibly refer to stretching or bending of groups common to both species, for example the band at 1080 cm^{-1}, which disappears at pH = 12-13 when all the phosphoric acid is dissociated. At pH 11 a band around 1005 cm^{-1} appeared: since its intensity increased at increasing pH values, it plausibly refers to PO_4^{3-} species (Stuart, 2004).

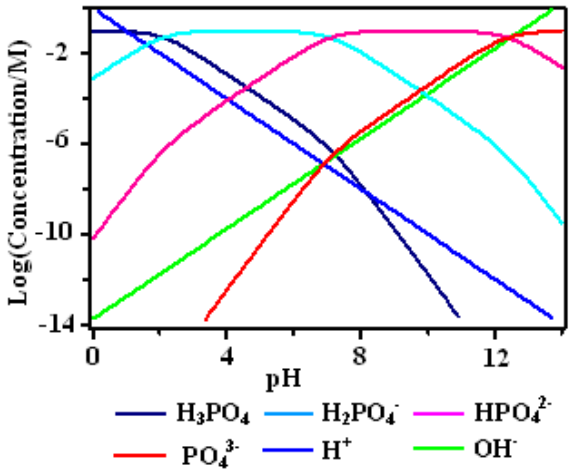

Figure 3.5: Distribution diagram of phosphoric acid.

Casein MIR spectra interpretation

Figure 3.6 shows the average MIR spectra of TG casein in PBS 0.1M at pH 6.8. Spectra were subtracted of buffer and water contributions, in order to make evidence to the absorption of casein compounds.

In water-subtracted spectra some absorption bands of the phosphate groups were still visible. It was possible to recognize the two broad bands related to phosphate at 990 and 1080 cm^{-1} and the weak bands at 940 cm^{-1} and 1160 cm^{-1} of stretching and bending of the mono-anion. At this pH value, in fact, mono-anion is not the prevalent specie.

In PBS-subtracted spectra, only phosphate bands at 990 and 1078 cm^{-1} were recognizable: these absorptions were plausibly assigned to phosphate groups present in the casein structure. This was confirmed by comparison with spectra of TG casein dissolved in TRIS buffer where these bands were clearly recognizable (data not shown).

On the right side of both spectra it was possible to recognize the amide I and amide II region, between 1500 and 1800 cm^{-1}. In particular the amide I consisted of a broad band centered around 1644 cm^{-1} related to the C=O stretching, while the amide II occurred at 1548 cm^{-1}. Amide II derives mainly from in-plane N-H deformation and from C-N and C-C stretching vibrations (Stuart, 2004).

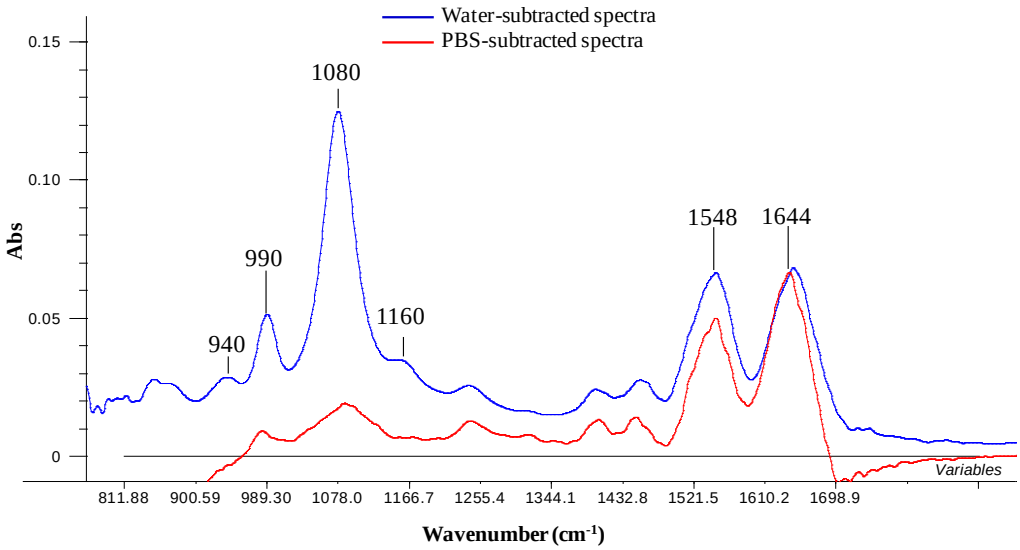

Figure 3.6: MIR water- and PBS-subtracted spectra of TG casein.

In order to analyze the remaining portion of the spectrum, whose interpretation is not detailed in the literature, considerations were made by comparing the spectrum of the casein TG as such and spectra of casein with the addition of Ca^{2+}, EDTA and citrate (Figures 3.7 and 3.8). The pH of casein solutions were kept at 7, in order to avoid modifications of phosphate bands.

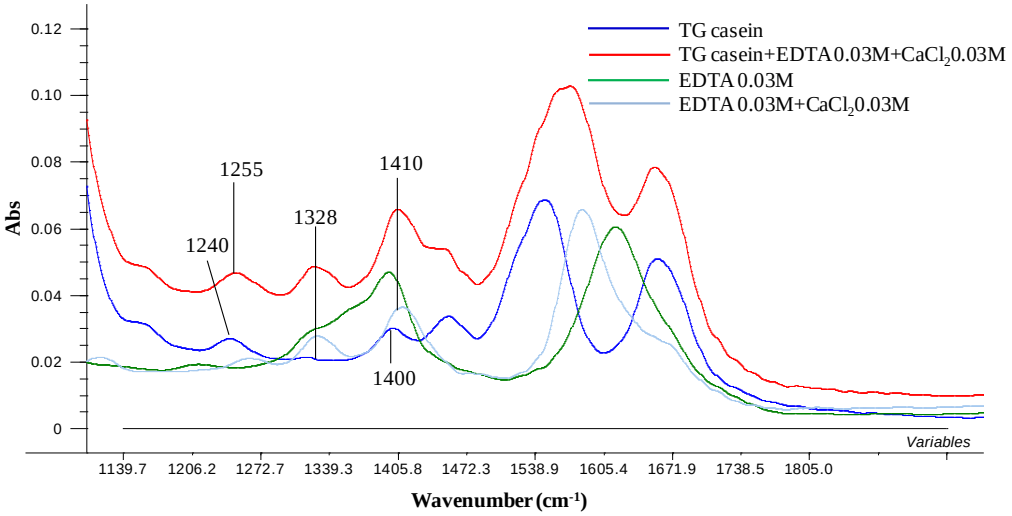

Figure 3.7: MIR spectra of TG casein, EDTA and their complexation with Ca^{2+} ion.

The band located at 1240 cm^{-1} is reported in literature as an overlapping region assigned to the vibrations of amide III (Stuart, 2004). In our experiments, in TG casein samples after adding Ca^{2+} and EDTA, this band showed a shift from 1240 to 1255 cm^{-1}. It means that upon removal

of calcium by EDTA, the signal moves to higher wave numbers. For this reason the band was assigned to a phosphate group bound to Ca^{2+}: in fact, the free phosphate group has stronger bonds than when it is coordinated with calcium; thus, losing calcium bond, phosphate absorption band moves to higher wave numbers, corresponding to higher frequency and higher bond strength.
The weak signal positioned around 1400 cm^{-1} in the TG casein spectrum shifted to higher wavenumbers (1410 cm^{-1}) as well by adding $CaCl_2$ and EDTA. By comparison with literature data (Mizuguchi et al., 1997) and with spectra of EDTA and Ca^{2+}- EDTA solutions, the band at 1400 cm^{-1} was assigned to the symmetric stretching of COO- group bound to calcium in the protein, while, the band at 1410 cm^{-1} was assigned to the symmetric stretching of the same group in EDTA. In the presence of EDTA, calcium is surrounded by four COO- groups, while in casein is bound to just one COO- group. In the two cases, the binding has a different strength and therefore, with or without EDTA, has a different frequency.
Conversely, in presence of citrate, another calcium complexing, the band shifted to lower wavenumbers, around 1397 cm^{-1}. This band appears to be also present in the spectrum of the citrate solution, occurring at 1390 cm^{-1}. In order to understand if the signal at 1402 cm^{-1} was influenced by citrate, the sum of the spectrum of casein without citrate and the spectrum of citrate (adjusted for the amount of citrate present in milk) was calculated (Figure 3.8).

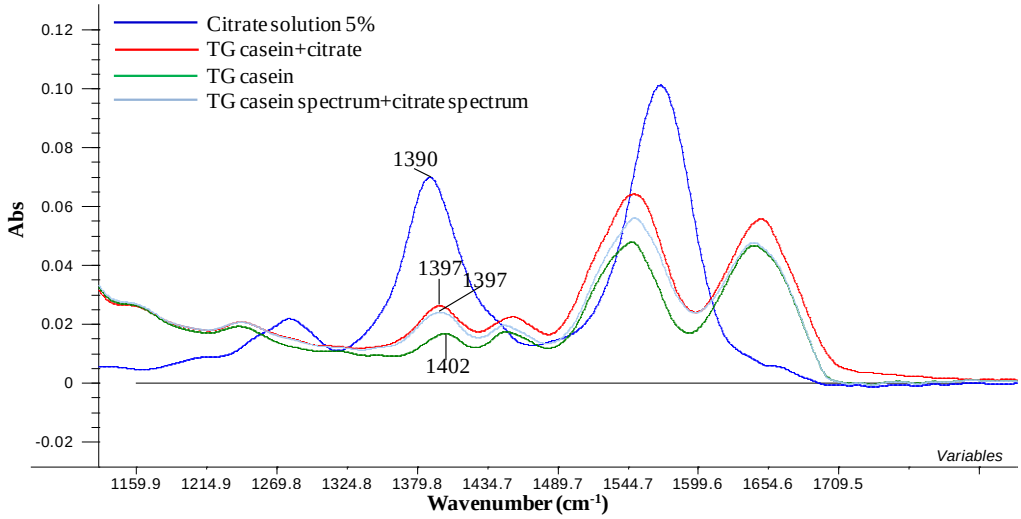

Figure 3.8: MIR Spectra of TG casein before and after adding citrate solutions.

The considered band still moved to higher wavenumbers and overlapped with that at 1397 cm^{-1}, present in the spectrum of casein with citrate. This means that the shift observed by adding citrate to casein, was actually due to the superposition of bands of casein and citrate rather than to an interaction between citrate and caseinic calcium.
By adding calcium and EDTA to casein solution, a new band appeared at 1328 cm^{-1}. This band was absent in the casein spectrum and increased intensity with increasing concentration of $CaCl_2$ and EDTA. This absorption was plausibly assigned to a EDTA-Ca^{2+} complex, being also present in the spectrum of a Ca^{2+}-EDTA solution.

Study of the influence of the buffer solution

The study of the influence of the buffer solution used as a solvent has highlighted the contribution to the absorbance of phosphate groups, which link together the casein sub-fractions in the micelle. These groups, resulting from the use of phosphate buffer as solvent, are no longer free in solution but involved in the micelle aggregation. Figures 3.9 and 3.10 report some examples of the effects of the two buffers, expressed as a mathematical difference between spectra obtained at the same pH (6.80) and at the same concentration (100 mM) using citrate or phosphate buffer solution in both MIR and NIR spectral regions.

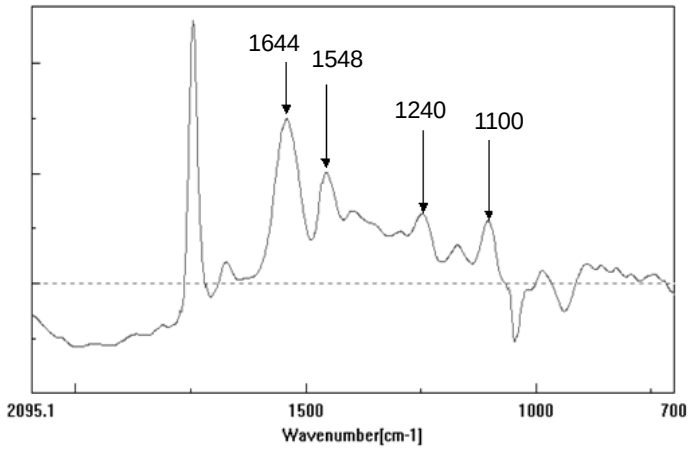

Figure 3.9: MIR spectrum of differences between phosphate buffer solution and citrate buffer solution (pH 6.80; 100 mM) of TG casein.

The main absorption groups, due to the structure of proteins, were clearly identified in the MIR region (Figure 3.9) in the presence of phosphate buffer as solvent. The presence of a peak at 1100 cm^{-1} confirmed the role of phosphate groups in the formation of intra-and inter-molecular bonds that help to stabilize the molecular structure of the casein micelle.
The main absorption bands (Williams & Norris, 2001) visible in the NIR region suggested a contribution of specific groups to the stabilization of the micelle structure, as shown in Figure 3.10. Data confirmed the formation of hydrogen bonds between the different peptides and phosphate groups that link the sub-micelles into a single macro-micelle.

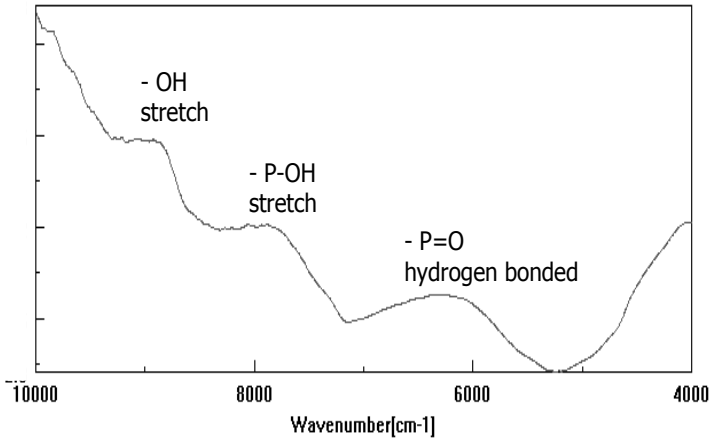

Figure 3.10: NIR spectrum of differences between phosphate buffer solution and citrate buffer solution (pH 6.80; 0.1 M) of TG casein.

Temperature-dependent MIR and NIR modifications

In order to evaluate temperature-dependent modifications in casein fractions, solutions of α_s-, β- and κ- casein in 0.1 M PBS pH 6.8 at 20°, 30°, 40°, 50° and 60°C were scanned in MIR region. Figures reported below show the spectra of each fraction at 20°C and 60°C.

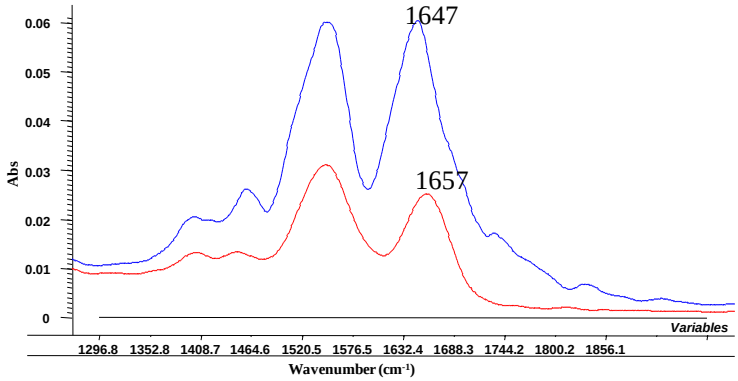

Figure 3.11: Amide I and II MIR spectra of α_s-casein (20°C blue; 60°C red).

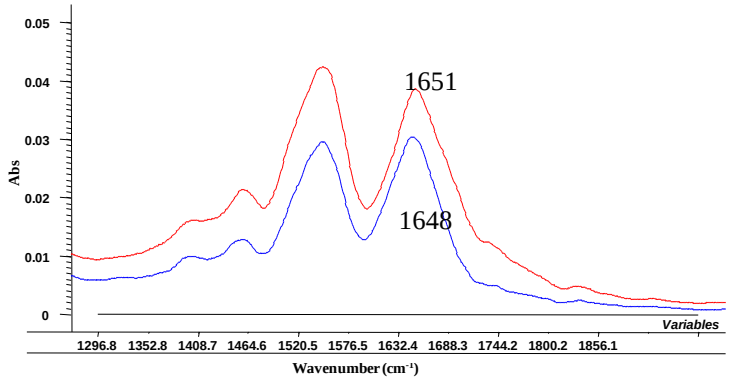

Figure 3.12: Amide I and II MIR spectra of β-casein (20°C blue; 60°C red).

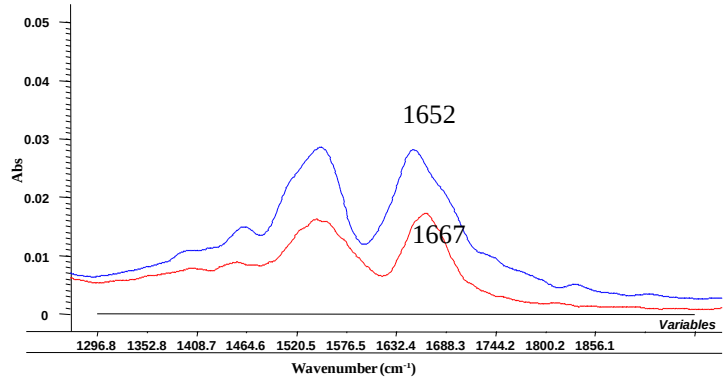

Figure 3.13: Amide I and II MIR spectra of κ-casein (20°C blue; 60°C red).

A shift of amide I band towards higher wavenumbers was detected for all fractions.
The amide I band of peptides and proteins, related to the carbonyl stretching vibration of the peptide backbone, is a sensitive marker of peptide secondary structure, depending on hydrogen bonding and the interactions between the amide units (Surewicz, 1993).
Each casein fraction showed different gap amplitude. As it can be seen in Figures, amide I band of κ- casein had the largest gap of 17 cm^{-1}, moving from 1652 cm^{-1} to 1667 cm^{-1}; β-casein presented the narrowest shift of 3 cm^{-1}, from 1648 cm^{-1} to 1651 cm^{-1}; regarding α_s-casein, the band moved from 1647 cm^{-1} to 1657cm^{-1} with a gap of 10 cm^{-1}. This behavior reflects molecules properties: κ-casein is the more hydrophilic casein and in an aqueous medium shows a more linear structure than β-casein, which is conversely the most hydrophobic (Horne, 2002). Thus, κ-casein is the most susceptible to variation induced by temperature, showing the largest gap in wavenumbers. α-casein hydrophobicity, which is higher than κ-casein, but lower than β-casein, produced an intermediate shift amplitude.

Figure 3.14 shows an example of the differences occurred with changes in temperature in NIR spectra of TG casein in PBS (0.1 M pH 6.8).

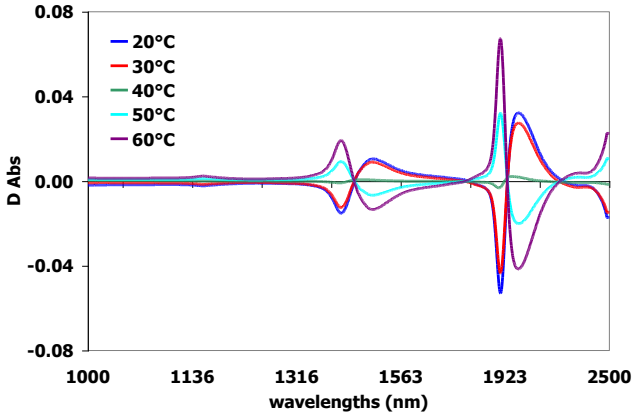

Figure 3.14: NIR spectra of TG casein in PBS 0.1 M pH 6.8, at different temperature.

In any case, regardless of the type of casein analyzed (single sub-unit, TG casein, UC preparation) in the NIR region were detected only changes related to the absorption bands of water. No changes in overtone or combination bands related to structural groups specific of casein molecules as a function of temperature were detected, in agreement with data reported in the literature (Czarnik-Matusewicz & Ozaki, 2005).

pH-dependent MIR and NIR modifications

Commercial preparations of casein diluted in phosphate solutions at different pH from 6.8 to 10 were scanned in MIR range. Spectra subtracted of phosphate and water contribution are reported in Figures 3.15 and 3.16.
Appreciable changes were noticed only in the area of absorption of phosphate groups in the spectra without the aqueous component. Again, it was possible to notice the two bands related to phosphate at 990 and 1080 cm^{-1} present in all the samples. Conversely, the band at 940 cm^{-1} of the monoanion was present exclusively in samples with the lowest pH.

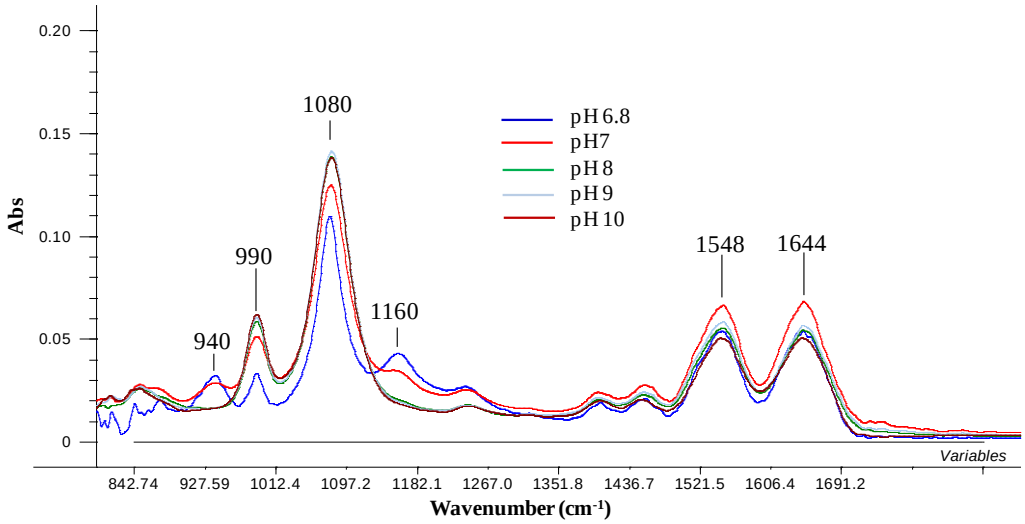

Figure 3.15: MIR water-subtracted spectra of TG casein at pH 6.8-10.

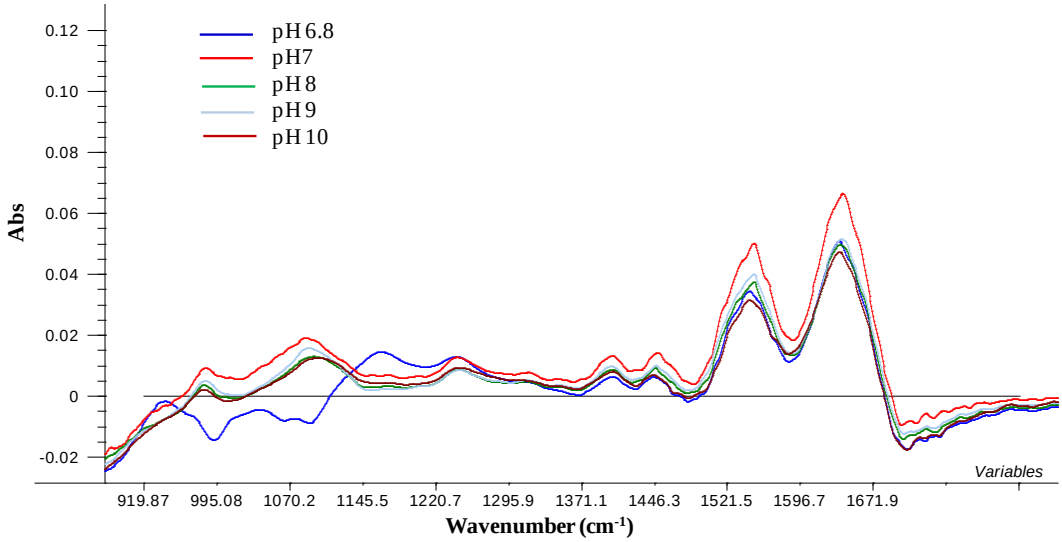

Figure 3.16: MIR PBS-subtracted spectra of TG casein at pH 6.8-10.

pH variations didn't induce observable modifications in bands of amide I and II.

Figure 3.17 finally shows the variations which occurred in the analyzed solutions dissolved in 0.1 M PBS in response to changes in pH, expressed as differences of absorbance (Δ Abs) from the mean NIR spectrum.

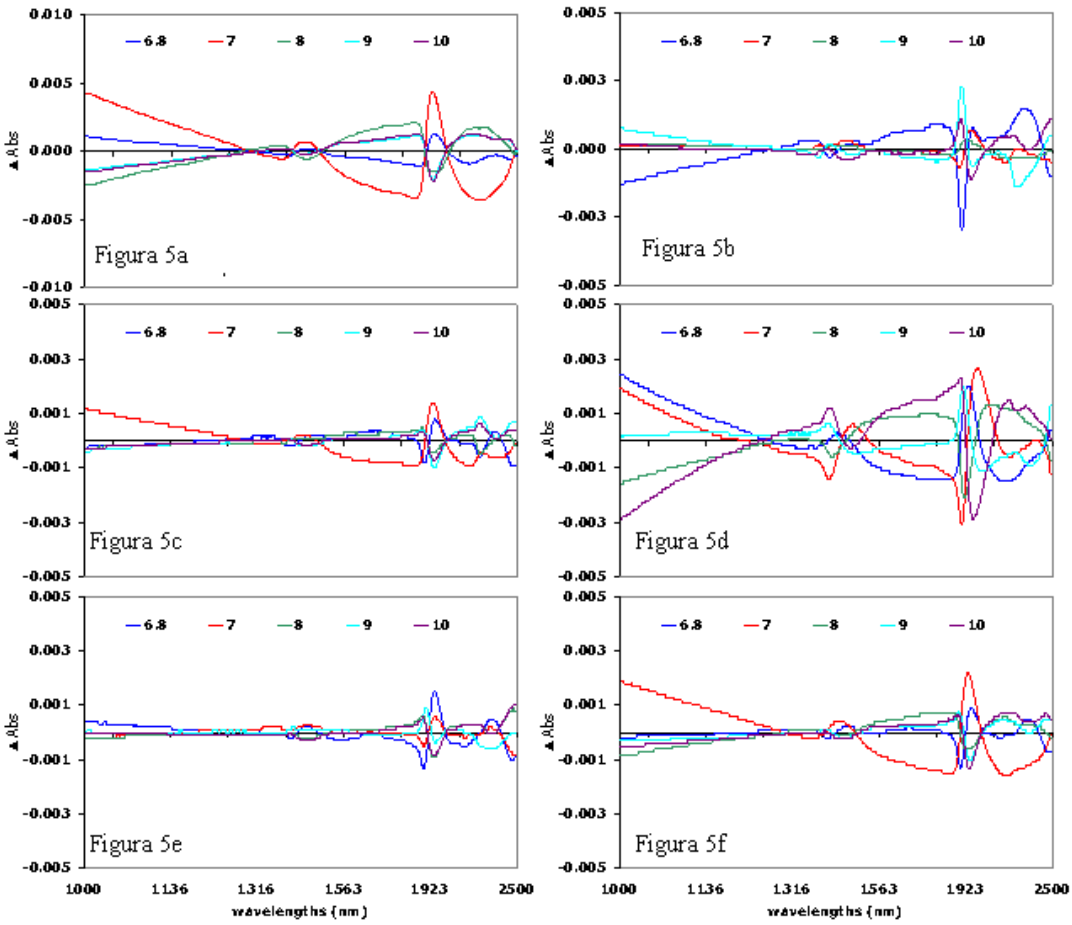

Figure 3.17: pH effect (6.80 – 10) on solution of: α_s-casein [a)]; β-casein [b)]; κ-casein [c)]; TG casein [d)]; UC casein [e)]; SC casein [f)] scanned in NIR region.

It was interesting to note that the series are no longer ordered, such as in the case of temperature changes, but some reversals or changes in the linearity were observed, caused by different interactions of the basic groups of proteins. In particular, in the series of α - (Figure 3.17a) and β-casein (Figure 3.17b), the reverse around 1900-1940 nm occurred at pH 8, while in the spectra recorded for κ - casein (Figure 3.17c), this inversion occurred at pH 7.

The number of amino acid residues, which are ionized at these pH values, reported in Table 3.1, provides a biochemical explanation of the different observed behaviors. The reversal recorded at pH 7 in the case of κ-casein is also justified by the more hydrophilic nature of this fraction compared to the others.

In the case of the spectra of synthetic casein (SC, Figure 3.17f), obtained by calculating the sum of the spectra of individual casein sub- fractions, the reverse occurred at pH 8. This behaviour can be explained by considering that the signal strength of the fractions α - and β -casein is higher than the κ-casein, thanks to their higher concentration.

Reversals in the series of TG casein (Figure 3.17d), as well as those of the UC casein (Figure 3.17e) occurred at pH close to 7. This behavior is consistent with the localization of κ-casein micelle in the whole micelle: in fact, according to its hydrophilicity, it is located in the outer region, being able to interact more and for first with external agents.

AA residues	α_s-casein	β-casein	κ-casein
Asp	11	4	3
Glu	49	19	12
His	8	5	3
P-Ser	19	5	1

Table 3.1: Number of negative charged amino acid residues at pH $\geq$ 6.80 in the casein sub-fractions (Swaisgood, 1992).

3.1.4 Conclusions

These results proved the adequacy of the NIR and MIR spectroscopic techniques for the study of intermolecular interactions of milk micellar proteins in aqueous environment. Interesting informations was provided on the effects of solvent. The spectral response, otherwise, was less affected by modifications of the temperature parameter. MIRS detected shifts in peaks maxima of amide I bands of casein fractions, related to modifications of H bonds. These shifts were related also to hydrophobicity properties of caseins. NIRS could detect modifications of only water bands.
Regarding pH, MIR could detect modifications of only phosphate groups of PBS. ΔAbs from the NIR mean spectrum evidenced some modifications of linearity due to the number of negative charged amino acid residues at pH $\geq$ 6.80 in the casein sub-fractions.
These techniques allowed to detect the presence of inorganic phosphate groups in the whole micelle, even if these groups are not linked directly to individual sub-fractions.

3.1.5 References

Czarnik-Matusewicz B, Ozaki Y Analysis of the aggregation process of b-casein by near infrared spectroscopy. Proceedings of XII ICNIRS, Auckland, NZ, 2005, pag.837.

Holt C, Horne DS, 1996, The hairy casein micelle: Evolution of the concept and its implications for dairy technology. Neth Milk Dairy J, 50: 85-111.

Horne DS, 2002, Casein structure, self-assembly and gelation. Curr opin colloid In 7:456-461.

Mizuguchi M, Nara M, Kawano K, Nitta K, 1997, FT-IR study of the Ca^{2+}-binding to bovine α-lactalbumin: Relationships between the type of coordination and characteristics of the bands due to the Asp COO^- groups in the Ca^{2+}-binding site. FEBS Lett 417: 153-156.

Mucchetti G, Neviani E Microbiologia e tecnologia lattiero-casearia. Qualità e sicurezza. Tecniche Nuove, Milano, Italy, 2006.

Rollema HS Casein association and micelle formation. In Advanced Dairy Chemistry, Vol. 1: Proteins (ed. P.F. Fox), Elsevier Science Publisher, Ltd., Essex, 1992, pp. 111-140.

Stuart BH, Infrared spectroscopy: fundamentals and applications. John Wiley and Sons, Ltd, The Atrium, Southern Gate, Chichester, West Sussex, England, 2004.

Surewicz WK, Mantsch HH, Capman D, 1993, Determination of protein secondary structure by Fourier transform infrared spectroscopy: a critical assessment. Biochem 32:389–394.

Swaisgood HE Chemistry of the caseins. In Advanced Dairy Chemistry, Vol.1: Proteins (ed. P.F. Fox), Elsevier Science Publisher, Ltd., Essex, 1992, pp. 63-110.

Walstra P, 1999, Casein sub-micelles: do they exist? Int Dairy J, 9: 189-192.

Williams P, Norris K, Near-infrared technology in the agricultural and food industries. American Association of Cereal Chemists, Inc. St. Paul, Minnesota, USA, 2nd ed., 2001.

3.2. NIRS ability in predicting the casein content and in studying micelles interactions

3.2.1 Aim

The aim of this research activity was to investigate the near infrared spectra of different casein solutions in order to improve knowledge of the structure of casein aggregates and their sub-units, also on the basis of a suitable prediction of casein content with two types of equipment.

3.2.2 Materials and methods

Samples

Raw bulk milk samples were collected from different farms in the Asturias region (Spain) during one month period.

Chemical analyses (in duplicates) of Total Protein (TP%) and Non Caseinic Nitrogen (NCN%) contents were performed by Kjeldahl's method (Standard ISO 8968-1:2001/IDF 20; Standard ISO 17997-1/IDF 029-1:2004)and casein content was calculated as the difference between TP and NCN contents. Milk samples were split into two aliquots: the first one was ultra-centrifuged at 100 000 g for 1 hour at 4°C ±1°C in order to obtain the native casein by sedimentation; the second one was acidified with HCl 3 N until pH=4.6 and then centrifuged at 30 000 g for 30 min at 4°C ±1°C to get the acid casein. The two types of casein, for a total of 116 samples, were then reconstituted to the final concentration equal to their initial concentration in milk by diluting the centrifuged samples in adequate amounts of phosphate buffer (PBS 0.1M, pH=6.8).

Electrophoretic analyses

Capillary Zone Electrophoresis (CZE) analyses were also carried out on reconstituted samples with a Beckman P/ACE MDQ apparatus (Beckman Instruments, Fullerton, CA, USA). Separations were performed under denaturant conditions at 38°C ±1°C in a coated fused-silica capillary, by applying a 25kV voltage, as reported by Recio (Recio & Olieman, 1996).

Near infrared spectroscopy

Spectra of reconstituted casein were collected at 37°C ±1°C with two types of equipment, an FT-NIR (Perkin-Elmer, USA) and a Foss-NIRSystem 6500 (Foss, Denmark). FT-NIR analysis was performed in transflectance mode (1112-2500 nm; resolution=4cm^{-1}). Each spectrum was averaged from two duplicates.

Samples were also scanned in 400-2498 nm region with the Foss-NIRSystem 6500 equipped with a transport module. In particular, a first subsample was placed in a 50 mm-diameter gold transflectance cell, with 0,1 mm sample thickness cam-lock cell and scanned at 2 nm intervals. The second subsample was analyzed in reflectance mode with an opaque liquid cell. In both cases, samples were analyzed in duplicate and each spectrum was averaged from 32 scans.

Data were processed by the Unscrambler software v.9.2 (Camo Inc., Norway).

3.2.3 Results and discussion

Milk is a very complex matrix, consisting of proteins in colloidal dispersion, fat in emulsion and minerals in solution. Therefore, it was decided to work with a simplified model, in order to

focus the attention only on the caseinic portion, but maintaining the same properties and proportions present in milk (solution state, pH and casein concentration on the basis of Kjeldahl's results). Furthermore, under these conditions it's possible to evaluate the sensitivity of the spectroscopic technique when applied to a single matrix but using different instrumentations and procedures.
The electrophoretic analysis performed on samples of reconstituted casein allowed the separation of the different casein fractions. The obtained results, expressed as normalized area (area / migration time), are shown in Figure 3.18.

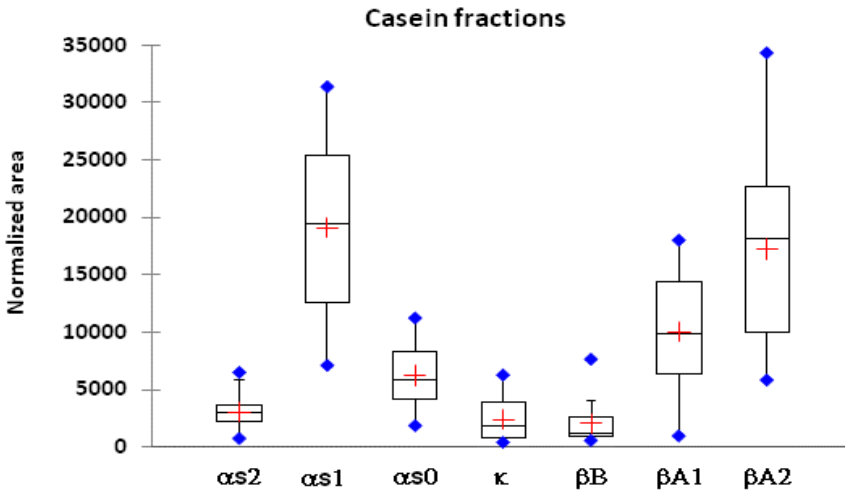

Figure 3.18: Box plot representation of casein fractions content in reconstituted samples. Line in the centre of the rectangular box represents the median, cross represents the mean value and diamonds indicates the maximum and minimum values of the data set.

Figures below show some examples of NIR spectra of reconstituted caseins obtained with different instruments and different sample presentation modes.

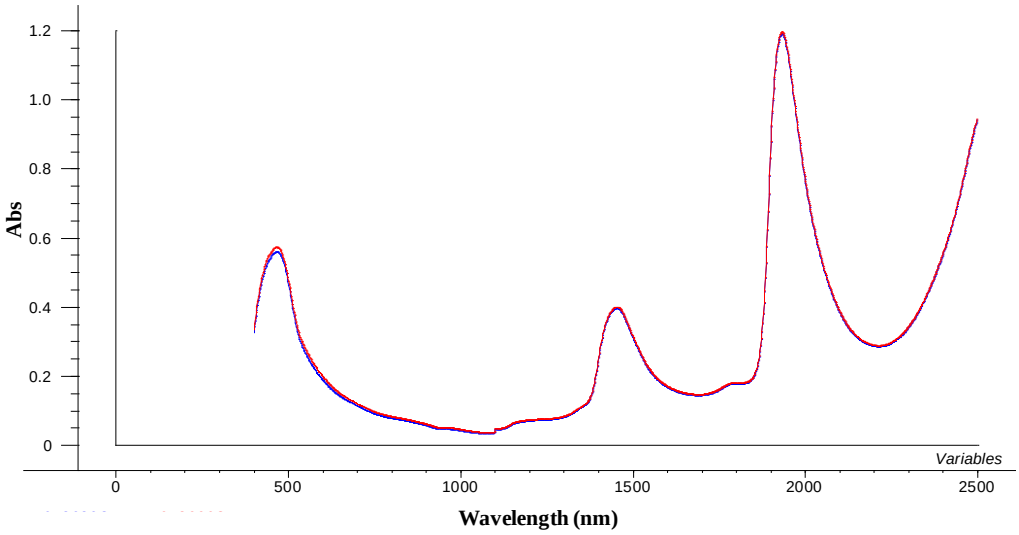

Figure 3.19: Examples of NIR spectra of reconstituted native (blue) and acid casein (red) obtained in transflectance mode with Foss-NIRSystem 6500.

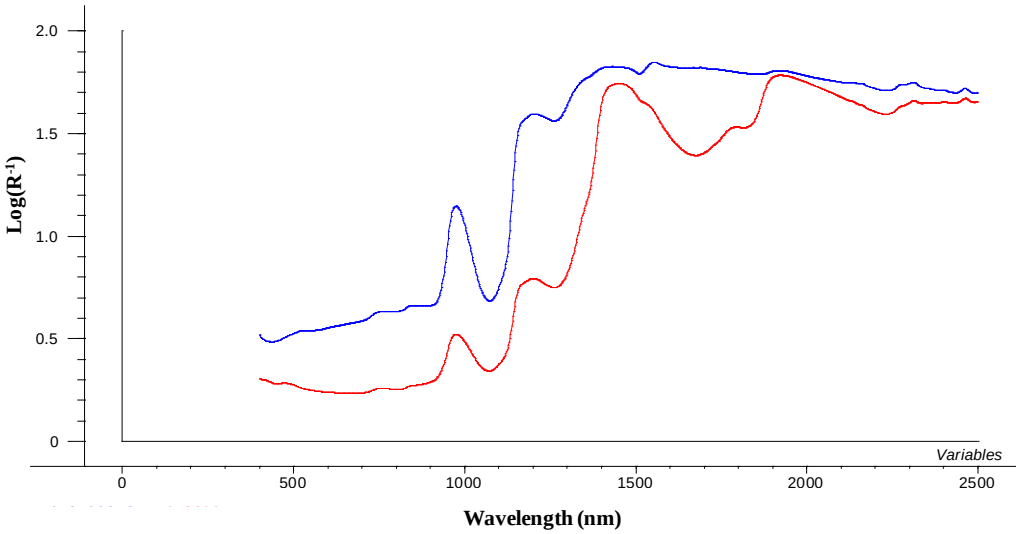

Figure 3.20: Examples of NIR spectra of reconstituted native (blue) and acid casein (red) obtained in reflectance mode with Foss-NIRSystem 6500.

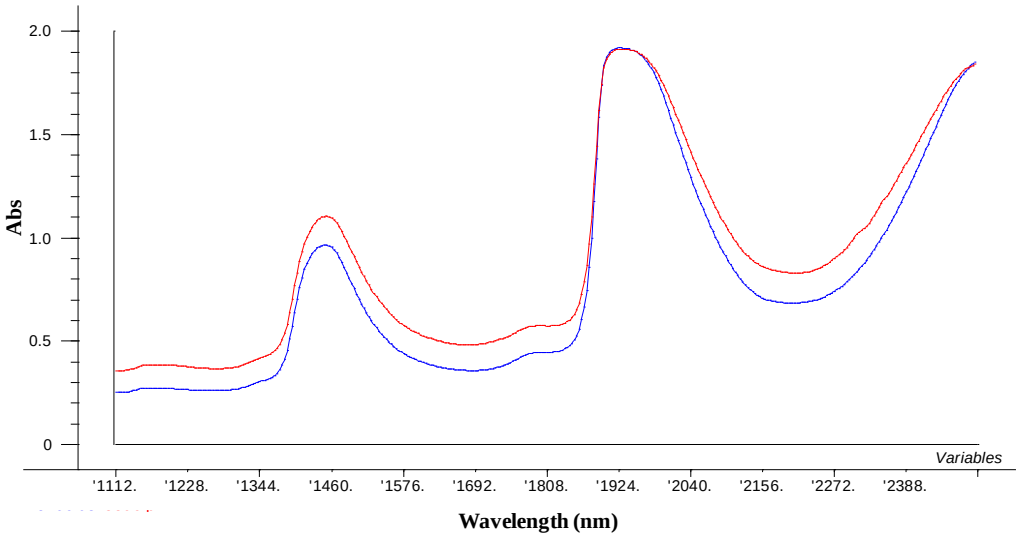

Figure 3.21: Examples of NIR spectra of reconstituted native (blue) and acid casein (red) obtained in transflectance mode with FT-NIR Perkin-Elmer.

Spectra acquired in NIR transflectance mode (Fig.3.19) did not show substantial differences among the two types of samples and were characterized by the strong absorption bands related to water: 1450 and 1940 nm, representing the O-H first overtone stretching and the O-H second overtone bending respectively (Williams & Norris, 2001).
Spectra acquired in FT-NIR transflectance mode (Fig. 3.21) were still dominated by water absorption bands, but in this case a weak separation between ultra centrifuged native casein and demineralised acid casein samples was noticeable.
More interesting was the case of spectra obtained in reflectance mode (Fig. 3.20): in this case NIR spectroscopy was able to well separate the two types of reconstituted casein.
PLSR (Partial Least Square Regression) analysis was performed by using all NIR spectra collected by the different instruments and electrophoretic data. Table 3.2 shows the statistical parameters obtained, in terms of number of Latent Variables (LV), coefficient of correlation in calibration (Rcal) and in cross-validation (Rval), root mean square of standard error in cross-validation (RMSECV); also the pre-processing procedures applied to spectra (SG: second derivative Savitzky-Golay, 5 points, polynomial order 2; SNV: Standard Normal Variate) are reported.

Instrument	Spectral range	Variable	LV	Rcal	Rval	RMSECV	Pre processing
FT NIR transflectance	1112-2500 nm	αs_2		poor	poor		
		αs_1	4	0.918	0.864	3206.36	none
		αs_0	1	0.837	0.813	1346.24	none
		κ	10	0.999	0.801	1207.78	SG
		βb		poor	poor		
		βa_1	3	0.991	0.750	3414.98	SG
		βa_2		poor	poor		
NIR transflectance	400-2498 nm	αs_2	6	0.847	0.667	1085.12	none
		αs_1	3	0.888	0.861	3504.54	SNV
		αs_0	3	0.88	0.862	1260.51	SNV+SG
		κ	7	0.963	0.800	1261.66	SNV
		βb		poor	poor		
		βa_1	7	0.915	0.823	3262.47	None
		βa_2	2	0.895	0.858	4426.92	None
NIR reflectance	400-2498 nm	αs_2		poor	poor		
		αs_1	3	0.905	0.863	3311.70	SNV+SG
		αs_0	3	0.938	0.898	978.78	SNV+SG
		κ	5	0.949	0.920	759.72	SNV
		βb	9	0.983	0.675	716.48	SNV+SG
		βa_1	4	0.842	0.810	3213.80	None
		βa_2	6	0.933	0.810	4631.04	None

Table 3.2: Statistical descriptors for NIR calibrations of reconstituted samples casein fractions.

In general, the best performances were obtained with the reflectance measurements. This is due to the fact that reconstituted samples are similar to opaque solutions and the reflectance mode exhibits dependency on the light scattering phenomena. NIR reflectance measurements allowed the use of path-lengths longer than in transflectance mode with a depth of light variable for each wavelength. This fact can explain the great variation when measuring non-homogeneous samples (Williams & Norris, 2001).

Satisfactory results were obtained in calibration, with the exception of αs_2 casein, while statistics in validation could be improved by increasing the sample set and creating a reference data set. However these results were in line with those available in literature, considering the fact that the bibliography reports data referred to the milk matrix (Díaz–Carrillo et al., 1993; Barzaghi et al., 2008).

To verify the role of the width of the spectral region on the different performances, a comparison within calibrations was made in a common region chosen between 1112 and 2498 nm. These new models showed a general worsening in calibration and validation results (data not shown). It seemed therefore that in this case the enlarged VIS-NIR spectral region was essential to create good predictive models.

In order to assess the ability of NIR to discriminate between the application of physical and chemical treatments, PCA analysis was applied on the second derivative of reflectance spectra.

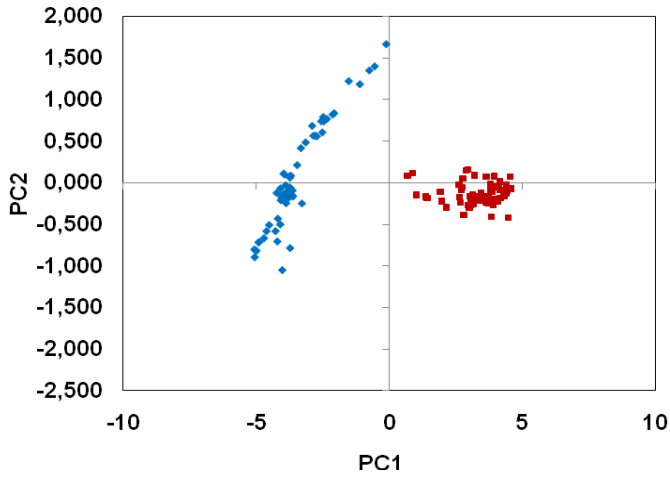

Figure 3.22: Scores plot obtained from the PCA analysis performed on the second derivative of reflectance NIR spectra of native (blue dots) and acid (red dots) casein reconstituted solutions.

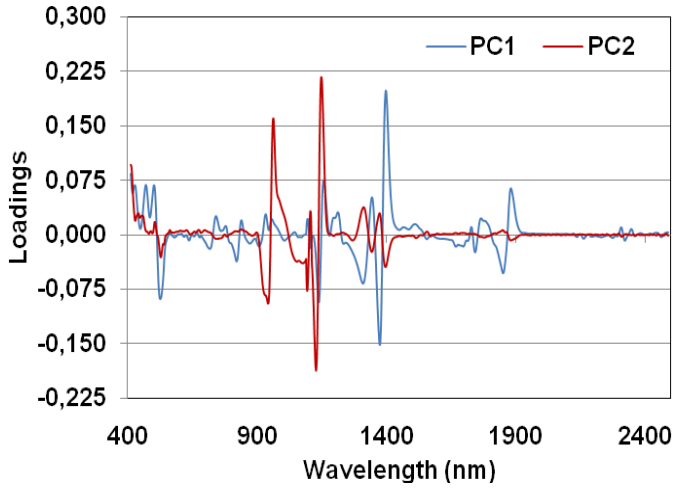

Figure 3.23: Loadings plot on PC1 and PC2 obtained from the PCA analysis.

As shown in figure 3.22, the two groups of samples are perfectly separated along the first principal component (PC1), which was able to explain 98% of the total variance. The second principal component (PC2) explained the remaining 2% of the total variance and seemed to be able to weakly separate inside the group of reconstituted samples of native casein.
The loadings plot (Fig.3.23) indicated that the separation of the two groups was mainly based on wavelengths related to P-OH stretching (1300, 1876 nm), P-H stretching (1370, 1394 nm) and some related to C-H bond stretching (Williams & Norris, 2001).
These results can prove the ability of NIR to recognize changes in the mineral equilibrium induced by acidification. In fact, caseins are phosphorylated aggregated proteins present in milk in a micellar state which may be separated by acidification, ultracentrifugation, and enzymatic

coagulation. Casein separated by acidification is called acid, demineralized or isoelectric, because it's obtained by acidifying the skimmed milk to pH of 4.6, corresponding to the casein isoelectric point (Fox & McSweeney, 2003). Acid casein is also known as demineralized casein because, as a result of the pH change, it loses part of the calcium and phosphate responsible of the micellar state. Casein obtained by ultracentrifugation is called 'native casein' and maintains the same structure as in milk (Fox & McSweeney, 2003). Thus, although it's the same protein on the basis of its primary structure, the two types of casein show variations in micelles interactions and links between sub-units.
To better understand the molecular differences between native and acid caseins, the second derivative of mean reflectance spectra of the two types of reconstituted samples was compared. In particular, it was possible to distinguish between the specific absorption bands exclusively related to nitrogen compounds and those related to the bonds involved in the stabilization of the micelle structure.

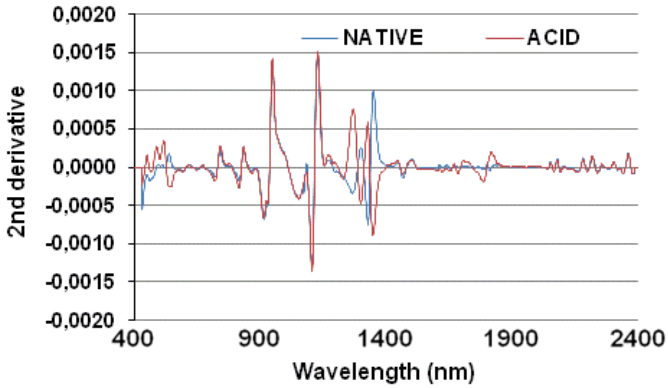

Figure 3.24. Second derivative mean spectra of native (blue line) and acid (red line) casein reconstituted samples.

As shown in Figure 3.24, the portion of the spectrum between 2000 and 2300 nm appeared to be superimposed in the two types of casein. Indeed in this area it's possible to recognize the absorption bands related to the stretching and bending of the N-H bond, in particular: 2120 nm N-H str + C=O str of amino acids, 2148 and 2176 nm combination bands of amide I and III; 2248 nm N-H str + NH_3 def of amino acids; 2290 nm N-H str + C-H def of amino acids (Williams & Norris, 2001).
The absorptions at 2440 and 2482 nm are related to the free P=O group (Williams & Norris, 2001). Casein contains both colloidal organic phosphorus in the form of phosphoserine, and colloidal inorganic phosphorus salified to amino-terminal or carboxylic groups of proteins through calcium. In both cases, the free P=O groups are present (Fox & McSweeney, 2003). These groups were therefore detectable in both the native and the acid casein samples.
In the region around 1050 nm, the second overtone of the N-H group stretching and the combination of the free P=O with the amide I could be recognized (Williams & Norris, 2001).
Another common area of the spectra was identified between 1500 and 1580 nm, where there are bands related to the first overtone of the N-H stretching (Williams & Norris, 2001).

Otherwise, the two types of samples showed a very different behavior in the area between 1200 and 1400 and between 1800 nm and 2000 nm, ascribable to changes in phosphate bonds and water bands (Williams & Norris, 2001).
In the reconstituted acid casein samples, two bands at 1234 and 1294 nm were noticeable. These wavelengths can be assigned to the P-OH bond stretching (Williams & Norris, 2001). When phosphate is bound to serine, two acid functions are free for any salification with cations, especially calcium. It was evident that these bands should be found in reconstituted acid casein: in this case the two acid groups remain free since calcium- phosphate bound is lost (Fox & McSweeney, 2003). The same phenomenon occurred more markedly in the region between 1850 and 1950 nm. In fact, the spectrum of acid casein reconstituted samples showed stronger absorption bands related to the O-H and P-OH groups stretching (Williams & Norris, 2001).
The possibility of a more robust models was explored by applying the PLSD (Partial Least Square Discriminant) technique on the data matrix of raw reflectance spectra. Samples were divided into two groups according to the applied treatment and the belonging to that groups was used as the independent variable. In the model, the native casein samples have a value 0, while acid casein samples have value 1. Figure 3.25 shows the result obtained by applying PLSD, correlating the NIR data set with the treatment applied to obtain casein samples.

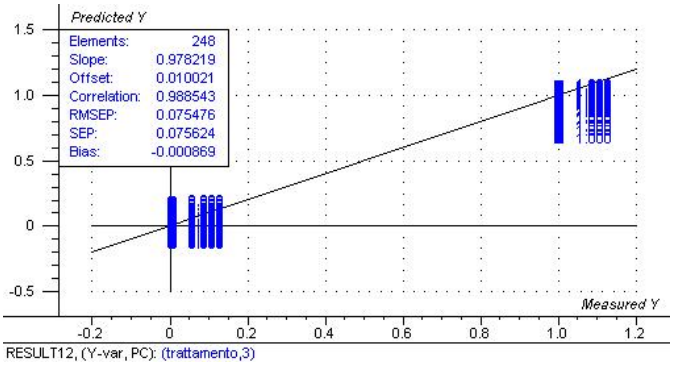

Figure 3.25. Second derivative mean spectra of native (blue line) and acid (red line) casein reconstituted samples.

The regression line, characterized by a good correlation coefficient in prediction of 0.978 and an error in prediction equal to 0.07, showed the ability of NIR technique in discriminating casein samples obtained with different treatments.

3.2.4 Conclusions

In this work a comparison of the performances in calibration of different NIR apparatus and sample presentation modes was made. In the case of casein spectra, the spectral range was found to be more influential than the type of instrument.
These preliminary results confirmed the applicability of NIRS to investigate the structure of casein micelles. Further studies coupled with investigation in the mid-infrared region can help to collect more information for a better characterization of the secondary structure of this protein complex.

3.2.5 References

Díaz –Carrillo E, Muñoz -Serrano A, Alonso -Moraga A, Serradilla –Manrique JM, 1993, Near infrared calibrations for goat's milk components: protein, total casein, α_s-, β- and κ casein, fat and lactose. J Near Infrared Spec 1: 141-146.

Fox PF, McSweeney PLH, Advanced Dairy Chemistry: Volume 1 – Proteins, Fox PF & McSweeney PLH, eds., Springer, New York, USA, 2003.

Recio I, Olieman C, 1996, Determination of denatured serum proteins in the casein fraction of heat-treated milk by capillary zone electrophoresis. Electrophoresis 17: 1228-1233.

S. Barzaghi, E.V. Panarelli, K. Cremonesi, R. Giangiacomo, Capacità predittive della tecnica FT-NIR per la valutazione del contenuto in proteine e caseine del latte destinato alla caseificazione Proceedings of 3rd Simposyum of NIR Spectroscopy Lazise, Italy, 2008.

Williams P, Norris K., Near-infrared technology in the agricultural and food industries. American Association of Cereal Chemists, Inc. St. Paul, Minnesota, USA, 2nd ed., 2001.

3.3 Determination of milk macronutrients by FT-IR and FT-NIR spectroscopic techniques: performance comparison

3.3.1 Introduction

In dairy farms and quality control laboratories, macro-composition of milk is usually determined by appropriately calibrated MIR spectrometers. However, this type of analysis is performed off-line, in the lab. NIR spectroscopy is often presented as a suitable alternative to the MIR for the on line controls of the production. In fact, it allows to use longer pathlengths and optical systems based on quartz optical fibers (Per Waaben, 1998). The main disadvantage might lie in a lower sensitivity. However the literature is poor of studies that directly compare the two techniques.
The aim of the study was to highlight the potential and limitations of using FT-NIR spectroscopy in transmission of non-homogenized raw milk as an alternative to the MIR standard methodology. For this purpose, a same data set of milk samples was analyzed, evaluating the characteristic signals in the two spectral regions.

3.3.2 Materials and methods

173 individual samples of raw milk (78 cows) were collected from 6 different farms of Lombardy.
The samples were analyzed with MilkoScan FT2 (FOSS Italy, Italy) for the determination of protein and fat content, acquiring the MIR spectra in the spectral range 926-5000 cm^{-1}, using a pathlength of 45 μm at a constant temperature 40 °C + 1 °C.
The near-infrared analysis were carried out with FT-NIR instrumentation NIRFlex N-500 (Buchi Italia, Italy), maintaining a constant temperature at 40 °C + 1 °C by temperature control system. The transmittance spectra were recorded in the whole spectral range (4000-10000 cm-1, 32 scans, resolution = 8 cm-1) in quartz cuvettes with optical paths of 200 μm. The samples were kept in agitation and circulated in a cuvette with a peristaltic pump (Madatec, Italy). To minimize the sampling error measures were conducted in triplicate and the average spectrum was calculated. The data set was divided into two groups made respectively by independent 123 (calibration) and 50 samples (validation).
Spectral data were processed by software Matlab R2009a (The Mathworks Inc., USA) combined with PLS Toolbox 5.8 (Egenvector, USA).

3.3.3 Results and Discussion

The chemical composition of the studied individual milk samples is shown in Table 3.3.

	Minimum	Maximum	Mean	Standard Dev.
Fat	2.27	6.89	3.92	0.78
Proteins	2.72	4.48	3.46	0.36

Table 3.3: Chemical composition of milk samples.

The concentration range of the two investigated constituents is wider than those usually referred to bulk milk samples, since these samples are related to individual productions and the composition is highly influenced not only by the breed, but also by milking conditions (system,

time and duration) (Alais, 2000). Figures 3.26, 3.27 and 3.28 show examples of a milk MIR spectrum subtracted of water contribution and a milk NIR spectrum as it and one subtracted of water contribution.

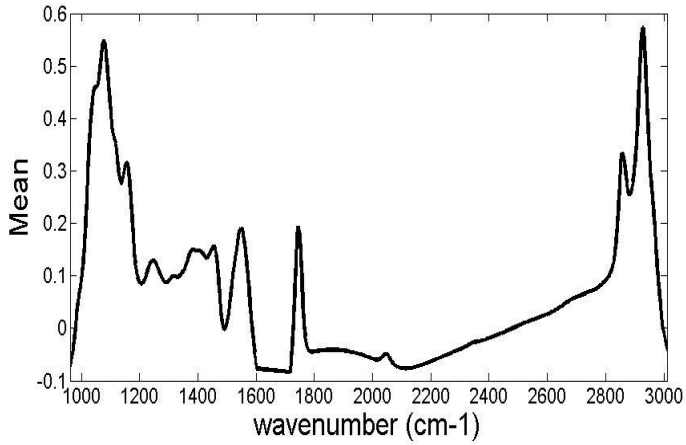

Figure 3.26: Example of milk MIR spectrum.

The MIR spectrum is proposed by the data collection software already subtracted of the aqueous component, as it's included in the instrumental background (Figure 3.26). Despite the complexity of the milk matrix, IR spectrum presents bands which are easily recognizable and easily attributable to the several milk constituents. In particular, signals related to the sugar component around 1080 cm^{-1} (stretching of the CO bond) and 1160 cm^{-1} (asymmetric stretching of the COC bond of the hemiacetal ring) were indentified. The proteic component was recognizable by the presence of the amide II bands at about 1550 cm^{-1} (stretching of the C = O bond). At about 1260 cm^{-1} on the band related to the COC stretching was detectable. The spectral region between 2800 and 3000 cm^{-1} appeared to be dominated by the stretching of the CH bonds. Finally, at 1745 cm^{-1} the stretching of the esters carbonyl group was recognized (Sivakesava & Irudayarai, 2002; Soyeurt et al., 2006).

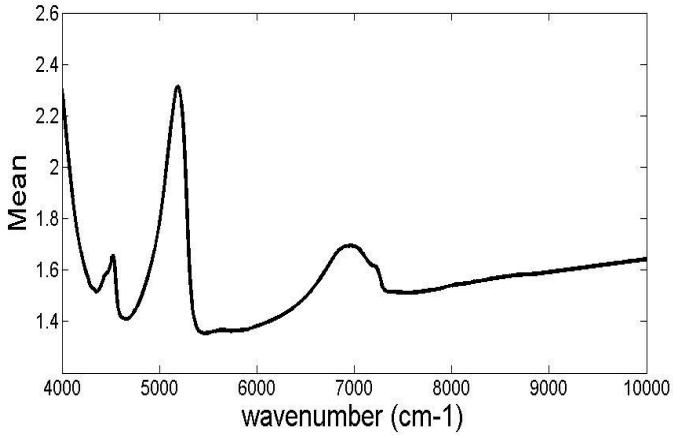

Figure 3.27: Example of milk NIR spectrum.

Because of the presence, in the NIR spectrum (Figure 3.27), of two strong absorption bands at 5100 and 6900 cm^{-1} attributed to the deformation and stretching of the OH bonds of water and the first overtone of the OH stretching, the assignment of spectral bands for the other components of milk is quite difficult. In fact, the spectrum of milk is the sum of each individual components and their specific interactions.

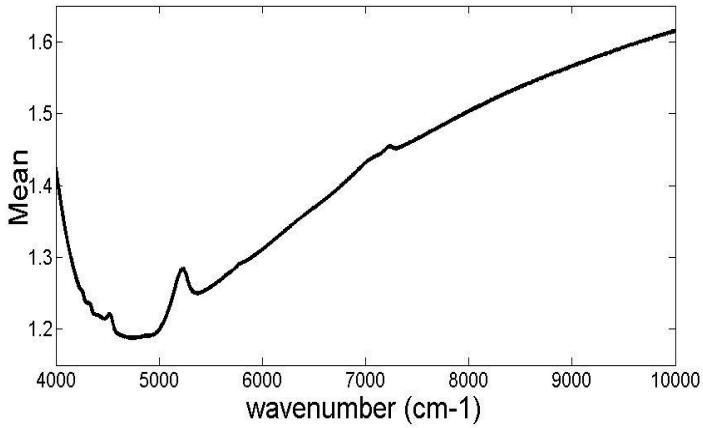

Figure 3.28: Example of milk NIR spectrum subtracted of water contribute.

Looking at the spectra subtracted of the water contribution (Figure 3.28), specific absorption were recognizable: the peak at 4320 cm^{-1} was due to the combination band of bending and asymmetric stretching of the $-CH_2$ group; in the spectral region around 4520 cm^{-1} stretching bands of –CH, C=O and NH bonds and bending of $-NH_3^+$ of the protein component could be recognized; the band at 5228 cm^{-1} was attributable to the second overtone of the stretching of the proteic C = O bond while that around 7240 cm^{-1} was assignable to the bending and stretching of the CH bond of methyl groups (Williams & Norris, 2001).
The comparison between the two spectroscopic techniques was made on the basis of VIP (Variable Importance in Projection from regression model) scores (Chong & Jun, 2005) calculated for each component from the calibration curves obtained for each component in the two spectral regions.
In the MIR region, the response between the sample concentration and the absorbance signal is linear and follows the law of Lambert-Beer. An interesting aspect is that the MIR instrument analyzes the sample after homogenization. This aspect is extremely important, since in milk the variability in the distribution of fat globules, present as an emulsion, would affect the accuracy of the calibration model (Andersen et al., 2002). In the NIR region, the same milk samples were analyzed under conditions as similar as possible to those of MilkoScan, except for the homogenization phase, which was compensated by means of peristaltic pumping.
Data of fat and protein content, expressed as percentage, obtained with MilkoScan were used to build calibration models in the NIR region. Regarding the fat parameter, very good calibrations were obtained without data pre-treatments with values of R^2 in validation of 0.97 and an error in prediction (SEP) equal to 0.14 g/100g. As far as proteins concerned, the best results were obtained using the second derivative (Savitzy Golay, 85, 2) spectra. The coefficient of determination in validation was equal to 0.86 and the SEP equal to 0.19 g/100g. Figure 4-7 shows the VIP scores for fat and protein obtained with both instruments.

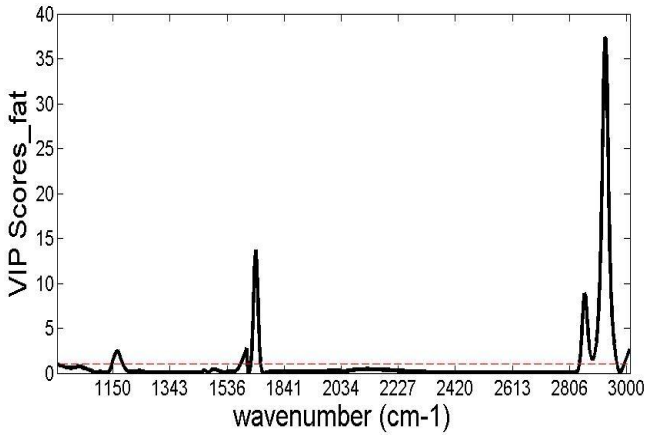

Figure 3.29: VIP scores for fat in the MIR region.

Looking at the VIP scores concerning MIR calibrations (Figures 3.29 and 3.31), wavenumbers responsible of the calibrations performance, previously discussed (1745, 2860 and 2929 cm^{-1} for fat, 1550 cm^{-1} for proteins) were well evident.

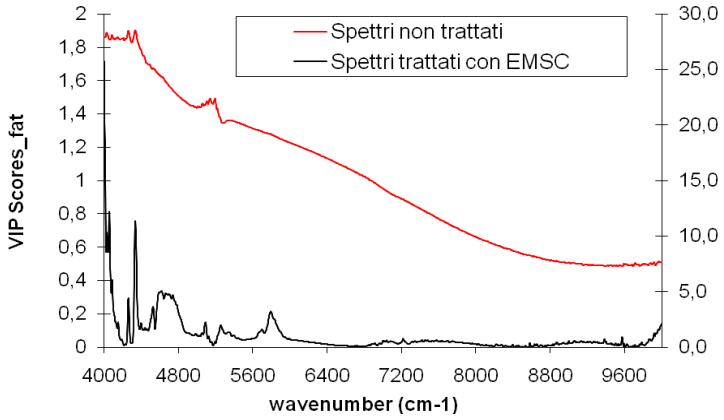

Figure 3.30: VIP scores for fat in the NIR region: raw data (in red) and after EMSC (in black).

In the case of NIR calibration for fat, by considering the VIP scores of original spectra (Figure 3.30), it was impossible to identify specific wavenumbers for this variable, while after pretreatment with EMSC (Enhanced multiplicative scatter correction: fourth-order polynomial) algorithm, peaks at 4530 and 4620 cm^{-1}, characteristic of stretching of the CH and C = O bonds, and at 5256 cm^{-1}, region of the second overtone of the stretching of the C = O group, were recognizable. This can be explained on the basis of the presence in milk of fat globules in emulsion with a few microns size, which, interfering with the wavelengths from 1 to 2.5 μm, cause the scattering of the near-infrared radiation (Cattaneo et al., 2009), modifying the spectrum in a way dependent on the fat concentration. The EMSC pretreatment was used to remove the contribution of the scattering and the interpretation of the data was made on the basis of the variation of the signals of the specific constituent.

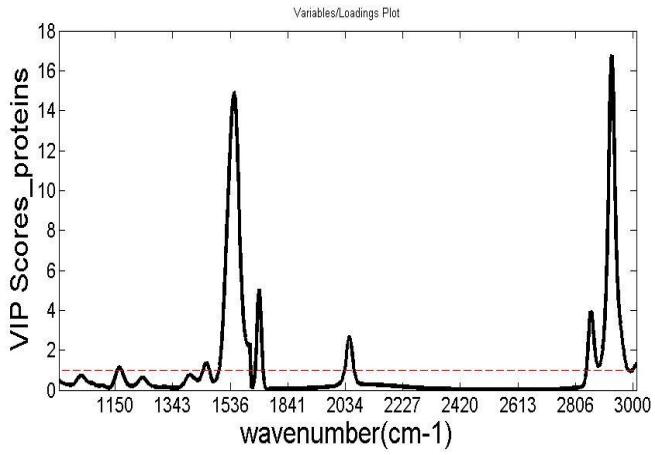

Figure 3.31: VIP scores for proteins in the MIR region.

This was confirmed by observing the VIP scores for proteins calculated in the NIR region (Fig. 3.32).

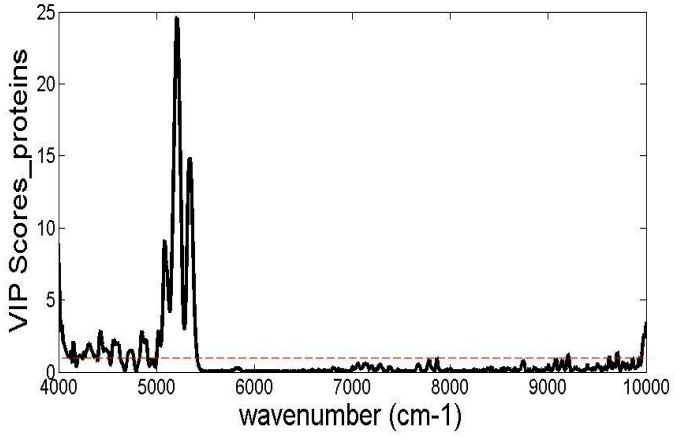

Figure 3.32: VIP scores for proteins in the NIR region.

Proteins don't cause the scattering phenomenon and the VIP scores pattern showed three signals recognizable between 5000 and 5500 cm^{-1}, which refers to the symmetry stretching of the NH bond and to bands of amide II, and to the second overtone of the stretching of the C = O amide group (Burns & Ciurczak, 2008). This interpretation was confirmed by two-dimensional correlation analysis (2D NIR-MIR). Figures 3.33 and 3.34 shows the 2D maps obtained using the NIR raw spectra and spectra after EMSC pretreatment.

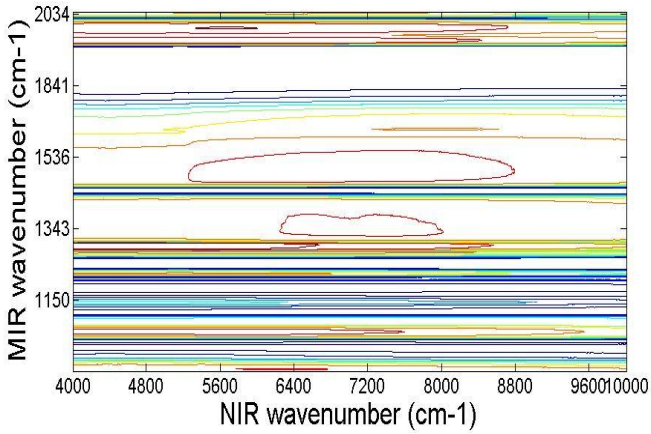

Figure 3.33: NIR-MIR 2D Contour Map (NIR raw spectra).

While in the first case the correlation did not provide easily interpretable results, it was clear that the EMSC pretreatment allowed a clear identification of wavenumber ranges which could be used for a more precise spectral interpretation.

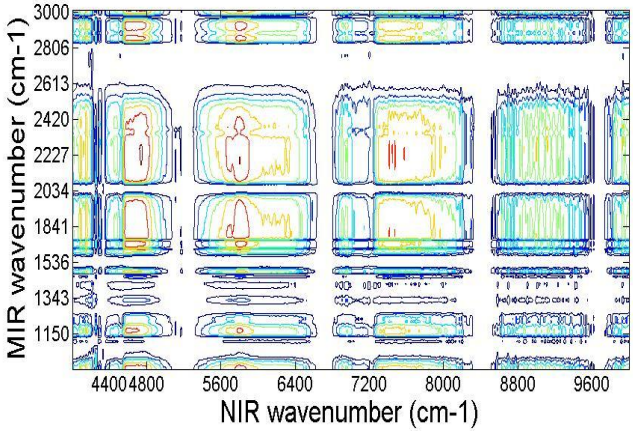

Figure 3.34: NIR-MIR 2D Contour Map (NIR EMSC spectra).

3.3.4 Conclusions

Regarding the fat parameter, NIR calibration provided results comparable with those obtained by MIR. Lower sensitivity of the NIRS was observed for the proteins parameter, justified on the basis of lower intensity signals and greater overlap of absorption in the NIR region. The best performances, in the case of fat, appeared to be dependent, however, also of the spectral contribution of the scattering caused by fat globules in emulsion and not just by the vibrational absorptions as observed using the mid-infrared. The application of two-dimensional spectroscopy between the two spectroscopy allowed a easier and more precise attribution of signals related to the milk constituents in the near infrared region.

3.3.5 References

Alais C Scienza del latte. Ed. Tecniche Nuove, 3rd Edition, Milano, 2000.

Andersen SK, Hansen PW, Andersen V, Encyclopedia of vibrational spectroscopy. Wiley and Sons, New York, 2002.

Burns D, Ciurczak E Handbook of Near-Infrared Analysis. 3rd Edition, CRC Press, 2008.

Cattaneo TMP, Cabassi G, Profaizer M, Giangiacomo R (2009) Contribution of light scattering to near infrared absorption in milk. J Near Infrared Spectrosc 17: 337-343.

Chong I, Jun C, 2005, Performance of some variable selection methods when multicollinearity is present. Chemometr Intell Lab 78: 103-112.

Per Waaben H, 1998, Spectroscopic analyses on dairy products. Ph.D. thesis, Royal Veterinary and Agricultural University, Department of Dairy and Food Science.

Sivakesava S, Irudayarai J, 2002, Rapid determination of tetracycline in milk by FT-MIR and FT-NIR spectroscopy. J Dairy Sci 85: 487-493.

Soyeurt H, Dardenne P, Dehareng F, Lognay G, Veselko D, Marlier M, Bertozzi C, Mayeres P, Gengler N, 2006, Estimating fatty acid content in cow milk using mid-infrared spectrometry. J Dairy Sci 89: 3690-3695.

Williams P, Norris K., Near-infrared technology in the agricultural and food industries. American Association of Cereal Chemists, Inc. St. Paul, Minnesota, USA, 2nd ed., 2001.

3.4 Evaluation of the variability in the distribution of milk fat globules within breedings in Lombardy

3.4.1 Introduction

The lipid fraction of milk is considered as a fundamental component from a nutritional point of view and a key element in the structure and aroma of many dairy products (Michalski, 2007).
Cow milk has a fat content ranging from 3.5 to 4%, with large fluctuations dependent on animal individual characteristics and seasonal factors. Milk fat is present as an emulsion in the form of spherical globules, whose synthesis occurs at the level of secretory cells of the mammary gland epithelium. The size of fat globules ranges from 0.1 μm to 20 μm, with an average of about 3-4 μm and can be affected by breed, stage of lactation, feeding and seasonal variations. The structure of milk fat globules is not homogeneous, but constituted of concentric laminas, due to both the overlapping layers of triglycerides and the presence of a membrane that surrounds the fat globule (El-Loly, 2011). The membrane has a thickness of 10-20 nm and presents a complex composition and variable composition in function of some factors (diet, breed, health, stage of lactation) and plays a key role in the stability of fat globules (Michalski et al., 2003).
In recent years, the fat globules size has been the subject of several studies since it has been observed that the differences related to this parameter have a interesting effect on both the nutritional properties and sensorial and technological features for the dairy production (Michalski et al. 2003).
Therefore, the use of fat globules with different sizes could lead to the emergence of new products with different sensory and technological properties and for this reason, the size of fat globules could be considered as a parameter able to define and determine the nutritional quality of milk.
The aim of this research activity was to evaluate the variability in the fat content and in the fat globules size distribution within cow breeds in Lombardy. In fact, according to some authors (Michalski et al., 2003, Michalski et al., 2005, Michalski et al., 2007b), the different fat globules size could be related to some physical and chemical properties and to fatty acid composition of milk and therefore it could be used for the production of dairy food with particular characteristics.

3.4.2 Materials and methods

Animals and milk sampling

This research was carried out on animals deriving from eight farms of dairy cattle located in the provinces of Lodi and Lecco. Seventy cows were selected among three different breeds: Friesian, Brown and Jersey and were half sisters. Fathers were chosen among the best breeding bulls selected in Italy.
Individual milk samples were monthly collected from all the farms during two years period. Sodium azide (Sodium azide tablet 8 mg, Sacco, Italy) was added as preservative directly to the sampling tubes; samples were stored at 4°C immediately after collection and analyzed within 2 days.

Determination of milk fat content

Milk samples were analyzed with MilkoScan FT2 (FOSS Italy, Italy) for the determination of fat content. MIR spectra were acquired in the spectral range from 926 to 5000 cm^{-1}, using a pathlength of 45 μm at a constant temperature of 40°C±1°C.

Determination of particle size distribution of milk fat globules

The particle size analyses of fat globules were performed using a Mastersizer 2000 (Malvern instruments Ldt., UK) granulometer equipped with a single laser source at 633 nm. The instrument software was set to calculate particle size distribution according to Mie theory using the "general purpose model" for spherical particles. The working parameters were chosen as pointed out by Michalski et al. (2001): water was used as dilution medium (~1:600) in order to avoid multiple scattering phenomena; refractive indexes were set to 1.33 for water and 1.458 for milk fat; the absorption coefficient was measured on liquid fat and was set to $0.5*10^{-5}$. In order to avoid fat crystallization, all the measurements were done at 40°C±1°C. The high dilution factor used made negligible the obscuration due to casein micelles. Samples were evaluated for surface-weighted diameter (D [3.2]), volume-weighted diameter (D [4.3]), specific surface area, the 10th, 50th, and 90th (μm) percentiles of distribution and the span of distribution calculated as d90 - d10/d50*100. Among these output parameters, the surface-weighted diameter, also called Sauter Mean diameter (SMD), was chosen as the best descriptor of particle size distribution, since it's a more consistent parameter than d50. This linear parameter, is defined as the diameter of a sphere that has the same volume/surface area ratio as a particle of interest:

$$d_{3,2}=\Sigma(N_j d_j^3/\Sigma N_j d_j^2)$$

Statistical analysis

Analyses of variance (ANOVA) were performed with statistics package for Excel, XL Stat 2009.3.02. Post hoc analysis with multiple comparisons for couples was performed using Tukey test.

3.4.3 Results and discussion

Figure 3.35 reports three examples of size distribution of fat globules of individual milk samples from the three sampled breeds.

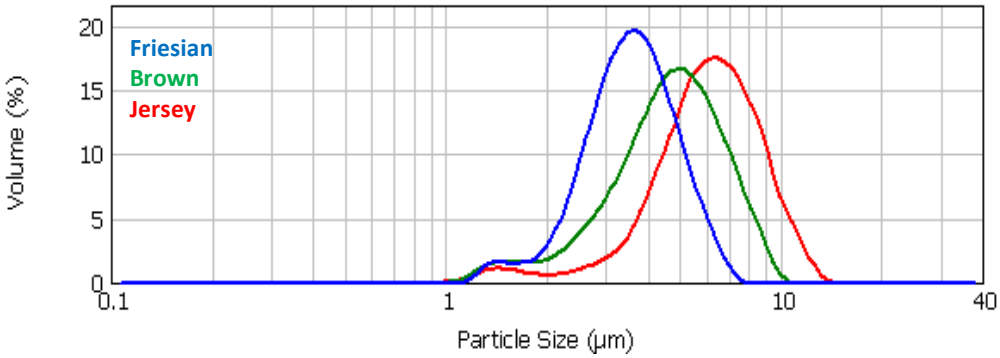

Figure 3.35: Examples of size distribution of milk fat globules of Friesian, Brown and Jersey cows.

According to literature data (Czerniewicz, 2006), milk fat from Jersey cows presented bigger globules than fat from Friesian and Brown cows. Regarding the examples in Figure 3.35 in Friesian milk 20% of fat globules has a diameter ranging from 3.3 and 4.5 µm with a SMD of 3.3 µm, in Brown milk 17% of globules ranged from 4.6 and 6.2 µm (D[3.2]=4.1 µm) while Jersey cow globules presented the higher diameter (5.7-7.8 µm; D[3.2]=5.3 µm).
Despite these differences, the post hoc analyses on SMD of two years measurements (Figure 3.36) revealed only two groups statistically different ($p<0.01$) in which Jersey breed constituted a single group with the highest D[3.2] value (4.2 µm). Thus, for a technological purpose, Brown and Friesian milk should not be different.

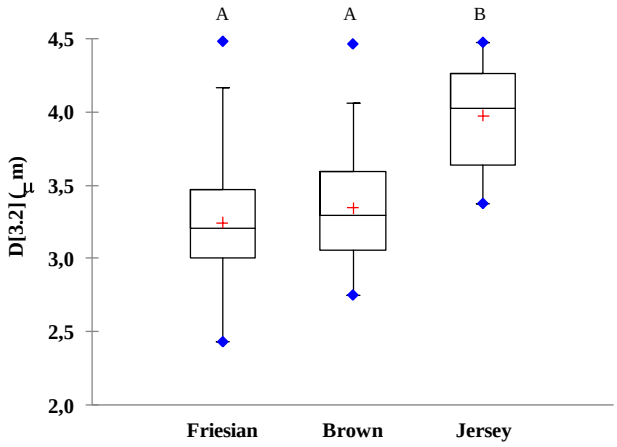

Figure 3.36: Average SMD (µm) for Friesian, Brown and Jersey cows

Our results are in agreement with literature data which assess that Jersey milk fat globules tend to have larger diameters than Friesian fat globules (Chandan, 2006). Major factors influencing milk fat dimension were considered.
Figures 3.37 and 3.38 show the correlation between SMD, fat content and fat production for Friesian milk.

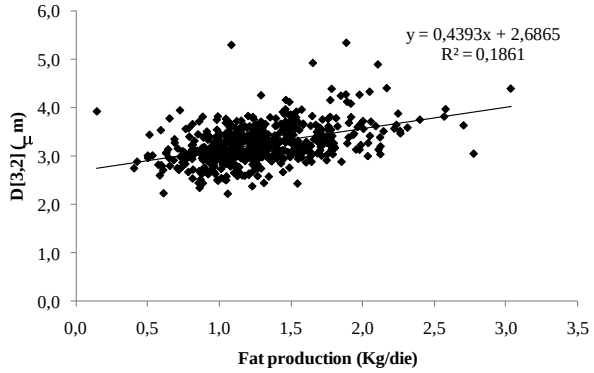

Figure 3.37: Correlation between SDM (μm) and fat production (Kg/die) for Friesian milk.

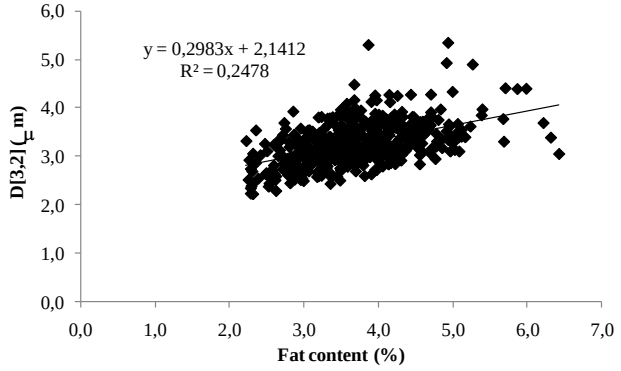

Figure 3.38: Correlation between SDM (μm) and fat content (%) for Friesian milk.

The SMD showed low correlations with both the percentage of fat in milk and the amount of fat produced.

About this topic, several authors are not in agreement. Menard et al. (2010) reported that the larger size of fat globules in buffalo milk compared to cow milk was related with the higher fat content and found a linear and positive relationship between fat globule size and fat content. El-Zeini (2006) reported that milk with high-fat content, such as buffalo milk, usually contains larger fat globules than milks with a lower fat content. Wiking 2004 found a correlation between the average diameter of milk fat globule and the diurnal fat production, indicating that when cows produce a high level of fat, the synthesis of membrane material is limited. Conversely, Walstra (1969) found no positive correlation between fat content and average globule size and King (1957) found a non-significant increase in the size of the fat globules with corresponding increase in the fat percentage in milk obtained from Ayrshires and Friesians.

The possible explanation for the formation of larger fat globules when the synthesis of milk fat is important is the limitation in the production of the Milk Fat Globule Membrane (MFGM) when fat globules are enveloped during their secretion from the epithelial cells of the mammary

gland. The amount of available membrane in the apical region of epithelial cells defines a physical limit to the number of cells that can be excreted with success. Thus, the MFGM could be a limiting factor in the formation of small fat globules in high-fat content milks such as Jersey cow milk (Ménard et al., 2010).
A two-way ANOVA was performed on SMD of Friesian samples in order to get evidence to the influence of father and farm variables and their interaction (Table 3.4).

Source	FD	Sum of Squares	Mean Squares	F	Pr > F
Farm	7	6.354	0.908	8.858	< 0,0001
Father	6	3.207	0.535	5.216	< 0,0001
Farm*Father	7	7.627	1.090	10.633	< 0,0001

Table 3.4: Effects of season on SDM (μm).

Both farm and father variables resulted statistically influencing milk fat globule diameter ($p<0.0001$).
The post hoc analysis found four significantly different groups for farm parameter (Figure 3.39) and two groups for father variable (Figure 3.40). An aspect to be considered is that the 'farm' parameter consisting of many sources of variability, including the feeding, the system and frequency of milking and hygiene practices.

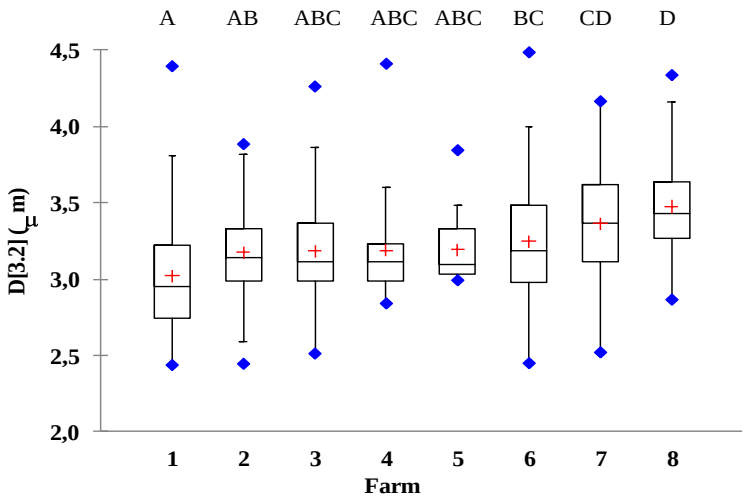

Figure 3.39: Farm influence on SMD (μm) for Friesian cows

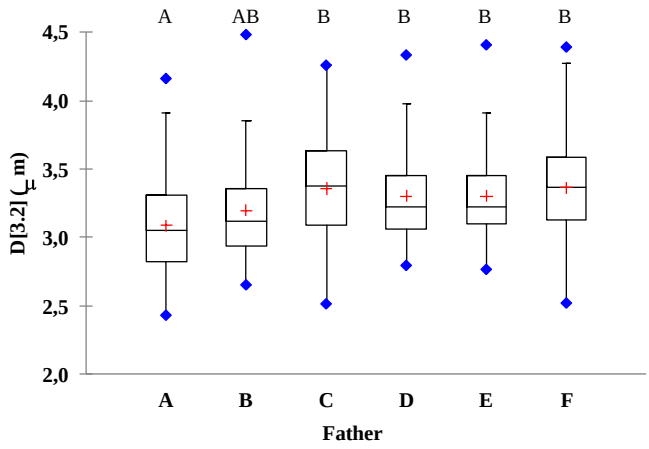

Figure 3.40: Father influence on SMD (μm) for Friesian cows

In order to highlight seasonal influence on milk fat globule dimensions, data were grouped according to season: summer milk was collected from June to August and winter milk from December to February. Spring and autumn milk were not considered. Table 3.5 shows the average value of SMD according to season for each breed.

		Summer		**Winter**		***p***
		Mean	Std Dev	Mean	Std Dev	
	Friesian	3.22	0.46	3.28	0.32	n.s.
D[3.2]	Brown	3.32	0.28	3.31	0.44	n.s.
	Jersey	4.10	0.47	4.11	0.61	n.s.

Table 3.5: Effects of season on SMD (μm).

This parameter was not statistically influenced by the season for any considered breed.
Literature data are confusing and discordant on this point: Mulder and Walstra (Mulder & Walstra, 1974) found that fat globules are smaller in spring than in winter, while our results are in agreement with a recent investigation on Polish milk (Barłowska et al., 2009) and the observed trend was similar than that found in a study on goat milk fat globules (ARSIA, 2005).
Moreover, literature data report that the amount of non globular fat, as a consequence of lypolitic phenomena, is greater in winter than during summer period, since the milk fat globule membrane has a lower stability in winter months. Thus, in cold months, milk has a lower amount of large fat globules, showing a lower average diameter.
Besides, milk fat globules possess a triglyceride core, with a complex composition due to the numerous fatty acids present in milk. Globules with different size have different triglyceridic composition (Lopez et al., 2011) and feeding plays an important role in defining fat globule core composition (Brunner, 1965). Since in our experiments the feed has not changed during the year, the changes observed are ascribable to heat stress.

Figure 3.41 shows two examples of the trend of the average value of SMD during lactation period. Data refer to milk samples collected in two farms breeding Friesian cows.

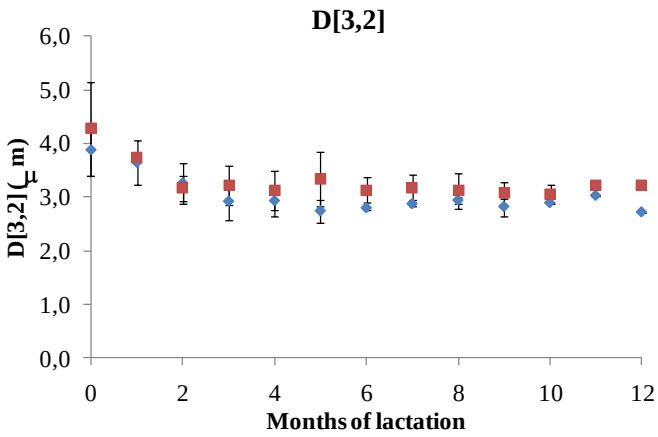

Figure3.41: Examples of effects of lactation stage on SMD (μm) for Friesian cows.

Fat globules diameter decreased during the first months of lactation and then remained fairly stable during the remaining period, reflecting partly the already observed trend of fat and protein contents.

These results are in agreement with literature data. It has been well documented that the average fat globule diameter is affected by the stage of lactation. In particular, several studies reported that fat globule diameter reaches the maximum in early lactation and decreases throughout lactation (Mulder & Walstra, 1974; Walstra, 1995; Singh, 2006; Hiu & Nip, 2006). Furthermore, recent results suggest that no significant change in the fat globule size distribution occurs after mid-lactation (Ye et al., 2002).

A significantly influence of the number of lactation on fat globule dimension was found. Figure 3.42 shows the SMD as a function of lactation number for Friesian cows.

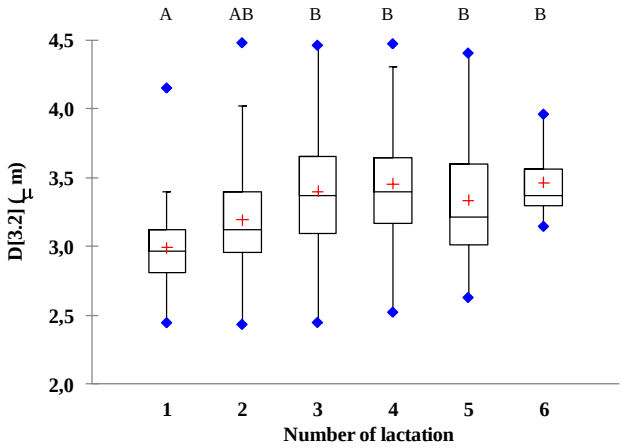

Figure 3.42: Effects of lactation number on SMD (μm) for Friesian cows.

Fat globules diameter increased during the four lactations remaining quite constant for the following lactations.
The post hoc analysis found that primiparous cows showed a statistically lower diameter than multiparous ones (D[3.2]=2.99 μm for primiparous vs. 3.45 μm for cows at the sixth lactation; $p \leq 0.01$).
In literature, few information is available on globule size as affected by lactation number. However, our results are in agreement with some recent studies. Couvreur & Hurtaud (2007) and Pandya & Khan (2006) found that lactation number influences size and number of fat globules in cow and buffalo milk respectively; Martini et al. reported that the ewes' age and consequently the parity number is an important factor in the variability of the fat globule size: younger animals' milk contained a higher percentage of medium-sized globules whereas older ewes showed a higher percentage of large-sized globules (Martini et al., 2004).
Another aspect which may influence the size of fat globules is the number of daily milkings to which cows are subjected. Of the eight farms involved in the trial, 7 took two daily milkings, while only one made three milkings. In order to reduce the unbalanced size of the two classes of samples, two groups have been created with the same dimension: the first group includes milk samples from three milkings while the second was created by selecting from the cows milked twice a day, the half sisters of the first group. The SMD average values of the two groups are shown in Figure 3.43.

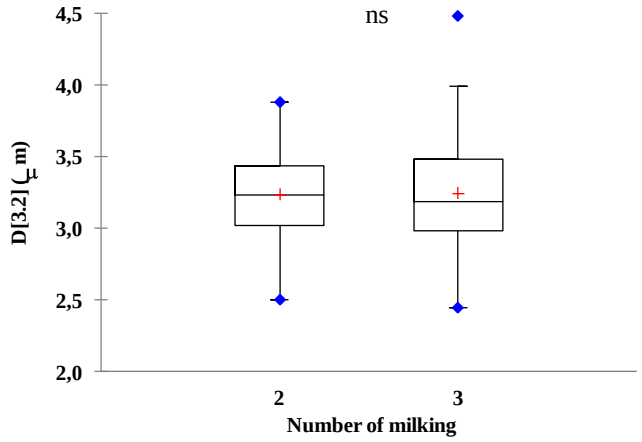

Figure 3.43: Effects of milking frequency on SDM (μm) for Friesian cows. ns=not significantly different.

From the post hoc analysis, the two groups were not significantly different ($p<0.01$). Literature data are discordant: Wiking et al. found that The d(0.1) of the milk fat globule was unaffected by milking frequency, while d(0.9) was larger in milk collected from four daily milking compared with that milked twice daily (Wiking et al. 2006).
Conversely, Abeni et al., supporting our results, reported that fat globule size D[3.2], globular surface area, and interglobular distance were not affected by milking interval (Abeni et al., 2005).

The effect of mastitis on fat globule size was evaluated as well.

Mastitis is an inflammation of the mammary gland, characterised by pathological changes in the mammary tissue; an increase in the number of somatic cells, physical, chemical and microbiological changes occur in milk during mastitis. Causative organisms include prototheca and human pathogens such as *E. coli* and *Staphylococcus aureus*, which cause high levels of somatic cell. In the dairy cattle population, both clinical and sub-clinical mastitis can affect the composition (changes in fat content, decrease in lactose and increase in mineral content, decrease in casein and increase in whey proteins concentration, especially immunoglobulins and non protein nitrogen) and manufacturing properties of milk with a decreasing in cheese yield (Auldist & Hubble, 1998, Barbano et al., 1991).
Somatic cells include any type of 'body' cell in the milk, such as skin cells (epithelial) from the cows' udders and leucocytes of several types, which are part of the cow's immune response to infection in the udder. Thus they are used as an index of mastitis.
In order to evaluate the influence of the mastitic infection on SMD, samples were grouped according to the limit of level of Somatic Cells Count (SCC) imposed by the legislation: milk with SCC < 400 000 per mL suitable for human consumption and milk with SCC > 400 000 per mL, which cannot be used for human consumption or for cheese making (European Regulation N° 853/2004).
Table 3.6shows the SMD [3.2] according to SCC for each breed.

	SCC < 400 *1000		SCC > 400 *1000		***p***
D[3.2]	Mean	Std Dev	Mean	Std Dev	
Friesian	3.34	0.38	3.40	0.35	n.s.
Brown	3.24	0.36	3.28	0.42	n.s.
Jersey	3.97	0.33	3.97	0.36	n.s.

Table 3.6: Effects of SCC, expressed as SCC*1000/mL, on SMD (μm).

In general, all breeds showed a slight increasing fat globule dimension with increasing SCC, with the exception of Jersey cows. However, these differences weren't statistically significant ($p<0.01$).
Literature data, however, report a general decrease in the size of fat globules, that can be traced to the fact that in mastitic milk, the fat globule membrane is more susceptible to spontaneous lipolysis and to the action of lipase enzymes produced by leucocytes that invade the mammary gland in response to infection (Auldist et al., 1995, Auldist & Hubble,1998, Holdaway, 1990). Damage to the membrane leads to the formation of not globular free fat. Since the large globules are more susceptible to lipolysis than small ones, the number of large particles decreases. Consequently the average diameter of fat globules tends to decrease (Hui & Nip, 2006).
An hypothesis of our evidence could be that the increase in D[3.2] is not due to an actual increase in fat globule size, but on the fact that the diffractometer could have measured somatic cell clusters.

3.4.4 Conclusions

The most influencing parameters on milk fat globules dimension (SMD) were found to be genetic factors (father), factors related to farm, stage and number of lactation. Conversely, season, daily milking number and the presence of higher level of somatic cells in milk didn't resulted significantly influencing the SMD.

The differences among farms could be determinant in planning the milk collection for the technological destination, while the differences among the breeding bulls can be used for the animals' selection.

3.4.5 References

Abeni F, Degano L, Calza F, Giangiacomo R, Pirlo G, 2005, Milk quality and automatic milking: fat globule size, natural creaming, and lipolysis. J Dairy Sci 88:3519–3529.

Agenzia Regionale per lo Sviluppo e l'Innovazione nel settore Agricolo-forestale, 2005, Relazione finale progetto A.R.S.I.A. Valorizzazione della qualità del latte ovino prodotto in Toscana, http://www.arsia.toscana.it/.

Auldist MJ, Coats S, Rogers GL, McDowell GH, 1995, Changes in the composition of milk from healthy and mastitic dairy cows during the lactation cycle. Aust J Exp Agr 35: 427-436.

Auldist MJ, Hubble IB, 1998, Effects of mastitis on raw milk and dairy products. Aust J Dairy Technol 53: 28-36.

Barbano DM, Rasmussen RR, Lynch J M, 1991, Influence of milk somatic cell count and milk age on cheese yield. J Dairy Sci: 74:369-388.

Barłowska J, Grodzicki T, Topyła B, Litwińczuk Z, 2009, Physicochemical properties of milk fat from three breeds of cows during summer and winter feeding. Archiv Tierzucht 52: 356-363.

Brunner JR Physical equilibria in milk: the lipid phase. In Fundamentals of dairy chemistry. Webb BH and Johnson AH Eds, AVI Publ Co Inc, Westport (USA) 1965, pp. 403-505.

Chandan RC, Manufacturing yogurt and fermented milks, John Wiley & Sons, 2006.

Couvreur S, Hurtaud C, 2007, Globule milk fat: secretion, composition, function and variation factors INRA Prod Anim 20: 365-382.

Czerniewicz M, Kielczewska K, Kruk A, 2006, Comparison of some physicochemical properties of milk from Holstein-Friesian and Jersey cows. Pol J Food Nutr Sci 15: 17-21.

El-Loly MM, 2011, Composition, Properties and Nutritional Aspects of Milk Fat Globule Membrane – a Review. Pol J Food Nutr Sci 61: 7-32.

El-Zeini HM, 2006, Microstructure, rheological and geometrical properties of fat globules of milk from different animal species. Pol J Food Nutr Sci 15: 147–154.

Holdaway RJ, A comparison of methods for the diagnosis of bovine subclinical mastitis within New Zealand dairy herds. Ph. D. Thesis, Massey University, 1990.

Hui YH, Nip WK, Food biochemistry and food processing, John Wiley & Sons, 2006.

King JOL, 1957, The association between the fat percentage of cow's milk and the size and number of the fat globules. Journal of Dairy Research 24: 198–200.

Lopez C, Briard-Bion V, Menard O, Beaucher E**,** Rousseau F**,** Fauquant J, Leconte N, Benoit R, 2011, Fat globules selected from whole milk according to their size: Different compositions and structure of the biomembrane, revealing sphingomyelin-rich domains. Food Chem 125: 355-368.

Martini M, Scolozzi C, Cecchi F, Abramo F,2004, Morphometric analysis of fat globules in ewe's milk and correlation with qualitative parameters. IJSA 3: 55-60.

Ménard O, Ahmad S, Rousseau F, Briard-Bion V, Gaucheron F, Lopez C, 2010, Buffalo vs. cow milk fat globules: Size distribution. zeta-potential. compositions in total fatty acids and in polar lipids from the milk fat globule membrane. Food Chem 120: 544–551.

Michalski MC, 2007, Metabolic importance of milk fat globule structure. INFORM 18: 86-88.

Michalski MC, Briard V, Juaneda P, 2005, CLA profile in native fat globules of different sizes selected from raw milk. Int Dairy J 15: 1089-1094.

Michalski MC, Camier B, Gassi JY, Briard-Bion V, Leconte N, Famelart MH, Lopez C, 2007b, Functionality of smaller vs control native milk fat globule in Emmental cheeses manufactured with adapted techologies, Food Res Int 40: 191-202.

Michalski MC, Gassi JY, Famelart MH, Leconte N, Camier B, Michel F, Briard V, 2003, The size of native milk fat globules affects physico-chemical and sensory properties of Camembert cheese. Lait 83: 131-143.

Michalski MC, Michel F, Sainmont D, Briard V, 2001, Apparent ζ-potential as tool to assess mechanical damages to the milk fat globule membrane. Colloids Surface B 23: 23-30.

Mulder H, Walstra P, The Milk Fat Globule Emulsion Science as Applied to Milk Products and Comparable Foods. 1974, Pudoc, Wageningen, The Netherlands, pp. 163–192.

Pandya AJ, Khan MMH Buffalo milk utilization for dairy products. In Handbook of non-mammalian animals. Park YW, Haenlein GFW eds, Blackwell Publishing Ltd, Oxford, UK, 2006.

Regulation of the European Community N° 853/2004 of European Parliament and of the Council, 30.4.2004, GU L 139/55.

Singh H, 2006, The milk fat globule membrane - A biophysical system for food applications. Curr Opin Colloid In 11: 154 – 163.

Walstra P, 1969, Studies on milk fat dispersion II. The globule-size distribution of cow's milk. Netherland Milk and Dairy Journal 23: 99–110.

Walstra P, Physical Chemistry of Milk Fat Globules. In Advanced Dairy Chemistry, Vol. 2: Lipids, Fox PF ed, pp. 131-178. 1995.

Wiking L, Stagsted J, Bjorck L, Nielsen JH, 2004, Milk fat globule size is affected by fat production in dairy cows. Int Dairy J 14: 909–913.

Wiking L,, Nielsen JH, Bavius A-K, Edvardsson A, Svennersten-Sjaunja K, 2006, Impact of milking frequency on the level of free fatty acids in milk, fat globule size and fatty acid composition. J Dairy Sci 89: 1004–1009.

Ye A, Singh H, Taylor MW, Anema S, 2002, Characterization of protein components of natural and heat-treated milk fat globule membranes. Int Dairy J 12: 393–402.

3.5 Development of a rapid and economic method for estimating the distribution of milk fat globules

3.5.1 Introduction

The size distribution of fat globules is an aspect of particular interest for the effect on technological and sensorial characteristics of milk, such as the creaming and the lipolysis phenomena. Their distribution depends on genetic factors, physiologic aspects related to nutrition and lactation stage, and technologic factors related to the type of the adopted farming and milking (Walstra, 1994; Wiking et al., 2004). When milk fat concentration increases it can be observed an increase of the large globule fraction in association with an increment in stearic, palmitic linoleic and oleic acids content in the backbone of triglycerides; at the same time the enzymatic activity associated with fat globule membrane decreases. Milk with bigger fat globules shows faster creaming and bigger skimming easiness. The cream obtained from this milk is better for whipping, but gives rise to butter with less water content, bigger fat crystals and it is less spreadable (Couvreur & Hurthaud, 2007). The size of globules affects the viscoelasticity of acid and enzymatic curds (Wiking et al., 2004). Recent studies on Camembert and Emmental cheese manufactured using milk either enriched in big fat globules (average diameter 6μm) or in small ones (average diameter 3 μm) highlighted effects on syneresis, proteolysis and cheese rheology of (Michalski et al., 2003; Michalski et al., 2004). In milk pasteurized products and in milk with extended shelf life, the dimension of homogenised globules plays a pivotal role in emulsion stability and palatability of the final product (Meyer et al., 2006). Thus, the study of factors that affect these qualitative aspects of milk fat may play an important role also in the dairy Italian typical productions.

Despite the importance of the knowledge of size distribution in several technological dairy processes, often laser diffractometers and other instrumentation for particle size analysis are not available in dairy laboratories and therefore such type of information is not easily accessible, except for research purposes. NIR instrumentation instead is largely used in dairy labs.

The interaction between the electromagnetic radiation in the near infrared region and the suspension of small particles in continuous media, such as fat globules in milk, give rise to scattering phenomena. The light scattering or light diffusion has been defined as a radiation redistribution inside a medium without loss of radiation. This phenomenon occurs in media characterized by fluctuations in density and thus in refractive index. (Kokhanovsky, 2009)

The NIR spectrum of whole milk arises from the absorbance due to both molecular vibrations and elastic scattering due to the presence of fat globules in emulsion. Numerically, about 80% of the fat globules has a diameter less than 3 μm and, having a different diffraction index from that of the aqueous medium, that interferes with the radiation wavelength from 1 to 2.5 μm with a dispersion of the radiation in all directions (Jääskeläinen et al., 2001). Consequently, the incident NIR radiation shows a behaviour which is not in agreement with the Lambert-Beer's law: NIR spectra of milk samples with high fat content show higher offset values than skimmed milk spectra.

The scattering phenomenon is often undesirable and usually reduced by operating at the level of both sample preparation (homogenization) and optical geometry (working in transflectance mode with an integrating sphere to collect the spreading radiation). Usually, also chemometric techniques, such as EMCS (Enhance Multiplicative Scattering Correction) algorithm, are applied in order to remove the scattering phenomenon. (Kokhanovsky & Zege, 1997; Prahl et al., 1989; Veach, 1997)

However, it's important to consider that the amount of photons that are deviated from their

straight trajectories depends on the wavelength and on the size of the scattering particles and therefore it is possible get information on particle size distribution from NIR spectrum.
Thus, the aim of this research was the development of a rapid and economic method for estimating the distribution of milk fat globules through a physical-mathematical model for the study of the scattering contribution in the NIR spectrum.

3.5.2 Materials and methods

Samples

Individual raw milk samples were collected during two year as described in the previous paragraph (3.4).

Gross composition

Gross composition of milk samples was determined with MilkoScan FT2 (FOSS Italy, Italy) as described in the previous paragraph (3.4).

Particle size analysis

The reference particle size analyses of fat globules were performed using a Mastersizer 2000 (Malvern instruments Ldt., UK) granulometer as described in the previous paragraph (3.4).

Spectral analyses

Spectral data were recorded using a Buchi NIRFlex N-500 (Buchi Italia, Italy) in transmission mode using a quartz flux cuvette with a path-length of 200 µm, 32 scans, resolution 8 cm^{-1}, three replicates for each sample. For the measurements, milk samples were placed in 40 ml tubes, heated at 40°C±1°C and fluxed trough the cell using a peristaltic pump. Spectra were collected in the spectral range from 1100 to 2500 nm using the NIRWare Operator v.1.2 software (Buchi Italia, Italy). Before milk scan, spectra of empty quartz cuvette and pure water were recorded.

The physical model was developed using both Matlab (the Mathworks, USA) and Microsoft Visual Basic for Excel.

3.5.3 Results and discussion

Some examples of transmission NIR spectra of milk samples showing different scattering behaviors due to either cow bred or fat concentration are reported in Figure 3.44.

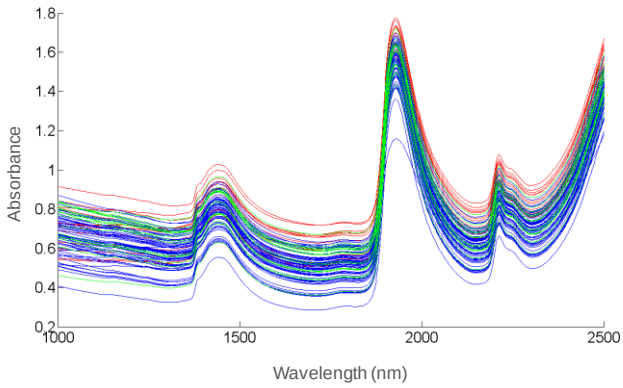

Figure 3.44: Examples of transmission NIR spectra of milk samples. Blue lines= Friesian milk; green lines= Brown milk; red lines= Jersey milk.

The spectra of whole milk are mainly characterized by water and quartz cuvette absorption.
The contribution of the scattering phenomenon is also recognizable by a different slope of the left portion of the spectrum. In fact, the NIR milk spectrum measured in transmission mode arises from both true absorptions due to constituents and from the varying intensity at different wavelengths of photon deviation due to scattering particles represented mainly by fat globules. Vibrational absorptions in the spectral region from 900 to 2500 nm are very small for all the milk constituents except for the strong water absorptions. In the spectral regions where water absorptions are absent, the extinction of radiation recorded by spectrometers is mainly due to scattering phenomena, which prevent photons from reaching the detector. To a first approximation, giving the geometry of a transmittance measurement in a FT-NIR spectrometer, it can be assumed that only the photons diffracted at a very small angle reach the detector. The photons that are deflected by a bigger angle from the straight trajectory don't reach the detector and give rise to an increase in optical density of the samples which isn't depending on true absorptions.
In this study, spectra were firstly subtracted of water and cuvette spectral bands in order to process the milk components absorption only (Figure 3.45), then two spectral windows were selected, characterized only by scattering contribution (Figure 3.46).

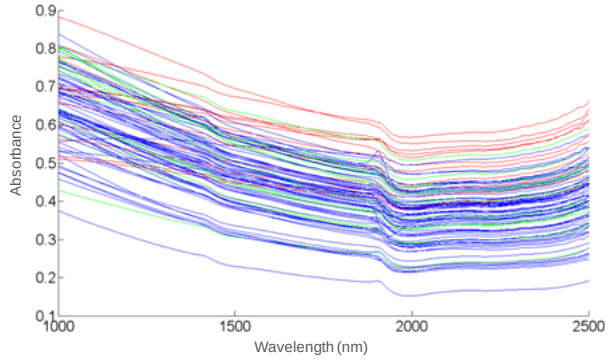

Figure 3.45: Milk spectra subtracted to water and cuvette contributions to the absorbance.

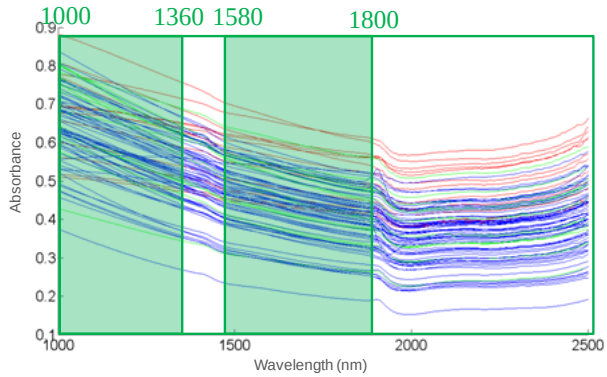

Figure 3.46: Selection of two spectral windows showing scattering contribution.

On the basis of these observations, in collaboration with an engineer of the University of Milan, a model was developed which calculates the optical density produced by milk fat globules, the fat concentration given. An example of model calculation is given in Figure 3.47.
In the model it was assumed that *n(d)*, the probability density function in number, follows a Weibull distribution, according to Brown (Brown & Wohletz, 1995):

$$n(d) = \frac{\beta}{\eta}\left(\frac{d-d_0}{\eta}\right)^{\beta-1} e^{-\left[-\left(\frac{d-d_0}{\eta}\right)^{\beta}\right]}$$

where: β is the shape parameter and η the scale parameter, two coefficients which describe and define the particle distribution.
The fat amount of milk and the fat and serum densities given, and assuming as a first approximation that the fat globules are spherical, the model calculates the amount, in number, *N*, of globules with a certain diameter range per volume unit of milk, returning a first distribution curve (step 1 in Figure 3.47).
Then the program calculates, in discrete form, the extinction coefficient $\tau(\lambda)$ due to the scattering for each wavelength in the region of interest:

$$\tau(\lambda) = \int_0^{\infty} \mu_{scatt}(d, \lambda) * N(d)\delta d$$

where μ_{scatt} (d,λ) represents the section of scattering.
To calculate μ_{scatt} the Evans Fournier approximation of the Mie theory, reported by Kokhalnovsky (Kokhanovsky & Zege, 1997), was used; to calculate the refractive index of water at each wavelength, the formula proposed in 1997 by the International Association for the Properties of Water and Stems was used; for the refractive index of milk fat the empirical formula proposed by Michalski (Michalski & Briard., 2001) was used. After this calculation, the program generates a theoretical spectrum.
Once put into the program the two portions of measured NIR spectrum (step 2 in Figure 3.47), the problem of the analytical inversion of the model in order to estimate the parameters of the fat globules distribution, known the weight percentage of fat in milk, was solved by using the Generalized Reduced Gradient method, a nonlinear optimization system. The model inversion was performed by minimizing the sum of squared differences between the measured spectrum of each sample and the calculated one (step 3 in Figure 3.47). At the end of the process, the new distribution curve is given with the distribution parameters (step 4 in Figure 3.47).

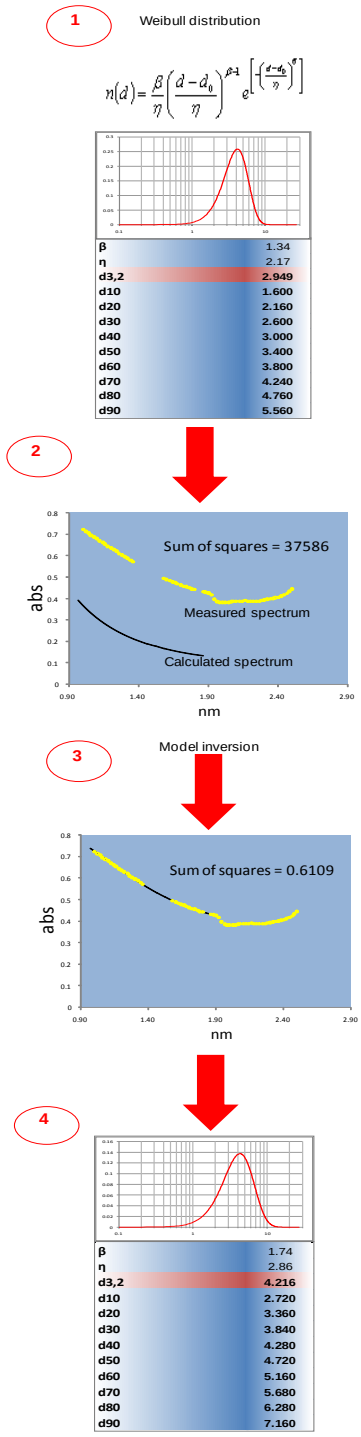

Figure 3.47: Example of model calculation.

Since the developed model is based on a single event for each photon scattering, the phenomena of multiple scattering, which lead to an overestimation of the size of fat globules, were avoided. The optimal sample dilution rate required to avoid multiple scattering events was identified by comparing the estimations obtained using the NIR model and the reference data obtained using the Mastersizer granulometer (Malvern instruments Ldt., UK). Using a dilution factor of 4, a good correlation between laser diffraction measurements and NIR estimations was obtained. Determination coefficients of 0.914 for the median value of particle size distribution (on volume basis), and of 0.94 for distribution span measured as difference between 20th and 80th percentile were obtained. No further improvements were achieved by increasing the dilution factor, as shown in Figures 3.48 and 3.49.

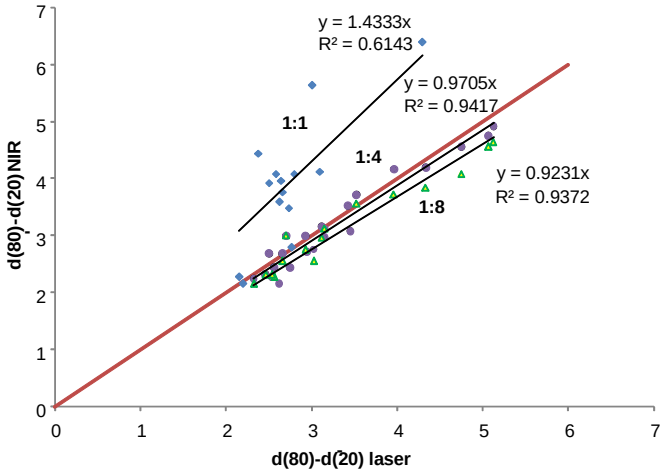

Figure 3.48: Correlation between fat globule size distribution span obtained using laser diffractometer and NIR scattering model at varying dilution rates (1:1 blue, 1:4 lilac; 1:8 green).

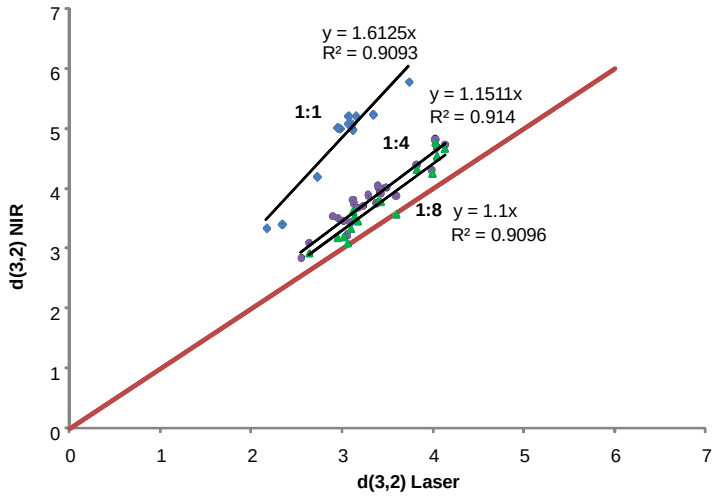

Figure 3.49: Correlation between Sauter mean diameter obtained using laser diffractometer and NIR scattering model at varying dilution rates (1:1 blue, 1:4 lilac; 1:8 green).

The performances of the model was tested by analyzing 180 external samples both with NIR and with the reference diffractometric technique.
The estimation of Sauter Mean Diameter D[3,2] showed a determination coefficient of 0.94 and a SEP of 0.120 µm (over a range from 2.22 to 5.34 µm, Figure 3.50); the R^2 for the span of the distributions was 0.88 (over a range from 0.79 to 1.70 µm) and the SEP was 0.185 µm. These results indicate a very robust model.

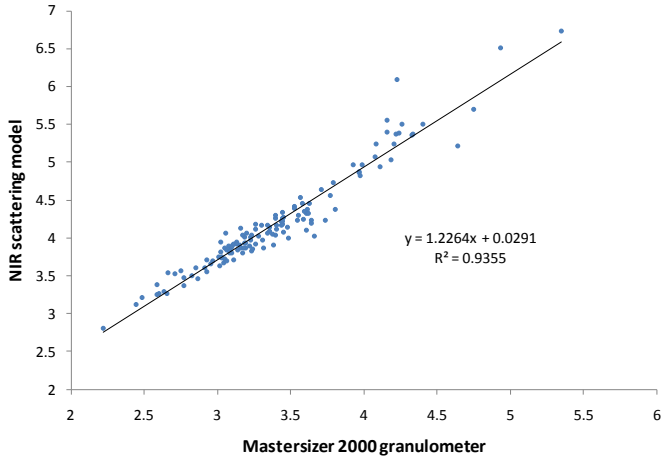

Figure 3.50: Correlation between Sauter Mean Diameter measured with NIR and with the reference diffractometric technique.

3.5.4 Conclusions

Although it is known that dairy composition can be monitored by NIR, the use of this technique for the study of fat globules distribution on the basis of a physical method is an innovative application.
The model developed in this research can be useful for a fast evaluation of milk fat globules distribution in place of a dedicated instrumentation. The possibility of a rapid estimation of milk fat globule size in dairy plant laboratories would be useful for a better evaluation of the technological fate of milk. Small fat globules are richer in phospholipids and well suited for new functional foods development than big fat globules, which are better for whipping purposes. The method can be useful in screening cows for mil fat globule sizes and in monitoring creaming processes.

3.5.5 References

Brown WK, Wohletz KH, 1995, Derivation of the Weibull distribution based on physical principles and its connection to the Rossin-Rammler and lognormal distributions. J. Appl. Phys, 78: 2758-2763.

Couvreur S, Hurtaud C, 2007, Globule milk fat: Secretion, composition, function and variation factors. Productions Animales 20: 369-382.

Jaaskelainen J, Peiponen KE, Raty JA, 2001, On reflectometric measurement of refractive index of milk. J Dairy Sci 84: 38-43.

Kokhanovsky AA Light Scattering Reviews 4: Single Light Scattering and Radiative Transfer. Springer, 2009.

Kokhanovsky AA, Zege EP, 1997, Optical properties of aerosol particles: a review of approximate analytical solutions. J. Aerosol Sci 28: 1-21.

Meyer S, Berrut S, Goodenough TIJ, Rajendram VS, Pinfield VJ, Povey MJW, 2006, A comparative study of ultrasound and laser light diffraction techniques for particle size determination in dairy beverages. Meas Sci Technol 17: 289-297.

Michalski MC, Briard V, 2001, Optical parameters of milk fat globules for laser light scattering measurements. Lait 81: 787-796.

Michalski MC, Camier B, Briard V, Leconte N, Gassi JY, Goudédranche H, Michel F, Fauquant J, 2004, The size of native milk fat globules affects physico-chemical, and functional properties of Emmental cheese. Lait 84: 343-358.

Michalski MC, Gassi JY, Famelart MH, Leconte N, Camier B., Michel F, Briard V, 2003, The size of native milk fat globules affects physico-chemical and sensory properties of Camembert cheese. Lait 83: 131-143.

Prahl SA, Keijzer M, Jacques SL, Welch AJ, 1989, A Monte Carlo model of light propagation in tissue, SPIE Proceedings of Dosimetry of Laser Radiation in medicine and biology, IS 5: 102-111.

Veach E, 1997, Robust Monte Carlo methods for light transport simulation, PhD thesis. Ed. By E. Veach Stanford University, Palo Alto, USA, 1997.

Walstra P Advanced Dairy Chemistry. Vol.2- Lipids. Fox PF, Ed., Chapman & Hall, New York, 1994.

Wiking L, Stagsted J, Bjorck L, Nielsen JH, 2004, Milk fat globules size is affected by fat production in dairy cows Int. Dairy J 14: 909-913.

3.6 Calibration transfer between bench-top and portable spectrometers for estimating the distribution of milk fat globules

3.6.1 Introduction

Quantitative applications related to NIR spectroscopy require the development of a multivariate calibration model. The typical procedure in calibration model development consists of obtaining a series of representative samples with a known concentration or property of interest, measuring the spectrum of each sample and constructing a model to predict the characteristics for new samples. In general, an accurate and robust calibration model is based on a large number of samples, that therefore requires considerable time and cost for preparation and measurement. However, because of differences between the instrumental responses and variations in environmental condition, a practical problem to multivariate calibration occurs when an existing model is applied to spectra measured under new environmental conditions or on a separate instrument (which is generally treated as the 'slave' and the original conditions or instrument is treated as the 'master'). For this problem, the traditional solution consists of performing full recalibration in the new situation, which involves the repetition of all calibration measurements with the aim of developing another similar calibration model. In some cases, this approach is very impractical in terms of the experimental burden, especially when the calibration samples are numerous, chemically unstable, hazardous (Tan & Li, 2007).
An alternative approach consists of performing a standardization that allows predicting the responses of new samples without performing recalibration, which is based on correcting the spectral difference between the master and slave instruments, and is more economical and cost effective than recalibration. In a broad sense, the term 'standardization' encompasses several approaches: calibration transfer, enhancement of the calibration robustness, model updating or response upgrading. The calibration transfer is the most popular form of standardization (Tan & Li, 2007). In the literature, several methods for calibration transfer have been proposed to perform the transfer of NIR spectra, such as a patented algorithm proposed by Shenk and Westerhaus, (Shenk & Westerhaus, 1991; Bouveresse et al., 1994) direct standardization (DS) and piecewise direct standardization (PDS) algorithms proposed by Wang (Wang et al., 1991) a two-block PLS approach suggested by Forina et al. (1995) an orthogonal projection (TOP) algorithm proposed by Andrew (Andrew & Fearn, 2004), a neural network-based approach (NN) (Despagne et al., 1998), a Fourier-based standardization method (Chen et al., 1997) and wavelet transform-based standardization techniques (Walczak et al., 1997).

In this work, the possibility to use portable spectrometer spectra for estimating the distribution of milk fat globules was evaluated trough standardization to bench-top instrument spectra.

3.6.2 Material and methods

Samples

Individual raw milk samples were collected during two year as described in the chapter 3.4. For the calibration transfer, 36 milk samples were selected with a fat content representative of the parameter variability.

Gross composition

Fat content of milk samples was determined with MilkoScan FT2 (FOSS Italy, Padova) as described in the chapter 3.4.

Instruments

The bench instrument, master, was a Fourier Transform NirFlex N-500 (Buchi Italia, Assago, MI, Italy) while the slave instrument was a Policromix DTS-1700 (LABPOD-MEMS) (Figure 3.51). This is a portable, compact, rugged and low-cost technology tool based on Digital Transform Spectroscopy (DTS™) Technology. The DTS-1700™ uses an innovative MEMS (Micro Electro-Mechanical Systems) spatial light modulator to deliver highly cost-effective solutions featuring excellent performance using a single InGaAs detector and no moving parts.

Figure 3.51: Master (right) and slave (left) spectrometers used in the calibration transfer.

The two instruments have different working principles: FT-NIR uses a Fourier Transform interferometer while LABPOD has a liquid crystal interferometer based on Hadamard transform; the two instruments have a different spectral resolution, 8 cm^{-1} for the FT-NIR and 12 nm for the LABPOD; FT-NIR has an extended range InGaAs detector while LABPOD has a single element InGaAs detector; the instruments also differ for the diameter of measurement spot, 2 mm for the FT-NIR and 5 mm for LABPOD, and for light collimation (in order to have a good illuminated surface for LABPOD, the distance between sample and light source was made up); moreover in LABPOD light passes trough fibers. NIR instruments with MEMS technology consists of a device (chips) consisting of a linear array of micro-mirrors. The device acts as a programmable micro diffraction grating able to select the wave lengths in a few microseconds. When all the elements are held in normal position -"up"-, the surface reflects light from each pixel. If any of these elements is activated, it acts as a diffraction grating, reflecting the light. Figures 3.52 and 3.53 show the operative scheme of a MEMS and the DTS system.

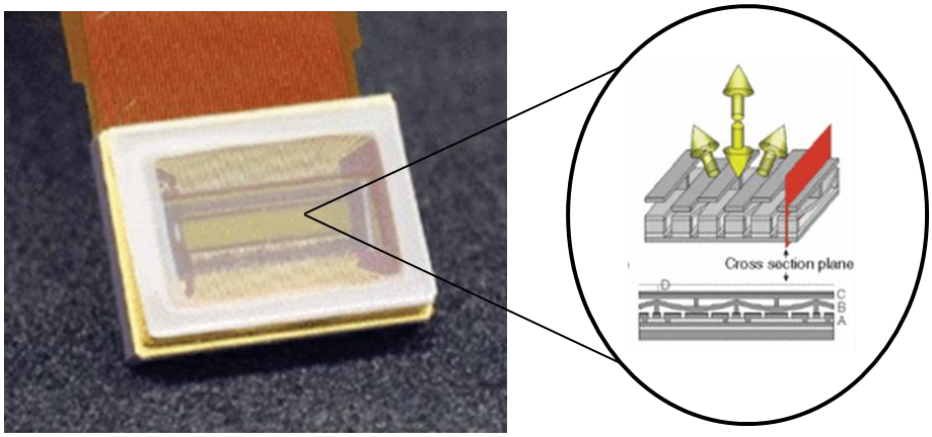

Figure 3.52: Operative scheme of MEMS.

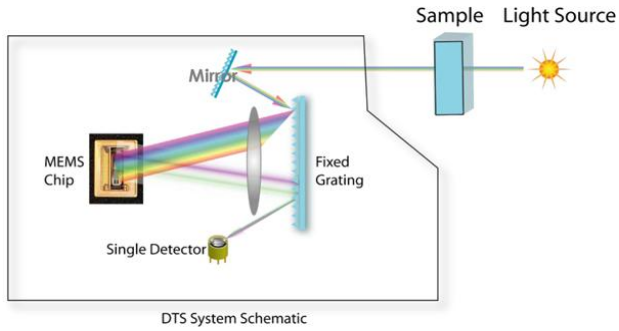

Figure 3.53: DTS system.

Spectral analyses

A set of 35 milk samples were scanned in parallel with two NIR apparatus.
Spectral data were recorded using a Buchi NIRFlex N-500 (Buchi Italia, Italy) in transmission mode using a quartz flux cuvette with a path-length of 200 µm, 32 scans, resolution 8 cm^{-1}, three replicates for each sample. For the measurements, milk samples were placed in 40 ml tubes, heated at 40°C±1°C and fluxed trough the cell using a peristaltic pump. Spectra were collected from 4000-10000 cm^{-1} (1100-2500 nm) using the NIRWare Operator v.1.2 software (Buchi Italia, Italy).
The same samples were scanned simultaneously with a Polychromix LAB POD Spectral Code at the same conditions, in the range from 935.4 to 1692.1 nm with a resolution of 12 nm. Each sample was scanned 100 times.

Software

All computations were performed using MATLAB (The Mathworks, Inc., USA) for Windows, using version 7.0. Routines, such as spectra pretreatment, calibration model establishment, performance evaluation were carried out with our own written programs in the MATLAB 7.0 environment (The Mathworks, Inc., USA).

Theory of the calibration transfer procedure

The standardization procedure was performed with MATLAB function '*stdgen'*, which allows using two common standardization methods: direct standardization (DS) and piecewise direct standardization (PDS). In DS, the whole spectrum on the secondary instrument is used to fit each spectral point on the primary instrument. For real spectroscopic data, however, spectral variations are often limited to a smaller region. Therefore, each spectral point on the primary instrument would more likely be related to the spectral measurement at nearby wavelengths than the full spectrum on the secondary instrument. The PDS method is developed to reconstruct each spectral point on the primary instrument from several measurements in a small window on the secondary instrument (Wang et al, 1991).
PDS was proposed specially to correct problems in transfer caused by shifts in peak wavelengths and by peak broadening. The superiority of the PDS algorithm over the other algorithms was mainly explained by the advantage of its piecewise fashion application giving the transfer a local character because of the use of a small number of neighboring slave wavelengths located in a moving spectral window to reconstruct each master wavelength (Tan & Brown, 2001).

3.6.3 Results and discussion

Spectral differences

Figure 3.54 shows the NIR absorbance spectra of a randomly selected sample measured on the FT-NIR and LABPOD spectrometers. A clear difference between the measured spectra was observed. This difference was mainly a shift of the signals of interest both on wavelength and on percentage of light absorbed due to differences in working principle.

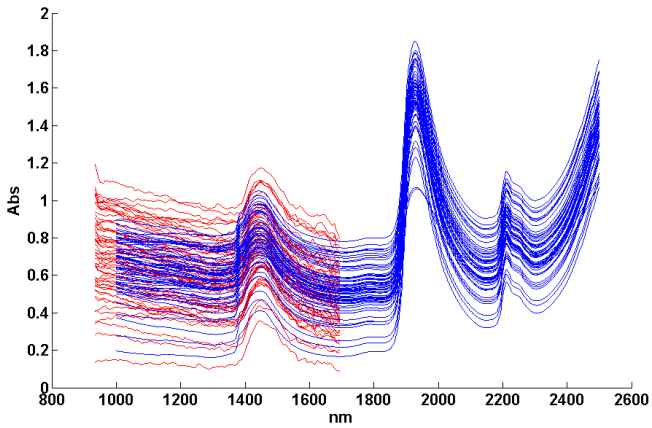

Figure 3.54: NIR absorbance spectra of milk sample measured with FT-NIR (blue) and LABPOD (red) spectrometers.

Standardization procedure

Usually, the first step in developing a standardization transform is to select samples to be included in the standardization subset, which best represent the variability of the considered parameter. A convenient method for choosing samples is based upon their multivariate

leverage, i.e. the sample with the greatest deviation from the multivariate mean of the calibration samples is selected. All other samples are then orthogonalized with respect to the first sample and the procedure is repeated (Wang et al., 1991). Another method is based on the PLS regression.
In this work, the best standardization performance was reached by selecting 5 samples on the basis of their leverage.
The standardization transform was performed on absorbance spectra.
Slave spectra were pretreated by applying the moving average smoothing with a segment size of 7 (Figure 3.55).

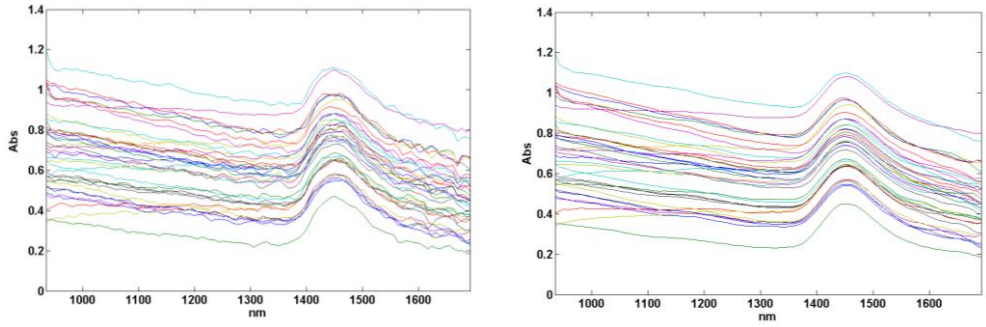

Figure 3.55: Original (left) and smoothed (right) slave spectra.

Spectra obtained from FT-NIR are comprehensive of quartz cuvette spectra. Thus, the average spectrum of quartz cuvette was subtracted from FT-NIR spectra, in order to have only the absorption due to milk constituents (Figure 3.56).

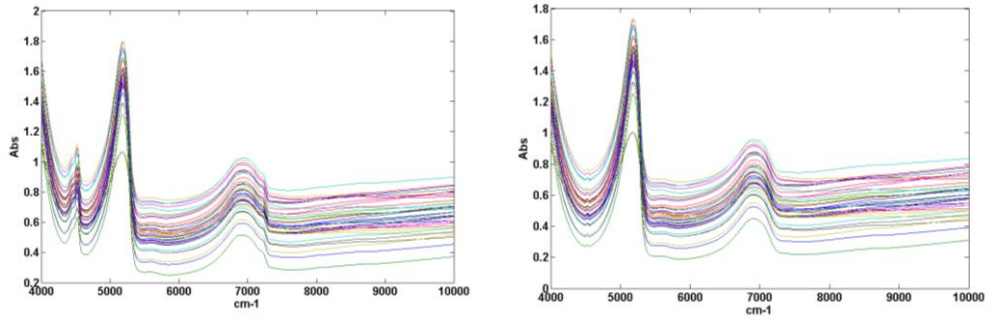

Figure 3.56: Whole master spectra (left) and spectra subtracted of quartz cuvette absorption (right).

Conversely, for LABPOD, before scan, the background measurements were made using, before scan, an empty quartz cuvette which is automatically subtracted by the software.
Besides, FT-NIR spectra have 1501 wavelengths, while LABPOD have only 100. Thus, the next step was to reduce FT-NIR matrix up to 100 wavelengths, choosing the most close to those of LABPOD. For this purpose, a Matlab routine called 'Mattdiff' was created. The routine is reported below.

```
function [MatCoppia]=mattdiff(VettA,VettB,ddiff)


%Sizing of wavelength vectors
CicloA =size(VettA);
CicloB =size(VettB);

 %creation of matrix of differences between wavelength
for i=1:CicloA(1,2);
   for j=1:CicloB(1,2);
       matdiff(i,j)=abs(VettA(i)-VettB(j));
   end
end

%creation of matrix of wavelength minima
MinRig=min(matdiff);
MinCol=min(matdiff');

%initialization of Matpos
Matpos(1:size(MinRig,2))=0;

%creation of matrix of correlations between wavelengths
rc3=size(MinRig);
for i=1:rc3(1,2);
    if find(MinCol==MinRig(i))
        if MinRig(i)<ddiff;
            posmincol=find(MinCol==MinRig(i));
            indc=abs(i-posmincol);
            valfincol=min(find(MinCol==MinRig(i)));
            if length(indc)>1
                k=1;
                for j=1:length(posmincol)
                    if find(Matpos==posmincol(j))
                        k=k+1;
                    end
                end
                valfincol=posmincol(k);
            end
            Matpos(i)=valfincol;
        end
    else
        Matpos(i)=0;
    end
end

%creation of matrix of matching position
rc4=size(Matpos);
j=0;
```

```
for i=1:rc4(1,2);
    if Matpos(i)>0;
       j=j+1;
       MatCoppia(1,j)=i;
       MatCoppia(2,j)=Matpos(i);
    end
end
```

'Mattdiff' crosses all FT-NIR wavelengths with those of LABPOD and calculates the differences, as absolute value, creating a matrix. Then it combines the wavelengths of the two instruments whose difference is less than 1 (arbitrary chosen value).
Figure 3.57 shows master and slave absorbance spectra with matching wavelengths.

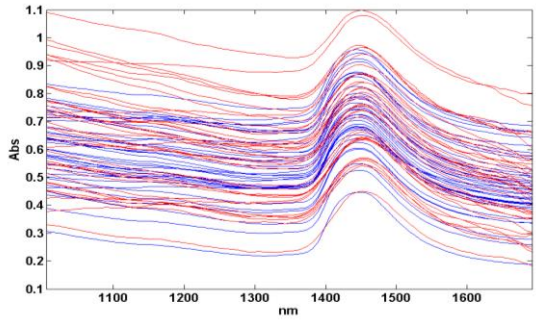

Figure 3.57: Master (blue) and slave (red) absorbance spectra with matching wavelengths.

Finally, the calibration transfer was carried out by the PLS_Toolbox function '*stdgen*' which calculates the standardization matrix and the background correction.

Performance of calibration transfer

Figure 3.58 shows master and standardized slave spectra. The difference between the master and the slave spectra after the PDS procedure has been reduced considerably indicating that most of the spectral differences have been compensated for through the standardization.

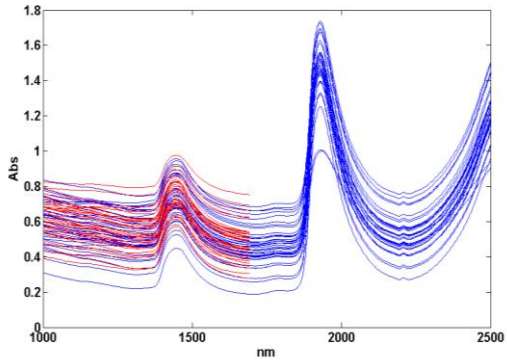

Figure 3.58: Master (blue) and standardized slave (red) spectra.

The standardization matrix was applied to transform an independent data set of 35 new slave spectra. Then, the mathematical model for the estimation of milk fat globules dimensions (par. 3.5) was applied. Figure 3.59 shows the correlation between D[3.2] calculated for master and standardized slave spectra.

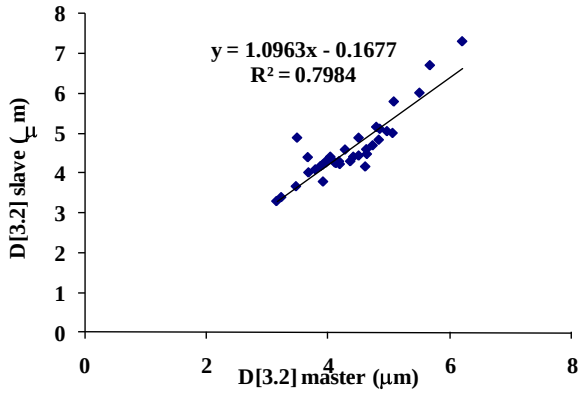

Figure 3.59: Correlation between D[3.2] calculated for master and slave spectra with the mathematical model (par. 3.5)

A good correlation between the two calculations was obtained, with a coefficient of determination R^2 of 0.867 and a SEP=0.39 μm, indicating a good spectra standardization.

3.6.4 Conclusions

Slave spectra after standardization were comparable with those of the master instrument. The calculation of milk fat globules diameter from slave standardized spectra through the mathematical model seen in chapter 3.5, gave comparable results with those calculated on master spectra.
The possibility of using a portable instrument offers many advantages, above all the possibility to perform on line analysis, such as analysis on milk directly in the parlor. Besides, this instrument is low cost, rugged since it has not moving parts and, being fully programmable, can be configured to operate in various scanning modes for a variety of general-purpose NIR applications that include quality control, R&D and industrial process control.
The good results obtained by PDS join all these advantages to the sensitivity and the precision of the tool bench.

3.6.5 References

Andrew A, Fearn T, 2004, Transfer by orthogonal projection: making near infrared calibrations robust to between-instrument variation. Chemom Intell Lab Syst 72: 51–56.

Bouveresse E, Massart DL, Dardenne P, 1994, Calibration transfer across near-infrared spectrometric instruments using Shenk's algorithm: effects of different standardisation samples. Anal Chim Acta 297: 405-416.

Chen CS, Brown CW, Lo SC, 1997, Calibration transfer from sample cell to fiber-optic probe. Appl Spectrosc 51: 744-748.

Despagne F, Walczak B, Massart DL, 1998, Transfer of calibrations of near-infrared spectra using neural networks. Appl Spectrosc 52: 732-745.

Shenk JS, Westerhaus MO, U. S. Patent 1991, 4866644, Sep., 12.

Tan C, Li M, 2007, Calibration transfer between two near-infrared spectrometers based on a wavelet packet transform. Anal Sci 23: 201-206.

Walczak B, Bouveresse E, Massart DL, 1997, Standardization of near-infrared spectra in the wavelet domain. Chemom Intell Lab Syst 36: 41-51.

Wang Y, Veltkamp DJ, Kowalski BR, 1991, Multivariate instrument standardization. Anal Chem 63: 2750-2756.

Tan H-W, Brown SD, 2001, Wavelet hybrid direct standardization of near-infrared multivariate calibrations. J Chemometrics 15: 647–663.

Forina M, Drava G, Armanino C, Boggia R, Lanteri S, Leardi R, Corti P, Conti P, Giangiacomo R, Galliena C, Bigoni R, Quartari I, Serra C, Ferri D, Leoni O, Lazzeri L, 1995, Transfer of calibration function in near-infrared spectroscopy. Chemom Intell Lab Syst 27: 189:203.

4. FINAL CONCLUSIONS

In this work, some aspects of cow milk casein and fat globules were studied applying NIR and IR techniques.

In dairy field, casein amount and quality have great influence on milk rennet properties and cheese yield. Caseins from milk of ruminants have been extensively studied, but the exact structure of the casein micelle is still debated. Despite the several applications of NIRS in food and agricultural sectors, the relevance of this technique to study the proteins structure has received minor attention.

In this research, the adequacy of the NIR and MIR spectroscopic techniques for the study of intermolecular interactions of milk micellar proteins in aqueous environment was proved. Good information was provided on the effects of solvent and the addition of bases. The spectral response, otherwise, was less affected by modifications of the temperature parameter.

NIRS was able to determine and quantify casein genetic variants in native and acid casein reconstituted samples, suggesting the possibility to select milk for its final purpose. Moreover, NIR spectroscopy was able to discriminate between caseins obtained after the application of physical and chemical treatments and to detect bonds involved in the micelle structure, especially phosphate group and its binding to calcium.

The second part of the PhD activity was focused on the study of the size distribution of milk fat globules, an aspect influencing the technological and sensorial milk characteristics. Despite the importance of this parameter in several dairy processes, instrumentations for particle size analysis are not available in dairy laboratories. NIR instrumentation, instead, is largely used in dairy labs.

This study firstly proved that for fat content, NIR calibration depends also on the spectral contribution of the scattering caused by fat globules in emulsion and not just by the vibrational absorptions, as observed using the mid-infrared. On the basis of these concerns, a rapid and economic method for estimating the distribution of fat globules in milk through a physical-mathematical model, based on the study of the scattering component in the NIR spectrum, was developed. The model showed very high performances in correlation with reference analyses results.

The model can be useful for a rapid evaluation of milk fat globules distribution with the possibility for a better evaluation of the technological fate of milk.

In order to improve the applicability of the model, a portable spectrometer was standardized to bench-top instrument spectra for estimating the distribution of milk fat globules showing a very good transfer of results.

Abstract: Study of chemical and molecular information related to NIR and IR spectroscopic data for dairy sector.

In the last decades, the spectroscopic techniques have acquired reliability, since they are sufficiently accurate and precise for analysis of the macro-composition of food.
In this work, NIR and IR techniques were applied to study some aspects of cow milk casein and fat globules.
In dairy field, casein amount and quality have great influence on milk rennet properties and cheese yield. Caseins from milk of ruminants have been extensively studied, but the exact structure of the casein micelle is still debated.
The research activity was addressed to verify the ability of spectroscopic techniques in the evaluation of modifications of casein fractions and sub-fractions as a function of pH and temperature. The NIRS ability in predicting casein fractions content and in detecting bonds involved in the micelle complex were also evaluated.
The study was carried out on both commercial preparations of casein fractions and reconstituted casein samples. These were obtained by ultracentrifugation (native casein) and by precipitation at the iso-electric pH (acid casein) of individual milk samples, collected during two months periods in the Austria's region.
The IR spectra of commercial caseins showed the phosphate band at 1100 cm^{-1}, confirming its role in the stabilization of casein micelle structure. When NIR casein spectra were measured as a function of temperature, exclusively changes in water bands were detected, while regarding pH, ΔAbs from the mean spectrum evidenced some modifications of linearity due to the number of negative charged amino acid residues at pH $\geq$ 6.80 in the casein sub-fractions.
Casein fractions content of reconstituted samples was determined by Capillary Zone Electrophoresis analyses. PLS analyses, performed with electrophoretic and NIR data, revealed the NIRS ability to determine and quantify casein genetic variants useful for milk selection for its final purpose. Moreover, the PCA analysis on the same samples proved the NIRS ability also to discriminate between samples obtained by physical and chemical treatments and to detect bonds involved in the micelle structure, especially phosphate group and its binding to calcium.
FT-NIR spectroscopy was also applied to study the size distribution of fat globules: an aspect influencing the technological and sensorial milk characteristics. In this contest, the variability in the distribution of fat globules within cow breedings in Lombardy was studied during two years period. The reference particle size analyses of fat globules were performed using a granulometer. The Sauter Mean Diameter (SMD) was chosen as the best descriptor of particle size distribution.
This parameter resulted to be more influenced by genetic factors than seasonal aspects. The differences among farms could be determinant in planning the milk collection for the technological destination, while the differences among the breeding bulls can be used for the animals' selection.
Despite the importance of this parameter in several dairy processes, instrumentation for particle size analysis are not available in dairy laboratories. NIR instrumentation, instead, is largely used in dairy labs. NIR spectrum of whole milk arises from absorbance due to both molecular vibrations and elastic scattering related to the presence of fat globules in emulsion. Moreover, the amount of scattered photons depends on their size and wavelength. A rapid and economic method for estimating the distribution of fat globules in milk through a physical-mathematical model based on the study of the scattering component in the NIR spectrum was developed. The model, working in Visual Basic for Excel, calculates the optical density produced by milk fat globules, given the fat concentration. On the basis of the Weibull distribution, the model calculates the amount of globules with a certain diameter range, returning a first distribution

curve. After the generation of a theoretical NIR spectrum, the model inversion was performed by minimizing the sum of squared differences between measured and theoretical spectra. At the end of the process, the new distribution curve was given. The performances of the model was tested by analyzing an external data set with both NIR and reference diffractometric data. For the SMD a very high coefficient of determination in prediction was found.
In order to improve the applicability of the model, the use of a portable spectrometer for estimating the distribution of milk fat globules was evaluated trough standardization to bench-top instrument spectra. The calculation of milk fat globules diameter by a portable instrument standardized spectra through the mathematical model, gave comparable results with those calculated on master spectra.

Riassunto: Interpretazione su base chimica e molecolare delle informazioni contenute in dati spettroscopici nel medio (IR) e vicino infrarosso (NIR) per lo studio di prodotti del settore caseario

Negli ultimi decenni, le tecniche spettroscopiche hanno acquisito caratteristiche di affidabilità, in quanto sufficientemente accurate e precise per l'analisi della macro-composizione degli alimenti. In questo lavoro, le tecniche NIR e IR sono state applicate allo studio di alcune caratteristiche chimico-fisiche di caseina e globuli di grasso in latte vaccino. La caseine del latte dei ruminanti sono state ampiamente studiate, ma l'esatta struttura della micella di caseina è ancora dibattuta. L'attività di ricerca è stata indirizzata alla verifica della capacità di tecniche spettroscopiche per lo studio delle modificazioni delle frazioni e sub-frazioni di caseina in funzione di pH e temperatura. Inoltre, è stata valutata la capacità della NIRS nel predire il contenuto di frazioni di caseina e nel rilevare i legami coinvolti nella struttura micellare. Lo studio è stato condotto su preparati commerciali di frazioni di caseina e su campioni di caseina ricostituita. Questi ultimi sono stati ottenuti ultracentrifugando (caseina nativa) o precipitando al pH isoelettrico (caseina acida) campioni di latte individuale, raccolti nella regione delle Asturie (due mesi). Dagli spettri IR delle caseine commerciali, la presenza a 1100 cm^{-1} della banda del fosfato ne ha confermato il ruolo nella stabilizzazione della micella caseinica. Negli spettri NIR di caseina misurati in funzione della temperatura, si sono rilevati esclusivamente cambiamenti nelle bande di assorbimento dell'acqua, mentre per quanto riguarda il pH, le modifiche registrate sono dovute al numero di residui amminoacidici carichi negativamente a pH> 6,80. Il contenuto delle frazioni caseiniche dei campioni ricostituiti è stato determinato mediante analisi in Elettroforesi Capillare Zonale. L'analisi PLS, eseguita sui dati elettroforetici e NIR, ha rilevato la capacità della NIRS nel determinare e quantificare le varianti genetiche delle caseine offrendo la possibilità di selezionare il latte a seconda della destinazione finale. L'analisi PCA ha rilevato anche la capacità della tecnica di discriminare tra campioni sottoposti a trattamenti fisici e chimici e nell'individuare i legami coinvolti nella struttura micellare.
La NIRS è stata applicata anche allo studio della distribuzione delle dimensioni dei globuli di grasso. La variabilità di tale parametro in allevamenti Lombardi è stata studiata durante un periodo di due anni. Le analisi di riferimento sono state eseguite utilizzando un granulometro, selezionando il Sauter Mean Diameter (SMD) come miglior descrittore. Questo parametro è risultato maggiormente influenzato da fattori genetici che da aspetti stagionali. Le differenze tra le aziende agricole risulterebbero determinanti nella pianificazione della raccolta del latte in funzione della destinazione tecnologica, mentre le differenze tra i tori possono essere sfruttate per la selezione degli animali.
Nonostante l'importanza di questo parametro, la strumentazione necessaria per la sua determinazione non è sempre disponibile nei laboratori di controllo, come lo è invece la strumentazione NIR. Lo spettro NIR di latte intero, deriva dall'assorbimento sia delle vibrazioni molecolari che dallo scattering legato alla presenza di globuli di grasso in emulsione. Inoltre, la quantità di fotoni deviati dipende dalla loro dimensione e dalla lunghezza d'onda. Conseguentemente, dallo spettro NIR è possibile ricavare informazioni sulla distribuzione delle dimensioni delle particelle.
E' stato sviluppato un metodo rapido ed economico per la stima della distribuzione dei globuli di grasso nel latte, attraverso un modello fisico-matematico basato sullo studio della componente di scattering nello spettro NIR. Il modello, sviluppato in Visual Basic per Excel, calcola, nota la concentrazione di grasso, la densità ottica prodotta da globuli di grasso del latte.
Sulla base della distribuzione di Weibull, il modello calcola la quantità di globuli in un certo intervallo di diametri, restituendo una prima curva di distribuzione. Dopo la generazione di uno

spettro teorico NIR, l'inversione del modello è eseguita riducendo al minimo la somma delle differenze al quadrato tra spettri misurati e teorici. Alla fine del processo, viene restituita la nuova curva di distribuzione. Le prestazioni del modello sono state valutate analizzando un data set esterno sia mediante NIR che con tecnica diffrattometrica di riferimento. Il parametro SMD ha fornito un coefficiente di determinazione in previsione molto elevato.
Al fine di favorire le possibilità di utilizzo del modello, sono state valutate le performances di uno spettrometro portatile, standardizzato contro lo spettrometro da laboratorio, per la stima della distribuzione dei globuli di grasso del latte. Il calcolo, attraverso il modello matematico, del diametro di globuli di grasso del latte ottenuto con strumentazione portatile, adeguatamente standardizzata, ha fornito risultati confrontabili con quelli ottenuti con strumento da ricerca.